United States
Naval Postgraduate School

THESIS

AN ALL-DIGITAL SIMULATION AND ANALYSIS OF THE CVA-63
BOILER AND AUTOMATIC COMBUSTION CONTROL SYSTEM

by

Charles Arthur Vinroot

June 1970

United States
Naval Postgraduate School

THESIS

AN ALL-DIGITAL SIMULATION AND ANALYSIS OF THE CVA-63

BOILER AND AUTOMATIC COMBUSTION CONTROL SYSTEM

by

Charles Arthur Vinroot

June 1970

An All-Digital Simulation and Analysis of the

CVA-63 Boiler and Automatic Combustion Control

System

by

Charles Arthur Vinroot
Lieutenant, United States Navy
B.S.E.E., North Carolina State University, 1964

Submitted in partial fulfillment of the
requirements for the degrees

ELECTRICAL ENGINEER

and

MASTER OF SCIENCE IN ELECTRICAL ENGINEERING

from the

NAVAL POSTGRADUATE SCHOOL
June 1970

ABSTRACT

An all digital simulation of the existing boiler and control system of CVA-63 was carried out. A significant savings in computer time over previous simulations was realized.

The parameter-plane method was used to search for new operating points for each of the system minor control loops. Individual loop transient response was tested with a simulation program to demonstrate improved response with new operating points.

The entire system response was then investigated to demonstrate the overall effects. Recommendations were made for new controller settings along with component variations in order to improve over-all system response.

TABLE OF CONTENTS

LIST OF DRAWINGS

TABLE OF SYMBOLS AND ABBREVIATIONS

GS	Steam Flow Rate (Lb/Hr)
GF	Fuel Flow Rate (Lb/Hr)
GW	Water Flow Rate (Lb/Hr)
PDS	Boiler Drum Pressure due to Steam Flow (PSIG)
PDF	Boiler Drum Pressure due to Fuel Flow (PSIG)
PDW	Boiler Drum Pressure due to Water Flow (PSIG)
PO	Boiler Drum Pressure (PSIG)
LF	Drum Water Level due to Fuel Flow (Inches)
LW	Drum Water Level due to Water Flow (Inches)
LSA	Drum Water Level due to Shrink/Swell (Inches)
LSB	Drum Water Level due to Steam Flow (Inches)
LST	Total of LSA+LSB
L	Drum Water Level (Inches)
PSA	Superheater Pressure Drop (PSIG)
POUT	Superheated Steam Pressure (PSIG)
PP	Pneumatic Steam Pressure Signal (PSIG)
PRP	Steam Pressure Reference Signal (PSIG)
PZP	Steam Pressure Error Signal (PSIG)
PS	Water Level Reference Signal (PSIG)
PL	Pneumatic Water Level Signal (PSIG)
PSL	Water Level Error Signal (PSIG)
PRL	Water Flow Reference Signal (PSIG)
PSW	Water Flow Demand Signal (PSIG)
PEQ	Pneumatic Air Flow Error Signal (PSIG)

PM	Air Flow Demand Signal (PSIG)
PQ1	Forced Draft Blower Actuating Signal (PSIG)
GB	Steam Flow Rate to Forced Draft Blower (Lb/Hr)
QA	Air Flow (%)
PQR	Pneumatic Air Flow Signal (PSIG)

ACKNOWLEDGEMENT

The author gratefully acknowledges the continuous encouragement and guidance of his advisor, Dr. George J. Thaler, throughout the duration of this project.

Also acknowledged is the helpful advice given by Mr. James W. Banham, Jr., of the Naval Ship Engineering Center, Philadelphia Division.

Last, but certainly not least, the author wishes to thank his wife, Sally, whose patience and understanding made this report possible.

I. INTRODUCTION

Naval boilers differ from most other stationary type boilers in that they are called upon to answer widely varying load demands in a minimum amount of time. Feedwater, fuel oil and combustion air must be supplied in varying, but accurate, amounts to maintain sufficient steam flow as required by ship operation. There are maneuvering conditions which might require boiler load to change from ten or twenty percent to over one hundred percent in a matter of a few seconds.

Automatic combustion control systems have been developed by various manufacturers to control the three inputs; oil, air and water. Most of the ACC systems up until the present have been of the pneumatic variety; i.e., pneumatic sensing and valve control. Individual components of systems of this type range from simple bellows type sensors to the extremely complex masses of springs, levers, valves, gages and nozzles found in pressure relays and transmitters.

This thesis will investigate the automatic combustion control system including a main boiler as found on USS KITTY HAWK (CVA-63). An all-digital computer model will be developed for testing and analysis purposes. Each of the three major control loops, fuel flow, air flow and feedwater flow, will be investigated independently and the effects of any changes or improvements will be tested in the system simulation. No radical changes to the overall system will be proposed but readjustment of variable parameters within the existing system will be stressed with emphasis on improved overall system performance.

A. THE BOILER

The boiler to be modeled is a Foster-Wheeler D-type as found on

CVA-63. The boiler consists of an upper steam drum connected by tubes to the lower water drum, screen wall and waterwall headers. A vertical superheater is integral to the boiler. This unit is capable of generating 318,000 lb./hr. of steam at 120 percent overload conditions. Cruising conditions are considered to be 117,500 lb./hr. of steam which is 44.7 percent of full boiler load. See Appendix A and Ref. 1 for more design and performance data. Two boilers are operated together and controlled by one ACC unit due to physical location on shipboard. Boiler transfer functions were obtained from Ref. 2 and were valid for cruising conditions only. For this reason, small variations in boiler load were used and the model developed was of the perturbation variety. When data on other conditions of load become available, the model may be easily modified to suit the design engineer.

B. AUTOMATIC COMBUSTION CONTROL

The automatic combustion control system encompasses two classifications of pneumatic control, combustion control and feedwater control. While the feedwater portion is not essential for combustion, it is usually included in any discussion of ACC systems since it is very necessary for operation of the overall system.

The primary function of the combustion control portion of the system is to maintain constant boiler superheater outlet pressure under all load conditions. It must also insure that fuel and air are mixed in the proper proportions to maintain optimum combustion efficiency. Normally, a safety feature is provided with the system whereby, in the event of loss of control air pressure, all valves return to a neutral position which reduces boiler firing to a stable minimum.

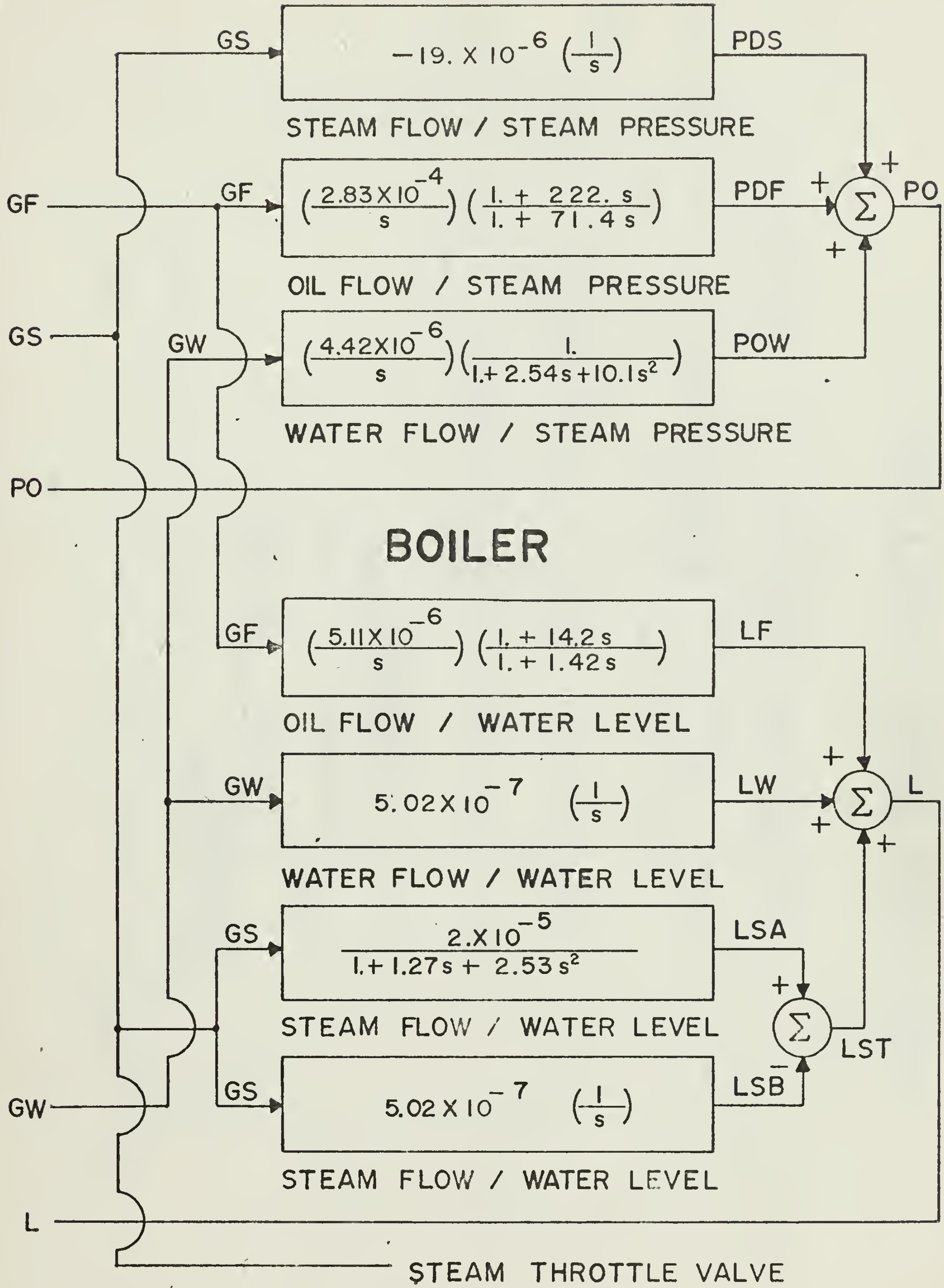
GS
$-19. \times 10^{-6} \left(\frac{1}{s}\right)$
PDS
STEAM FLOW / STEAM PRESSURE
GF
GF
$\left(\frac{2.83 \times 10^{-4}}{s}\right)\left(\frac{1. + 222.\, s}{1. + 71.4\, s}\right)$
PDF
+
+
+
PO
OIL FLOW / STEAM PRESSURE
GS
GW
$\left(\frac{4.42 \times 10^{-6}}{s}\right)\left(\frac{1.}{1. + 2.54s + 10.1s^2}\right)$
POW
WATER FLOW / STEAM PRESSURE
PO
BOILER
GF
$\left(\frac{5.11 \times 10^{-6}}{s}\right)\left(\frac{1. + 14.2\, s}{1. + 1.42\, s}\right)$
LF
OIL FLOW / WATER LEVEL
GW
$5.02 \times 10^{-7} \left(\frac{1}{s}\right)$
LW
+
+
+
L
WATER FLOW / WATER LEVEL
GS
$\frac{2. \times 10^{-5}}{1. + 1.27s + 2.53 s^2}$
LSA
+
STEAM FLOW / WATER LEVEL
LST
GS
$5.02 \times 10^{-7} \left(\frac{1}{s}\right)$
LSB
−
STEAM FLOW / WATER LEVEL
GW
L
STEAM THROTTLE VALVE

FIGURE 1(a.)

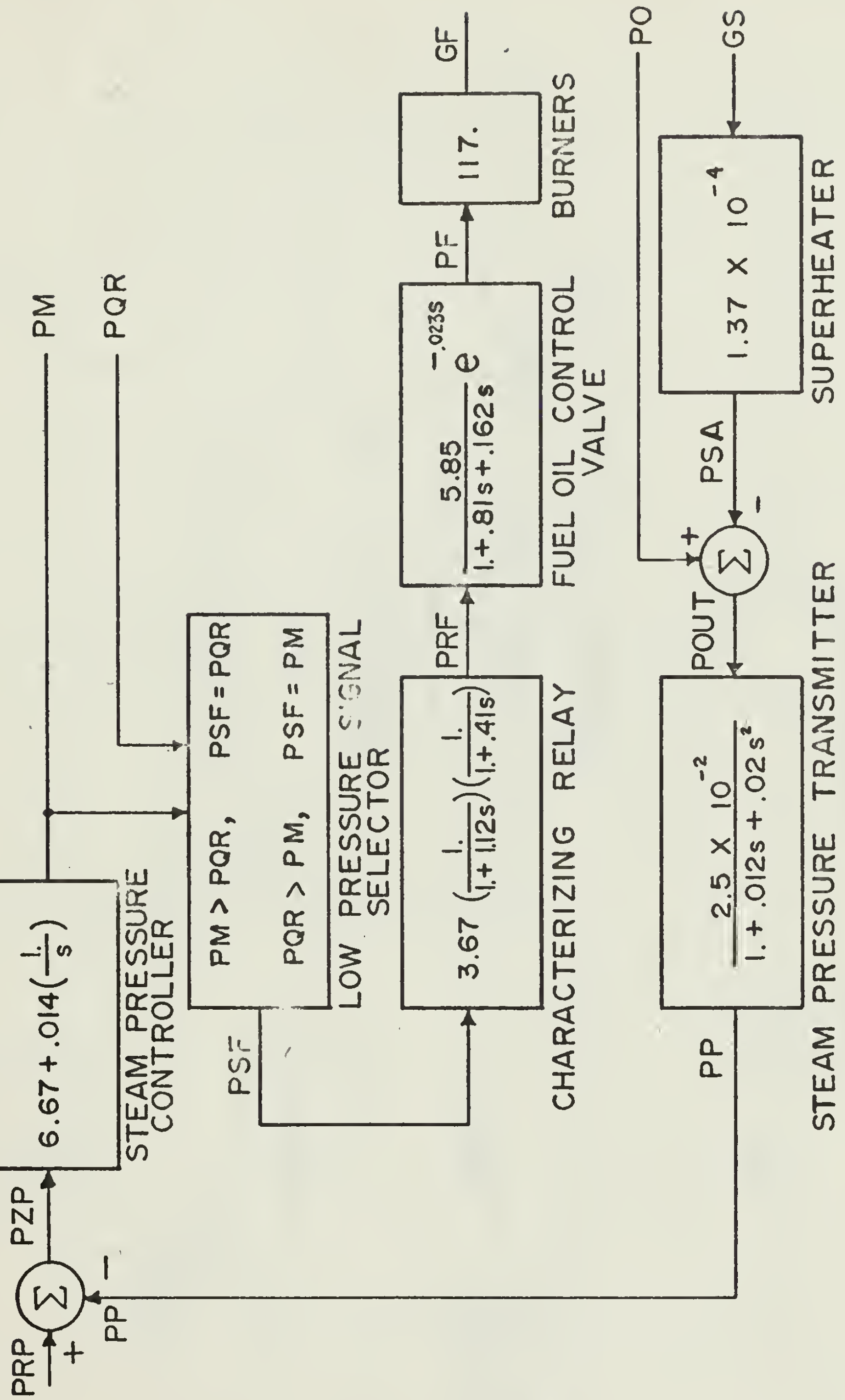

FUEL OIL FLOW CONTROL

FIGURE 1(b)

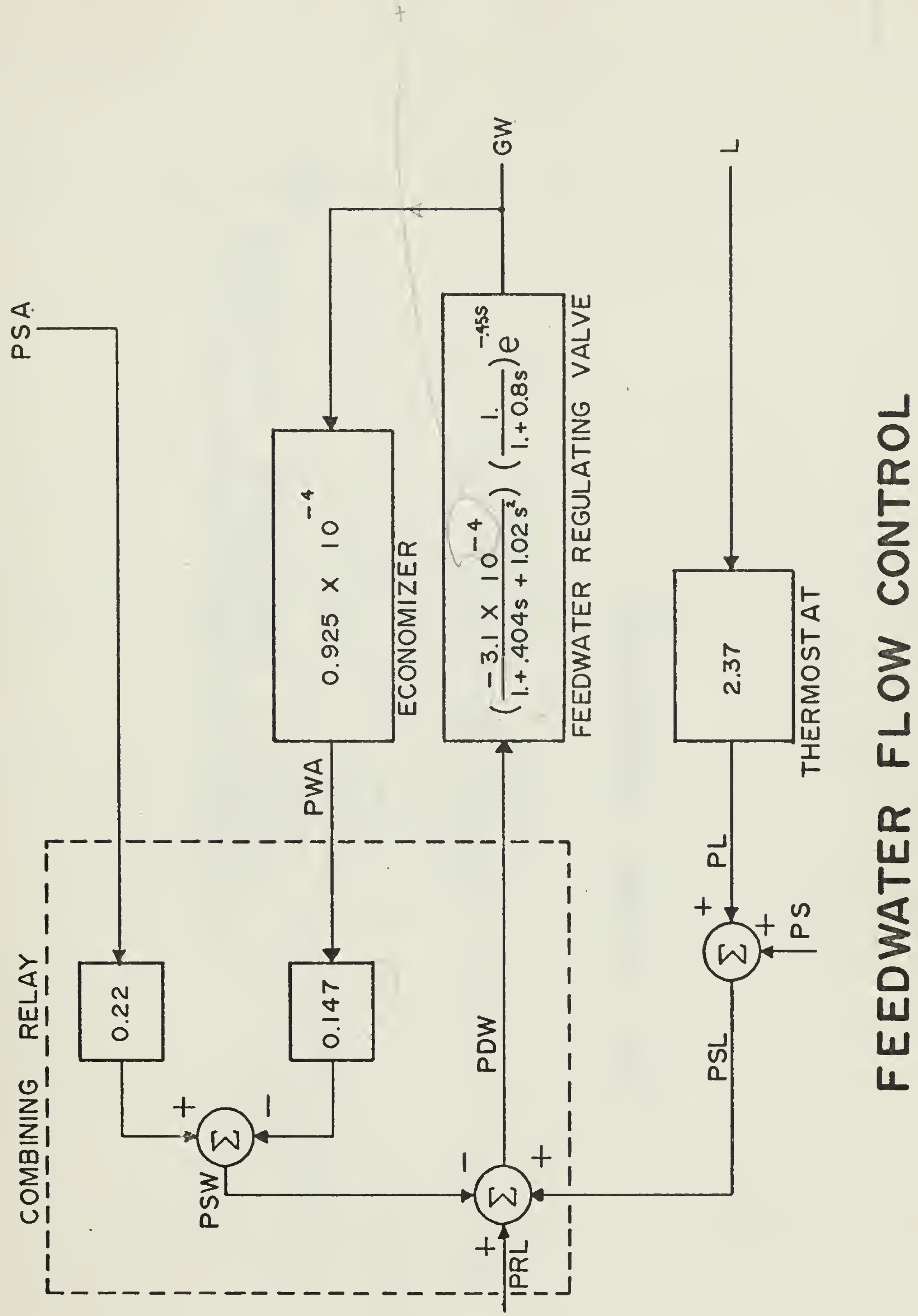
PSA
GW
L
0.925 X 10^-4
ECONOMIZER
(−3.1 X 10^-4 / 1.+.404s + 1.02s²) (1. / 1.+0.8s) e^-.45s
FEEDWATER REGULATING VALVE
2.37
THERMOSTAT
PWA
PL
PS
PSL
COMBINING RELAY
0.22
0.147
PDW
PSW
IPRL
FEEDWATER FLOW CONTROL

FIGURE 1(c.)

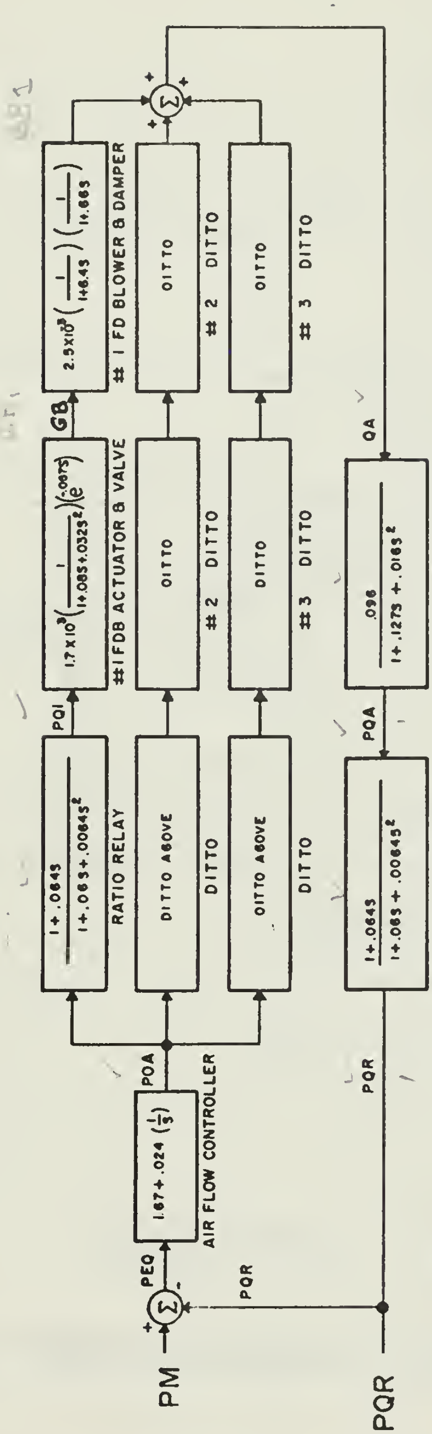

AIR FLOW CONTROL

FIGURE 1(d)

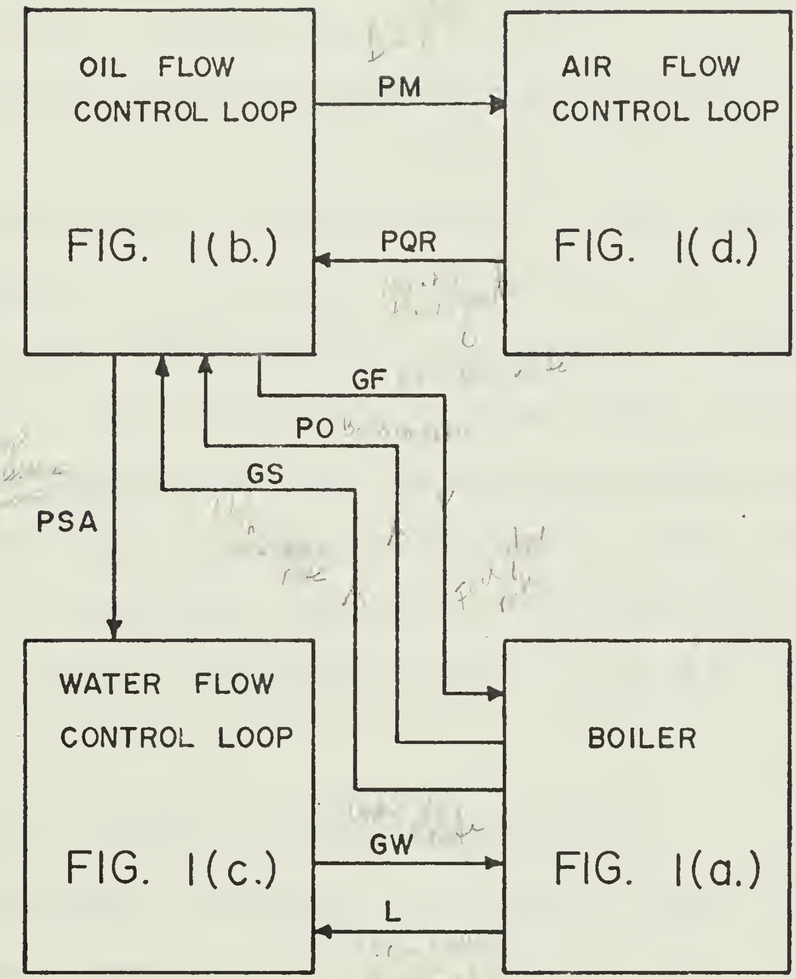

CONTROL SYSTEM

INTERCONNECTION DIAGRAM

FIGURE 2

The feedwater control portion of the system must maintain a balance between feedwater flow to the boiler and steam flow from the superheater. It must also maintain the water level in the steam drum at a normal steaming level under all conditions of boiler load. This level control is a most important function since high water level can mean possible liquid-state carryover into rotating turbines and subsequent destruction of blading while low water can expose the ends of tubes within the boiler leading to sagging and weakening due to extreme heat without adequate circulation cooling. Level control is complicated by the phenomena of shrink and swell. When boiler load is increased rapidly, large amounts of steam are removed from the boiler and the water in the steam drum will surge to a high level. The reverse is true when the load is suddenly decreased. The thermodynamic explanation of shrink and swell is to be found in Ref. 3 while more discussion is found in this paper in Section II.A.6.

C. OPERATION OF AUTOMATIC COMBUSTION CONTROL SYSTEM

The steam pressure transmitter (Fig. 1d) must transmit a linear pneumatic signal directly proportional to pressure variations in the two-boiler main steam header. At the normal operating pressure, 1200 psig., the output of the steam pressure transmitter is 9 psig. The steam pressure controller is of the set-reset variety, also known as proportional plus integral control. When the steam pressure signal from the steam pressure transmitter decreases, the output of the steam pressure controller increases proportionally and conversely. The proportional band setting of the controller determines magnitude of output variation for a given input and the reset needle valve of the controller determines the rate response.

The output of the steam pressure controller goes both to the air flow controller and to the low-pressure signal selector. This output becomes the demand signal for the air flow control loop. The air flow controller compares this signal to the actual air flow signal which is proportional to the flow of combustion air across the boiler air registers. The air flow controller is also of the proportional plus integral type and its output signal is sent to the airflow ratio relay and damper actuators. There are two factors which affect the quantity of air flow, damper position and forced draft blower turbine speed. The ratio relay preceeding each blower controller insures parallel operation of blowers for there can be one, two or three blowers in operation for each boiler at any one time. It has been found that the use of dampers is not only unnecessary but that they have actually contributed to some air flow loop instability problems. Dampers were completely eliminated on USS AMERICA (CVA-66) (See Ref. 4).

The air flow transmitter senses pressure differential between windbox and furnace and transmits a signal proportional to this difference. This signal, representing actual airflow across the burner registers, is sent to a ratio relay where the important air-fuel ratio may be adjusted for optimum combustion efficiency.

The output of the ratio relay goes to the air flow controller already discussed and to the low-pressure signal selector. This signal selector transmits the lower of its two input signals, boiler load demand from the steam pressure controller and air flow signal from the fuel-air ratio relay. The lower of these two signals is used as a demand signal to the oil flow portion of the system so that, under increasing load, oil supplied to the furnace can never exceed the required air flow for proper

combustion. This prevents the formation of black smoke in the furnace when the load is suddenly increased.

The output of the signal selector goes to a characterizing relay which converts it to a corresponding non-linear signal conforming to the burner curve of return oil pressure vs. burner oil rate. Fuel oil is supplied at a constant supply pressure and the amount burned in the furnace is controlled by closing down on the return valve in the recirculating system.

The feedwater portion of the control system consists of a thermostatic drum level sensor, a combining relay and the feedwater regulating valve.

The level sensor consists of a stainless steel expansion tube inclined across the steam drum with its center at normal steaming water level. The upper tube end is rigidly fixed and the lower end tube movement is amplified through a lever system attached to a pilot valve stem. Level sensing motion comes from contraction due to temperature difference between saturated steam temperature (upper half) and boiler water temperature (lower half). The pilot valve converts the mechanical motion into a proportional air output signal.

A boiler steam flow signal and water flow signal are combined with this level signal in the combining relay using a combination of diaphragms and levers. The resultant signal is a total water demand signal and controls the feedwater regulating valve. The feedwater valve positioner controls the flow of feedwater by converting the demand signal to mechanical valve motion.

Now that a general system description has been given, consider the effects of changing the boiler load.

1. <u>System Action During Increasing Boiler Load</u>

The first noticable effect on increasing boiler load is a drop in superheater outlet pressure. This is reflected by a decrease in the output of the steam pressure transmitter which causes a corresponding increase in the output of the steam pressure controller.

This represents an increasing air demand signal which is greater than the actual airflow signal. This causes an increase in blower speed and opens dampers further until flow matches demand.

When load increases, the signal transmitted by the low-pressure signal selector is the smaller air flow signal. As the air flow return system receives an increasing signal, the fuel oil return valve is closed proportionately causing more oil to be burned in the furnace. This, in turn, causes an increase in steam pressure until equilibrium is once again reached.

The effects of boiler water swell are reduced by the action of the combining relay. As load increases, the steam flow signal increases to a new, higher fixed position. The swelling water level produces a false signal (actually, more water is needed, not less as indicated at first) which is balanced by the steam flow signal. Relay settings determine sensitivity. As the level swell boils away, the level signal will decrease to its true value and a demand will be made for more water. As water flow increases to a higher value, its signal will offset the steam flow signal and equilibrium will be reached once again.

2. <u>System Action During Decreasing Boiler Load</u>

When boiler load is decreased, the superheater outlet pressure increases causing an increase in steam pressure signal from the steam

pressure transmitter. This increasing signal causes a proportional decrease in steam pressure controller output. Since air flow is now greater than necessary, the output of the minimum signal selector becomes the lower steam pressure signal, decreasing fuel oil demand. The air flow response lags behind at this point, providing an excess of combustion air until blowers slow and dampers close.

The decrease in fuel oil demand opens the return valve and the pressure returns to equilibrium due to the smaller quantity of fuel oil being burned in the furnace.

The water flow portion will act oppositely to the manner in which it acted for a load increase. Decreased steam flow demand will be partially (or fully, depending on adjustment of combining relay) offset by shrink in boiler water level signal. As this shrink effect dies out and the drum level starts to increase, the output of the combining relay will increase and the feedwater regulating valve will close. As water flow decreases, the water flow signal offsets the steam flow signal in the combining relay and equilibrium is reached.

D. IMPROVEMENTS NEEDED

Control of a boiler and its associated auxiliary equipment is complicated considerably by the interaction present among its control variables. The representation of the boiler and control system in Figs. 1(a) through 1(d) and the interconnection diagram of Fig. 2 demonstrate the coupling which exists. All three major system variables; steam flow, oil flow, and water flow affect both boiler steam pressure and boiler water level in varying ways. The transfer functions seem complicated enough at first inspection but when one stops to consider that these are valid for cruising

conditions only and that at varying boiler loads they become dynamic functions of the load and rate of load change the control problem becomes overwhelming.

Ideally, if the interaction between inputs and outputs could be removed or balanced in some way, the control problem would be greatly reduced in scope. In the case of the boiler, physically forcing non-interaction is impossible. The alternative then, is to design a non-interacting controller. This has, in fact, been done on paper (See Ref. 5), but the controller transfer functions which result for this system are not physically realizable and could not be simulated using the digital simulation language to be discussed in the next section. See Appendix B for design information on the non-interacting controller.

Any improvement then, in control of this boiler, is limited to complete redesign of the entire system, or optimization of the existing system.

Alternative control systems have been proposed. Digital control (Refs. 6 and 7) and analog fluidic control (Ref. 8) are two of the better known alternatives. The first was investigated by Naval Electronics Laboratory Center but this investigation was terminated in June 1968 due to unfavorable reaction by Naval Ship Engineering Center. Analog fluidic control is under test and development presently at NAVSEC, Philadelphia. It is safe to assume that this testing and design will come to fruition in a new, fast, state-of-the-art control system for ships of the future.

What are we to do with the ships of today? Economics forbids the complete replacement of several hundreds of ACC systems on ships which have a life expectancy of between twenty and thirty years. Hence, let us look into the possibility of improving present systems at a minimum of

expense. At the very least, we can hope to explore methods which will enable the future ship control designer to design better systems.

Exactly what is needed in the way of improvements? Basically, it is a faster responding system with less overshoot of variable response. For example, Ref. 9 states that specifications on several ships required boiler water level to remain within $\pm$ 4 inches of set point during linear changes in boiler load from ten percent to eighty percent in 45 seconds. Subsequent shipboard operation produced high water conditions out of sight in the boiler gage glass. This was due to maneuvering the ship within the load specifications but in only 10 seconds instead of the specified 45 seconds. Although the system would probably meet the original specifications, response could probably be improved somewhat through a judicious "tuning" of the control system.

This thesis investigates the CVA-63 system and makes recommendations for readjustment of controller settings or replacement of component parts as necessary for better (faster) overall system response. The parameter plane method of optimization is used and it is hoped that even if system response is not dramatically improved, the methods used will prove enlightening for others who may follow.

II. THE SIMULATION

The boiler and automatic combustion control system were simulated utilizing the IBM developed Digital Simulation Language (DSL). DSL is a non-procedural, problem-oriented language which will accept problems in ordinary differential equation form or as analog block diagrams. Since an excellent block diagram of the CVA-63 system was available (Ref. 2), this program provided a relatively simple, efficient means of simulation. References 10 and 11 describe the DSL program in more detail. The variables indicated in parenthesis refer to the system diagrams, Figs. 1(a) - 1(d) and the interconnection diagram, Fig. 2.

A. BOILER

The seven transfer functions appearing in Fig. 1(a) are the result of tests conducted at NBTL (Ref. 2). These functions are the result of a combination of both pulse testing (Ref. 12) and of periodic input frequency response analysis.

1. Steam Pressure / Steam Flow (PDS/GS)

This response essentially represents a mass balance situation and is accurately represented by a straight integration at cruising conditions.

2. Steam Pressure / Fuel Oil Flow (PDF/GF)

This can be represented by a first-order lag, first-order lead, and a straight integration, all series connected.

3. Steam Pressure / Water Flow (POW/GW)

A second-order lag (complex poles) and series connected integration represent the effects of feedwater flow on steam pressure at cruising conditions.

4. <u>Water Level / Water Flow (LW/GW)</u>

As in 1. on the preceeding page, a straight integration accurately represents this simple mass balance situation.

5. <u>Water Level / Oil Flow (LF/GF)</u>

Pulse tests by NBTL yielded a transfer function consisting of integration and series-connected lag-lead.

6. <u>Water Level / Steam Flow (LST/GS)</u>

The response of water level to steam flow rate is shown by the parallel combination with outputs LSA and LSB in Fig. 1(a). Water level in the steam drum should integrate proportionally to the mass balance of steam flow-water flow difference. This integration, however, is of low natural frequency and is initially overshadowed by the shrink/swell phenomenon discussed previously. Fig. 3 gives the response, LST, to a step input. Fig. 4 give^ the same response to the triangular pulse input used for response tests in the system (Fig. 5). It can be seen that the effects of the integration are not present for the first several seconds.

B. FUEL OIL FLOW CONTROL

Also called steam pressure control loop, the fuel oil flow control loop is a closed control loop consisting of the following elements;

1. <u>Steam Pressure Controller (PZP/PM)</u>

This is a typical proportional plus integral controller. Values for proportional and integral gain were measured by NBTL using sinusoidal testing techniques and are shown in Fig. 1(b). These gains are adjustable and will be utilized to set the loop to secure "optimum" performance.

2. <u>Low Pressure Signal Selector (PM, PQR/PSF)</u>

This acts as a switch only and, as such, has no measurable transfer function. It is conveniently simulated in DSL by using a Function Switch (see computer output).

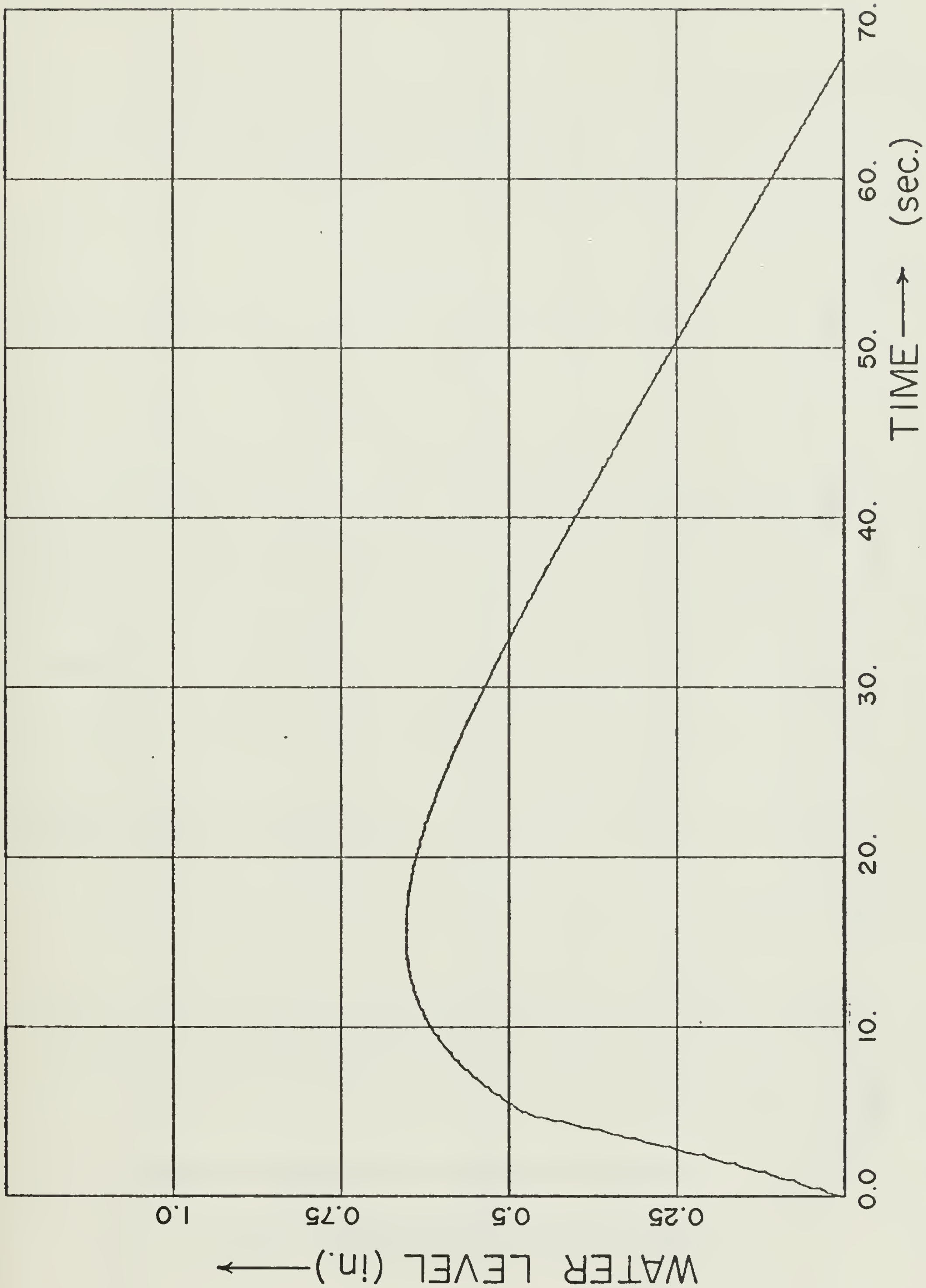

WATER LEVEL RESPONSE TO A STEP INPUT

FIGURE 3

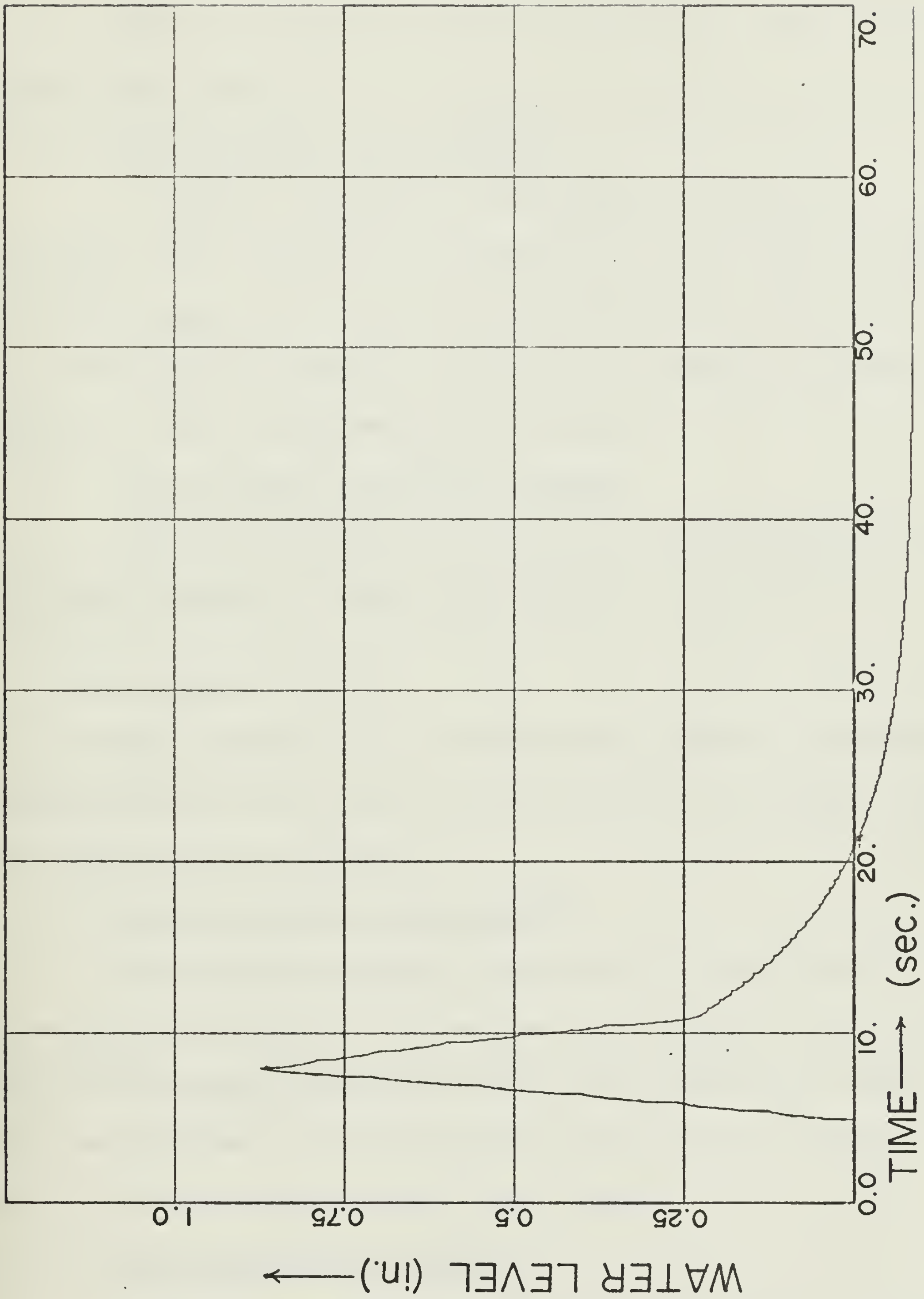

WATER LEVEL RESPONSE TO A PULSE INPUT

FIGURE 4

3. Characterizing Relay (PSF/PRF)

This has a two-pole response as determined by NBTL using the periodic input method.

4. Fuel Oil Control Valve (PRF/PF)

A quadratic lag function was obtained for this valve. A small time delay (0.023 seconds) is also present due to valve-stem stiction. This delay appears in all of the pneumatic/mechanical valves and is present due to the physical limitations of the valves themselves, and their inability to respond instantaneously to a demand.

5. Steam Pressure Transmitter (POUT/PP)

Analysis of transient response tests by NBTL yielded a quadratic lag transfer function as shown in Fig. 1(b).

C. WATER LEVEL/FLOW CONTROL

The water control loop is a "three-element" system, responding to changes in water level, water flow, and steam flow. Individual elements (see Fig. 1(c)) are as follows:

1. Feedwater Control Valve (PDW/GW)

The transfer function for this valve was found by NBTL to be third order, consisting of a first-order lag, attributed to the capacitance of the pneumatic diaphragm chamber, and a second-order lag due to the valve positioner. A 0.45-second pure time delay was thought to be due to valve-stem friction in the packing gland.

2. Combining Relay (PSA,PWA/PSW)

Dynamic measurement could not be made by NBTL and this component is approximated by pure gains.

3. Thermostatic Drum Level Indicator (L/PL)

At cruising condition loads, the thermostat may be represented

by a pure gain. NBTL was unable to make dynamic measurements due to limitations in the generation of a suitable water level input signal.

D. AIR FLOW CONTROL

The air flow loop is a typical feedback control system and the individual component transfer functions were derived by NBTL and are as follows:

1. Controller (POA/PEQ)

This controller is a typical set-reset controller with adjustable integral and proportional gains.

2. Ratio Relay (PG/POA and PQR/PQA)

The transfer function obtained by NBTL is as shown in Fig. 1(d).

3. Forced Draft Blower Actuator and Valve (GB/PQ)

The actuator and valve exhibit characteristic underdamped response and time delay which is normal with components of this type. Valve-stem friction is not as pronounced as in the feedwater control valve due to decreased valve-stem travel and the fact that the medium being controlled is steam instead of water.

4. Main Forced Draft Blowers (QA/GB)

Direct frequency response testing was used by NBTL to derive the transfer function shown in Fig. 1(d).

5. Air Flow Transmitter (PQA/QA)

This component is represented by a quadratic transfer function and appears in the feedback system of the air flow control loop.

E. INITIAL SYSTEM TESTS

Individual components were simulated and interconnected in DSL (see program listing) to produce a system simulation for transient response testing. Since transient response data for this boiler and combustion

control system are almost non-existent, the author had to rely on personal experience as Boiler Officer on USS INDEPENDENCE (CVA-62) from 1964 to 1966. General shape and accuracy of system response were also verified by J. W. Banham, Jr., head of the Machinery Automation Systems Department of the Naval Ship Engineering Center, Philadelphia Division.

Inspection of the completed simulation program on page 98 will reveal the manner in which individual components and loops are interconnected.

It was found necessary to put limitations on certain pneumatic signals to simulate the loading effects of a controller or relay being overdriven. This portion of the simulation appears at the end.

A triangular shaped input was selected for transient response testing. Since the model is of the perturbation variety, the use of a step input was deemed impractical and unrealistic. The triangular shaped input seemed to be the closest meaningful input signal which most nearly resembled a true impulse. The input is shown in Fig. 5.

System responses to this input are shown in Fig. 6 through Fig. 10. It must be remembered that variations are measured from a steady cruising condition value; i.e., a steam pressure variation of -8 psig is actually 1192 psig drum pressure, 8 psig below the nominal 1200 psig.

The value of a component by component simulation is readily apparent at this stage. Any intermediate signal may be designated as output for analysis purposes. Components which are overloaded or driven into saturation are easily discovered and individual components may be replaced with new or improved components to test the effects on the overall system response.

The effect of the underdamped feedwater control valve on water flow rate is readily apparent in Fig. 6. Later transient response tests show

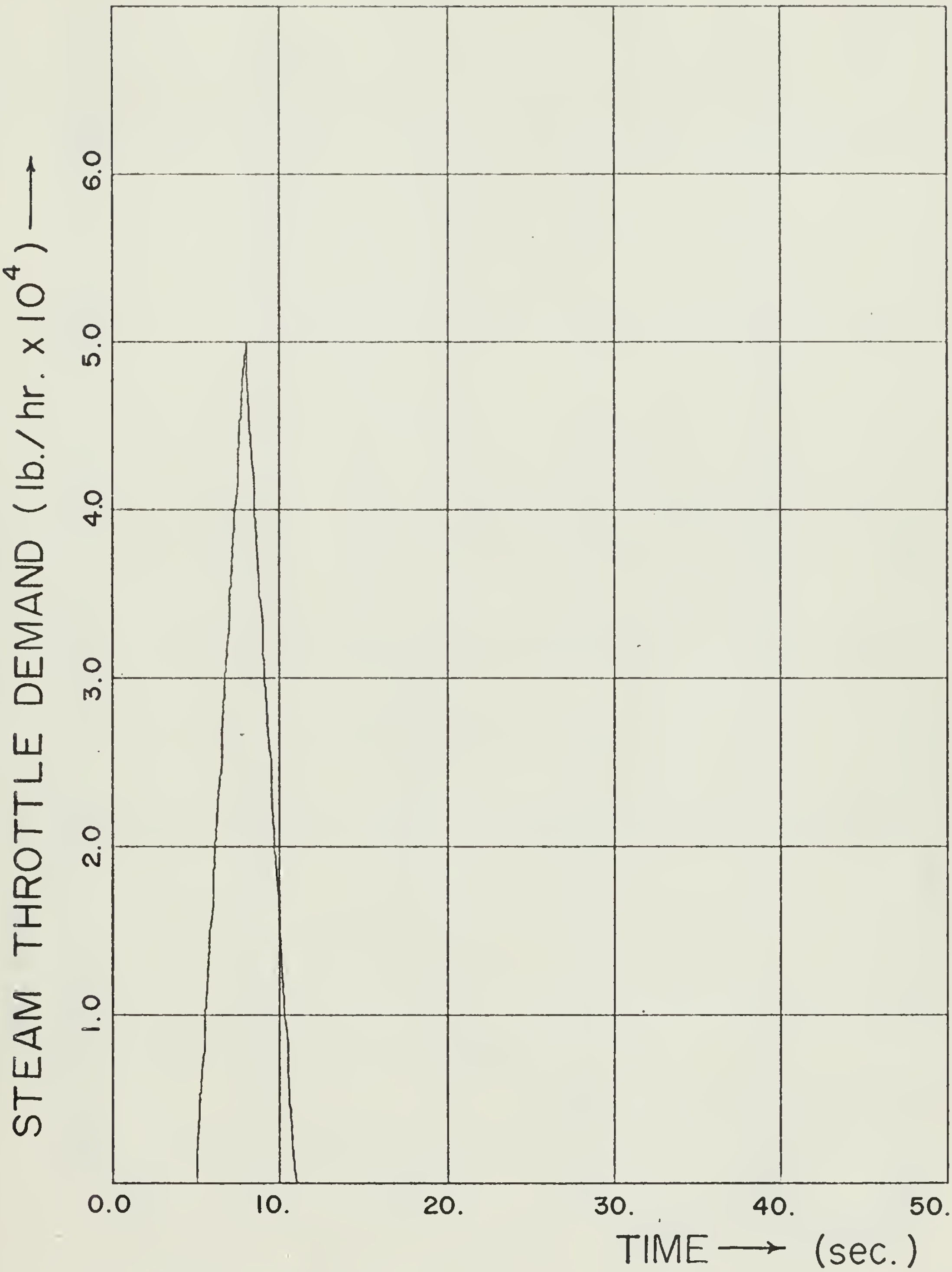

SYSTEM FORCING FUNCTION

FIGURE 5

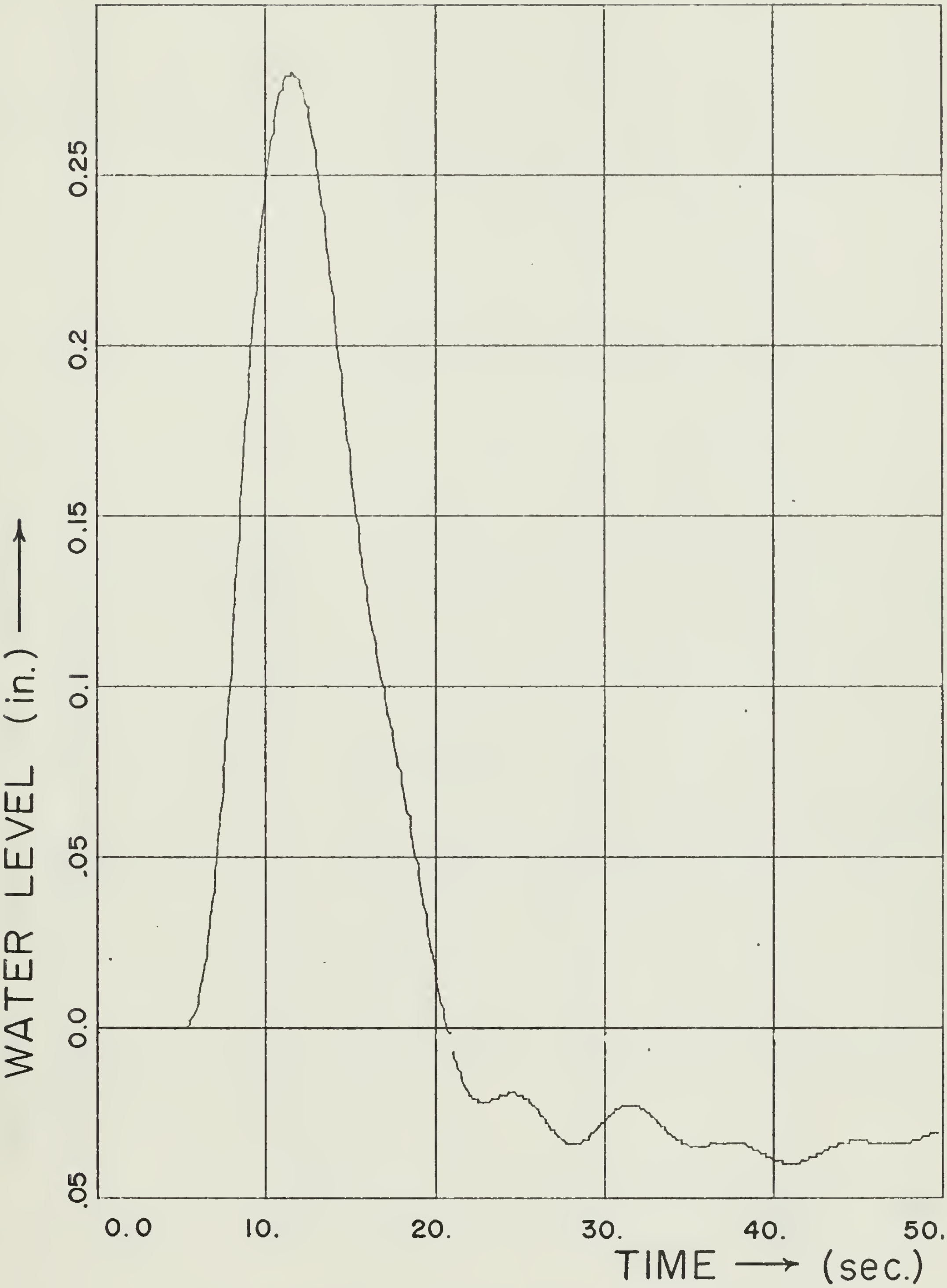

WATER LEVEL RESPONSE

FIGURE 6

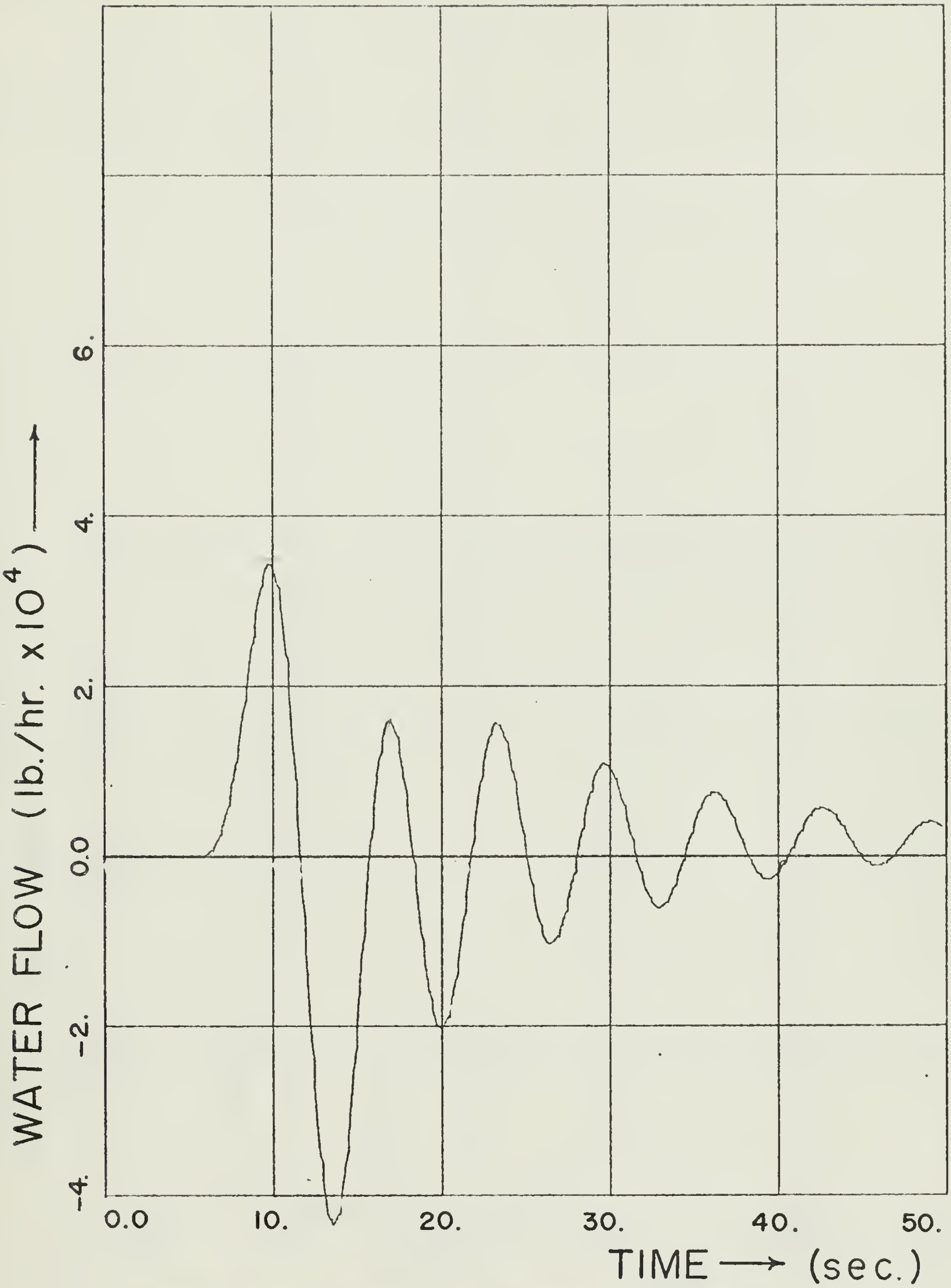

WATER FLOW RESPONSE

FIGURE 7

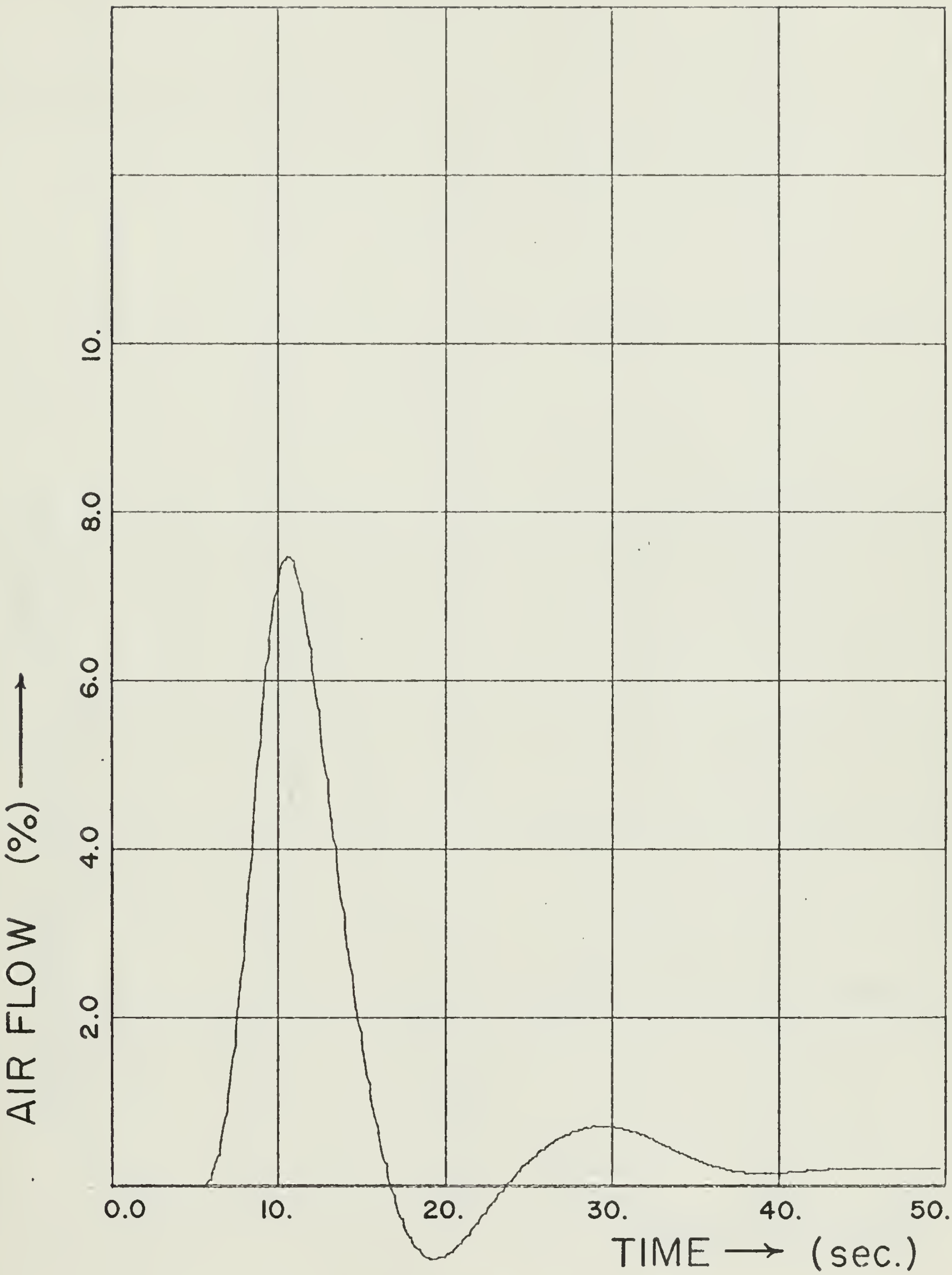

AIR FLOW RESPONSE

FIGURE 8

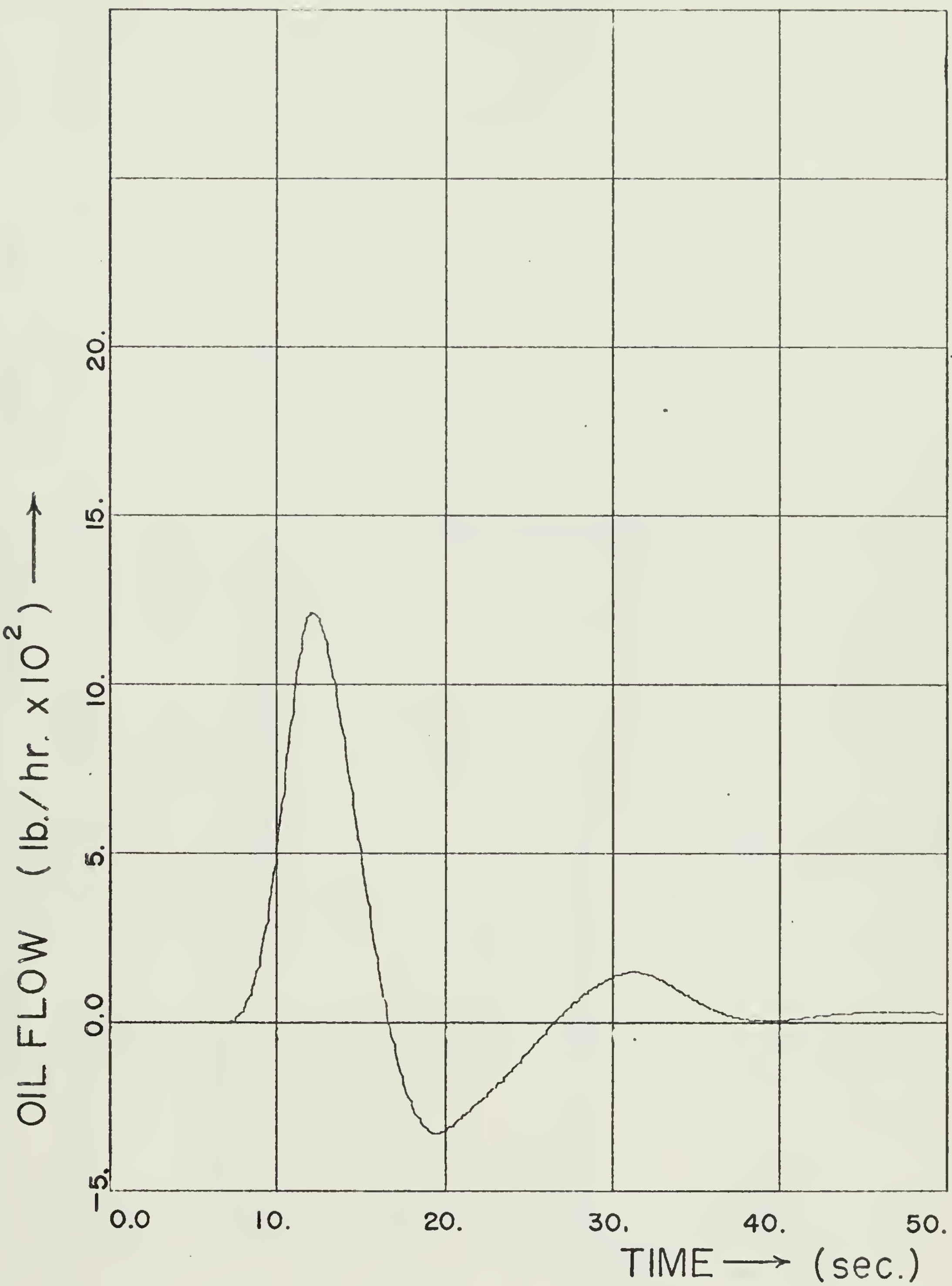

OIL FLOW RESPONSE

FIGURE 9

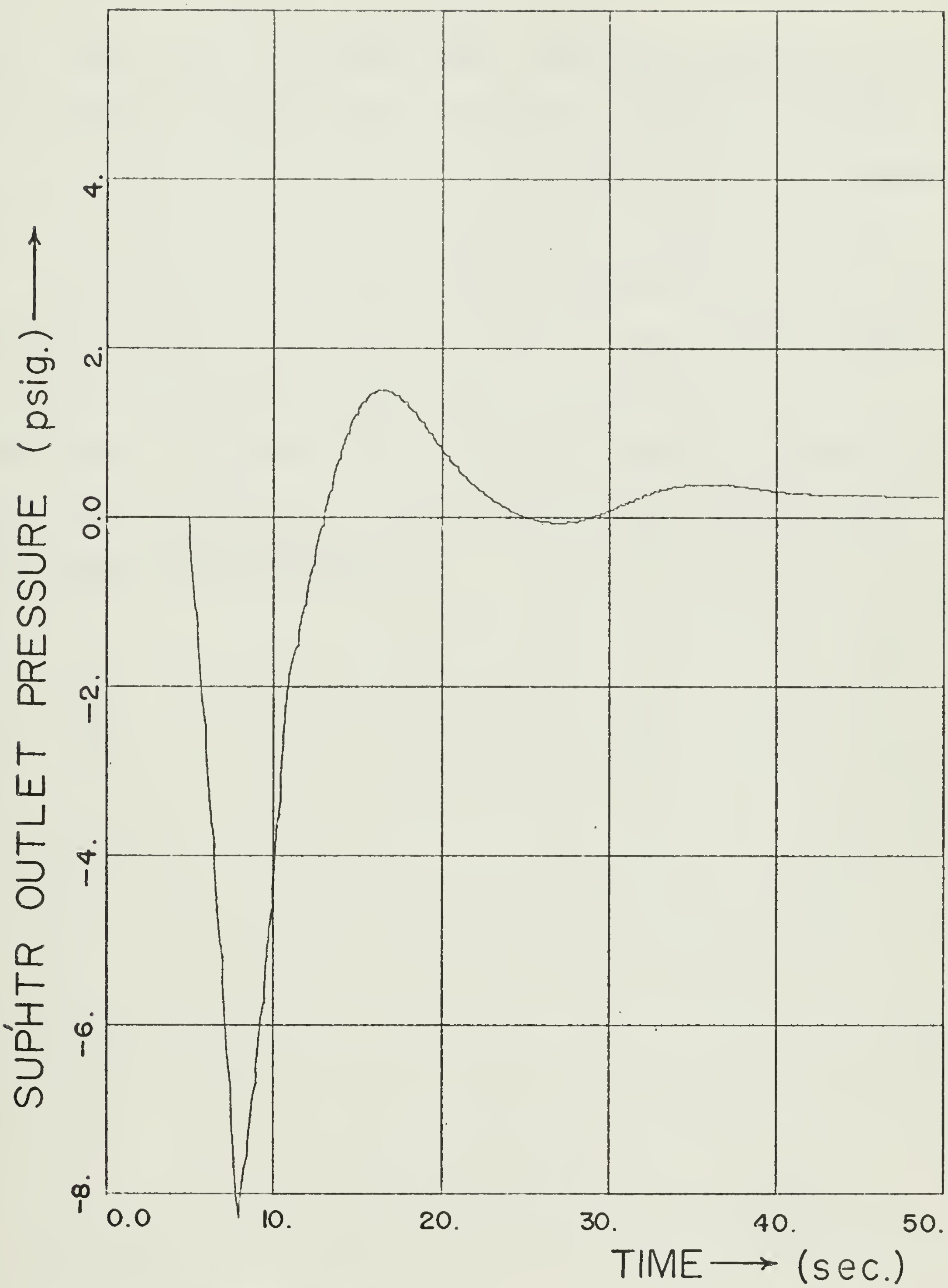

STEAM PRESSURE RESPONSE

FIGURE 10

the effects of varying time delay in the transfer function and of changing one of the gains in the combining relay.

The complete system simulation shows a great time saving over previous all-digital simulations (Refs. 7 and 13). Run time for the DSL program has a 2:1 correspondence with real or problem time. For example, two minutes of simulated boiler operation takes one minute of execution time on the IBM 360/65. While this depended somewhat on the size of the integration step and on the number of variables output, previous simulations were approximately ten times slower by comparison.

Simulation of individual loops was used for transient response testing but the simple programs used are subsets of the overall system program and do not merit further discussion.

III. INDIVIDUAL LOOP ANALYSIS

Since system complexity precluded mass analysis of the entire ACC system at one time, it was decided to separate the system into three minor loops. Obvious choices for analysis were the three major system variables, combustion air, fuel oil and feedwater. Although interaction is present throughout this system, it was ignored for individual loop analysis in the hope that improvements made in each loop would be significant in the whole system. This obviated the massive problem of trying to counter the effects of interaction to yield accurate loop responses.

Several analysis methods exist for determination of controller parameters to permit "optimum" performance. Reference 9 gives an excellent overview of individual component relationships to system performance. Essentially however, due to the demands of shipboard maneuvering, the performance requirement can be easily stated:

> The ACC system must be capable of maintaining stable operating conditions under widely varying load conditions with a given set of machinery (boiler, blowers, valves, etc.) and it must make transitions between operating points in a minimum amount of time.

This requirement is more easily stated than met. The designer is limited to passive components and more precisely, to the relative slow pneumatic-mechanical components which are presently available.

Root-Locus, Bode, and Black-Nichols are among analysis methods presently used in the design and analysis of systems of this type. Reference 14 is the first known to apply the parameter plane technique to the minor control loop of a boiler ACC system.

The parameter plane is a two-parameter method which determines the values of two parameters (α and β) that are required to insure that the characteristic polynomial has roots at a prespecified location in the s-plane. By choosing a suitable line on the s-plane and mapping it through certain algebraic transformations (see Ref. 15) one may obtain a curve on the α-β plane which may be used to select "optimum" values of α and β to give a desired response. In a dynamic system of this type where speed of response was important, three mapping transformations were deemed necessary. Constant-ω_n lines (ω_n is the natural frequency of an approximate second-order system) map from circles of constant radius on the s-plane. Constant-ξ lines (ξ is the damping ratio of the approximate second-order system) map from radial lines on the s-plane. Constant-σ lines map from real root locations on the real axis of the s-plane.

One difficulty encountered was the mathematical representation of pure time delay as present in all three minor loops. It was necessary to have this delay in a mathematical form to determine the characteristic polynomial for each of the loops. The Pade Approximation of transport lag is among the most widely known and was selected (Ref. 16). Varying degrees of approximations were available, ranging from first to twelfth order with accompaning increases in accuracy with higher order. Since the use of the parameter plane was dependent on the determination of the minor-loop characteristic polynomial, a fourth-order approximation was chosen for all transport lag representations. This approximation gave a satisfactory mathematical result and increased the highest power of the characteristic polynomial by four. The general form of the approximation appears in Appendix C along with the actual equation used in each of the loops.

Since hand calculation of mathematical mapping transformations would be prohibitive, a computer program, developed at the Naval Postgraduate School under the direction of Dr. George J. Thaler, was used for parameter plane graphical results.

Algebraic manipulation of transfer functions was also performed on the computer. FORMAC (FOrmula MAnipulation Compiler), an algebraic manipulation language (see Refs. 17 and 18) was extremely useful for development of loop characteristic polynomials and should prove useful to the control engineer faced with tedious algebraic manipulation.

All graphs presented in this thesis are the result of computer runs and were drawn directly by a CalComp plotter at the computer facility at the Naval Postgraduate School.

A. AIR FLOW LOOP ANALYSIS

The air flow control loop is a fairly typical feedback system and is shown in Fig. 11 which is a simplified version of Fig. 1(d). The resulting loop characteristic polynomial for the closed loop system is of fifteenth order and is shown in Appendix C.

The parameter plane approach was used and the selected variable parameters were the proportional and integral gains of the air flow controller. These variables were thought to be the most easily accessible and most easily adjusted. The proportional gain in the original system had been set at 1.67 and the integral gain at 0.024. For parameter plane purposes, integral gain was designated beta (β) and proportional gain alpha (α). The original system operating point is marked with an X on Fig. 12, the air flow loop parameter plane.

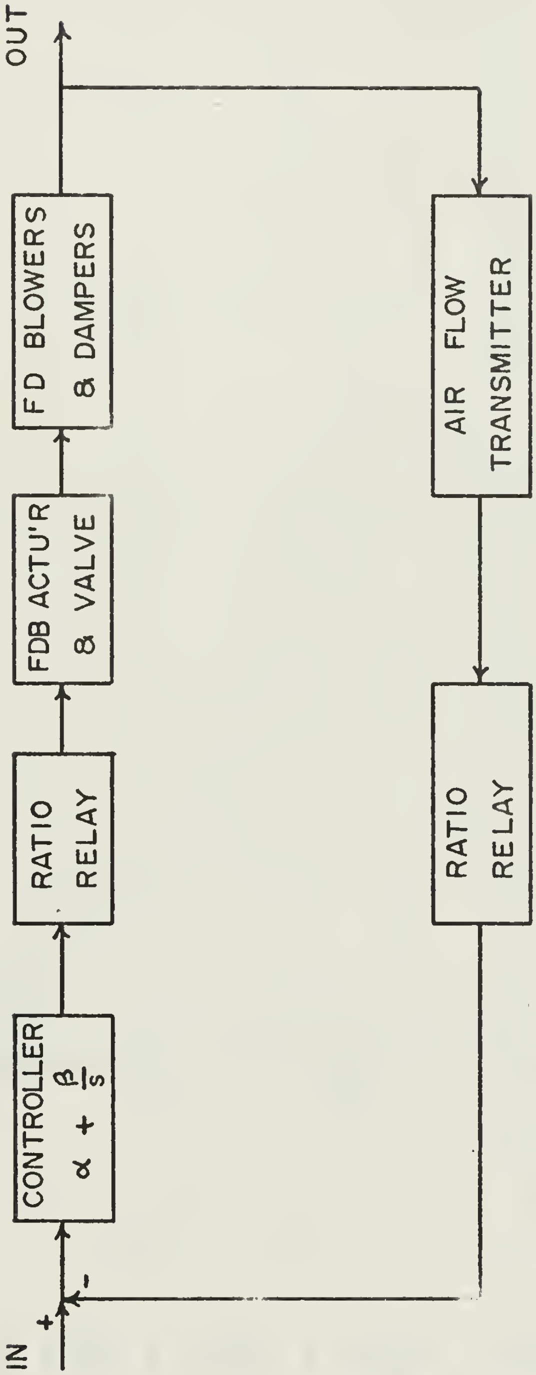

SIMPLIFIED AIR FLOW CONTROL LOOP DIAGRAM

FIGURE 11

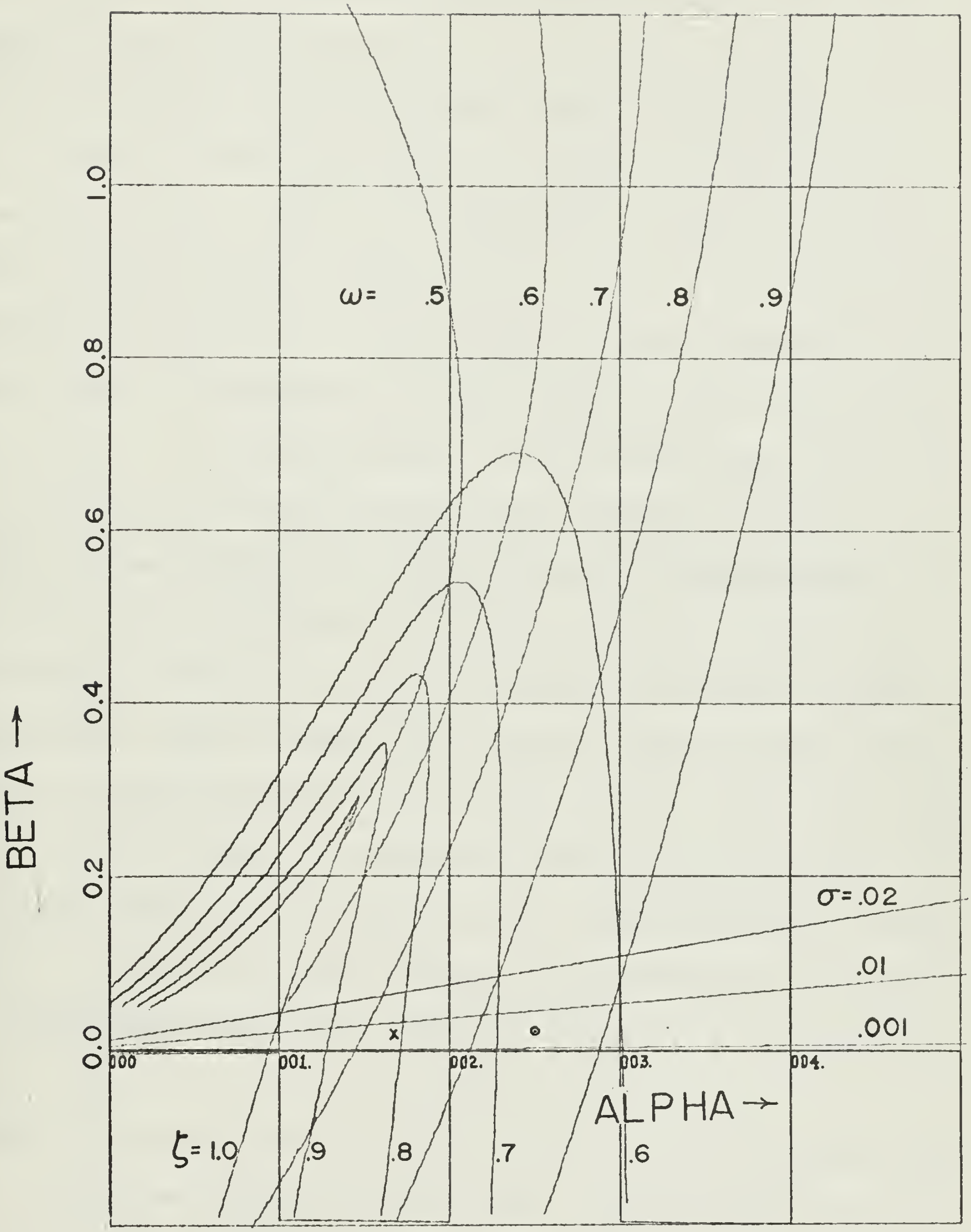

AIRFLOW LOOP PARAMETER PLANE

FIGURE 12

In order to demonstrate the accuracy and validity of the parameter plane, several runs of transient response were made using a simple DSL simulation of the system in Fig. 11.

It was decided to hold one parameter constant while varying the other in order to dramatize the effect of moving in a straight line on the parameter plane. In Fig. 13, alpha was held constant at 1.67 while beta was allowed to take on values of 0.01, 0.024, 0.1, 0.2. Note that the second curve; $\alpha = 1.67$, $\beta = 0.024$ is the transient response of the original system. Input for all transient response tests in this section was a unit step. Since motion along a line of constant alpha constituted motion along a line of nearly constant zeta (damping), no increase in response time was anticipated. Figure 13 bears out this expectation. Motion along a line of constant beta however, was nearly perpendicular to the lines of constant zeta, and rapid changes in transient response were expected. Figure 14 depicts such transient response; holding beta constant at 0.024, alpha was allowed to take on values of 1.0, 1.67, 2.0, 2.5, 3.0, and 3.5. Again, for comparison, the $\alpha = 1.67$, $\beta = 0.024$ curve is the response of the original system. At $\alpha = 1.0$, which is nearly on the $\zeta = 1.0$ curve, the system exhibited the characteristic response of a critically damped second-order system as predicted on the parameter plane.

While no one point could be selected as the "optimum" operating point, several qualitative statements could be made. It is obvious from Fig. 13 that beta, at least within the range of investigation, had little effect on the response time of the system. On the parameter plane, if alpha is allowed to remain constant, increasing beta will move the operating point

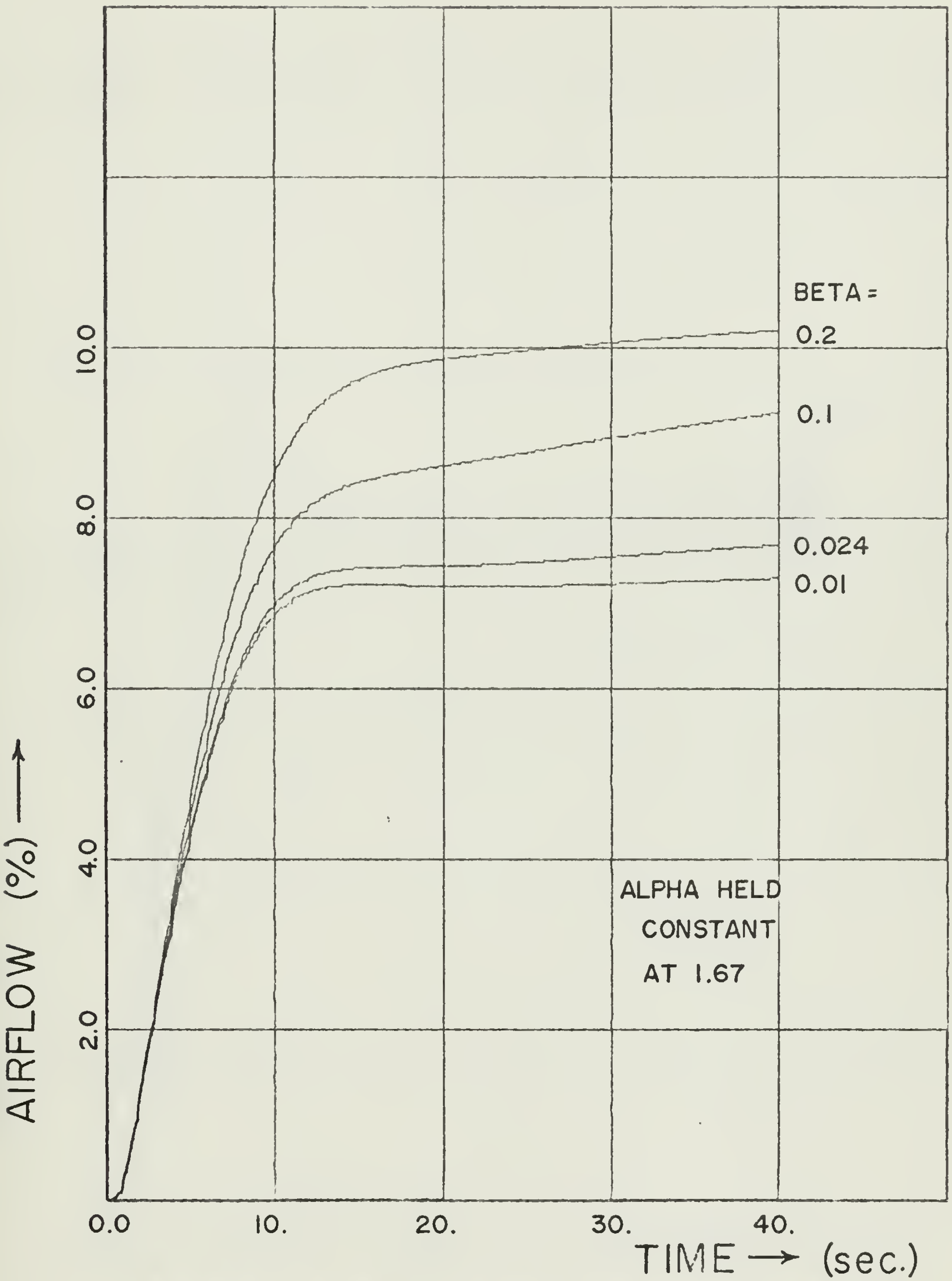

AIRFLOW LOOP TRANSIENT RESPONSE

FIGURE 13

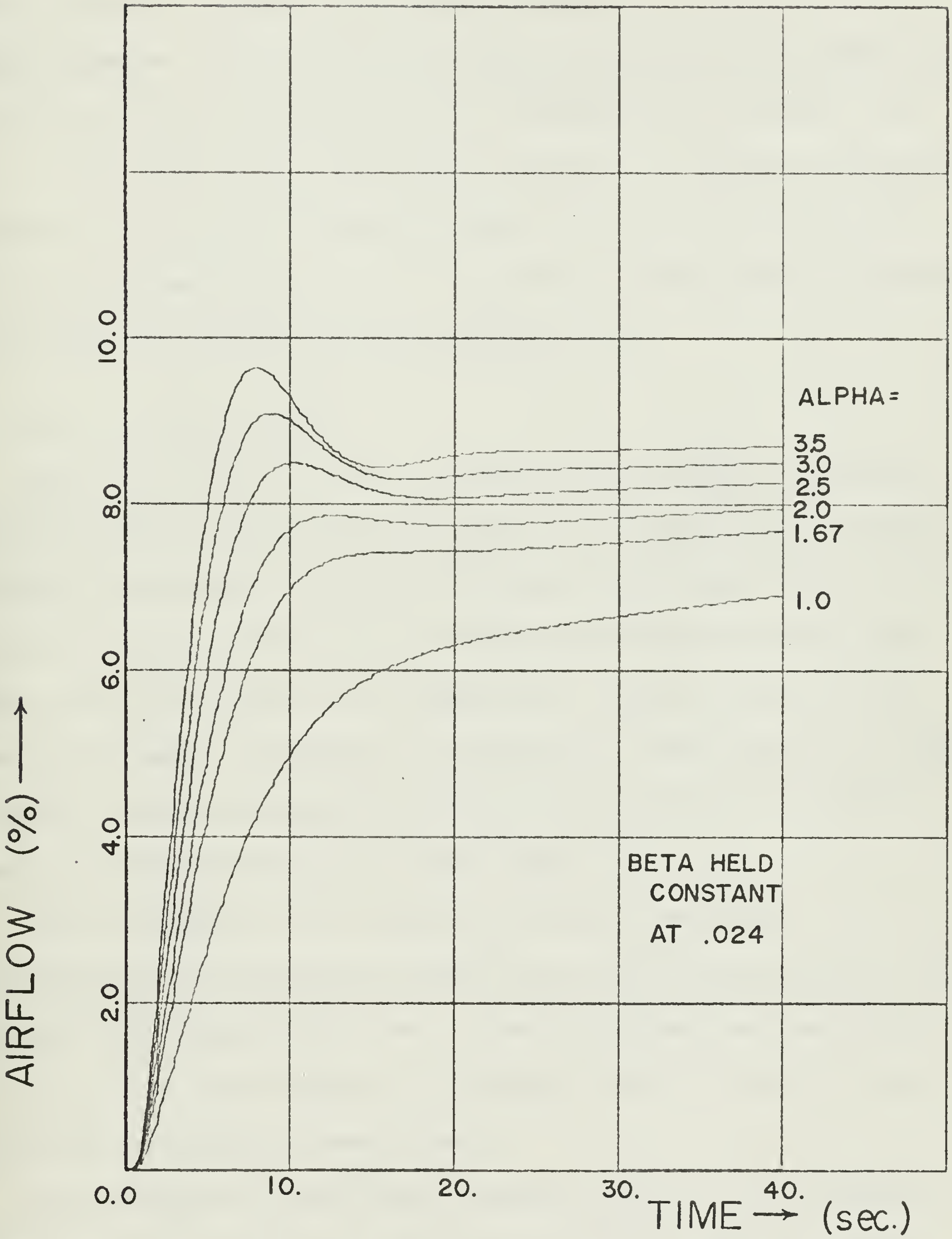

AIRFLOW LOOP TRANSIENT RESPONSE

FIGURE 14

along a nearly constant-ξ path until beta exceeds about 0.38 at which time ξ begins to decrease. The effect of variation of alpha was more readily apparent. Rise times were considerably improved with alpha values of 2.0 and 2.5 while overshoot was not considered to be excessive (Fig. 14). On the basis of this qualitative analysis, the "improved" operating point of $\alpha = 2.5$, $\beta = 0.024$ was selected. This point is marked with a Θ on the parameter plane, Fig. 12. Section IV demonstrates the response of the entire system with this new operating point.

B. OIL FLOW LOOP ANALYSIS

Since the position of the low-pressure signal selector determines the configuration of the oil flow control loop, a choice had to be made. During an increasing load, the air flow system lags behind and it is the output of this loop (PQR in Fig. 2) which becomes demand for oil flow. Hence, the air flow loop is an integral part of the oil flow loop when load is increasing. Increasing load conditions, before the air flow loop responds, the demand signal (PM) from the steam pressure controller is lower and therefore becomes the demand signal.

It was decided to try to improve the loop in the simpler of the two configurations since combination would have led to a characteristic polynomial of the twenty-eighth order. It was hoped that improvements made to the air flow loop would help the response when this loop was a part of the oil loop during a load increase.

The simplified oil loop diagram appears in Fig. 15. The resulting characteristic polynomial of thirteenth order was determined using the FORMAC program and is found in Appendix C.

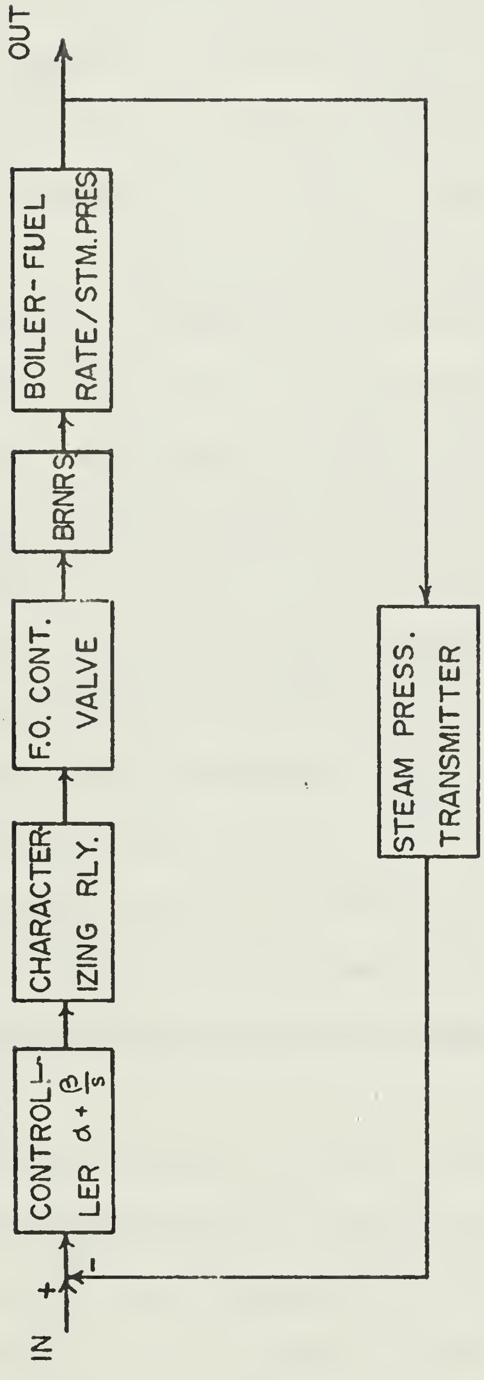

SIMPLIFIED OIL FLOW
CONTROL LOOP DIAGRAM

FIGURE 15

As was done with the air flow loop, the parameter plane was plotted. This time, the variables of the steam pressure controller were used for parameters. Alpha was chosen to be the proportional gain and beta the integral gain. The resulting graph is shown in Fig. 16.

Several points on the parameter plane were chosen for DSL simulation testing. With alpha held constant at 6.67, beta was allowed to take on the values 0.001, 0.014, 0.1, and 1.0. These curves are shown in Fig. 17. Note that $\alpha = 6.67$, $\beta = 0.014$ is the operating point of the original system as marked on the parameter plane with an X. Three curves are very close together, the result of moving vertically along a nearly constant-line as before. The fourth curve, $\beta = 1.0$, represents a point off the parameter plane but close inspection will reveal that the value of has been drastically reduced for this operating point. The transient response bears out this hypothesis, demonstrated by the large overshoot of a characteristically underdamped system. Again, with beta held constant at 0.014, alpha was allowed to vary from 4.0 to 10.0. These response curves are shown in Fig. 18. The critical damping ratio, $\xi = 1.0$, was not approached with the oil loop but extrapolation of the curves of Fig. 16 to an alpha of 2.5 will lead to the expected response. The original system response is shown for comparison as before ($\alpha = 6.67$, $\beta = 0.014$).

Again, it was difficult to make a quantitative analysis to determine an "optimum" operating point. It must be remembered that the results were valid only for an increasing load, the loop being considerably different during a decreasing load. A new operating point was selected on a qualitative basis at $\alpha = 8.0$, $\beta = 0.014$ and this point is marked with a $\odot$ on the parameter plane.

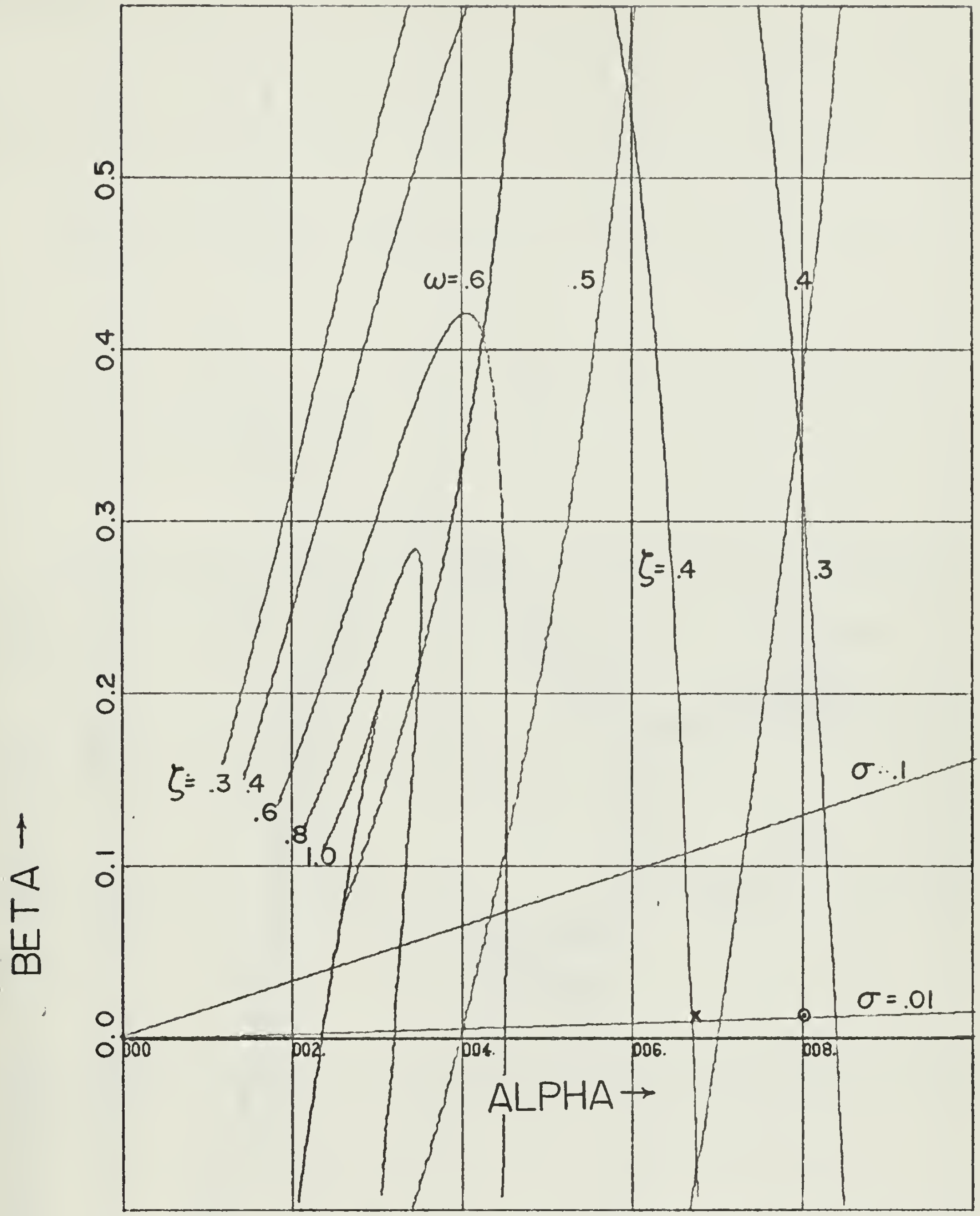

OILFLOW LOOP PARAMETER PLANE

FIGURE 16

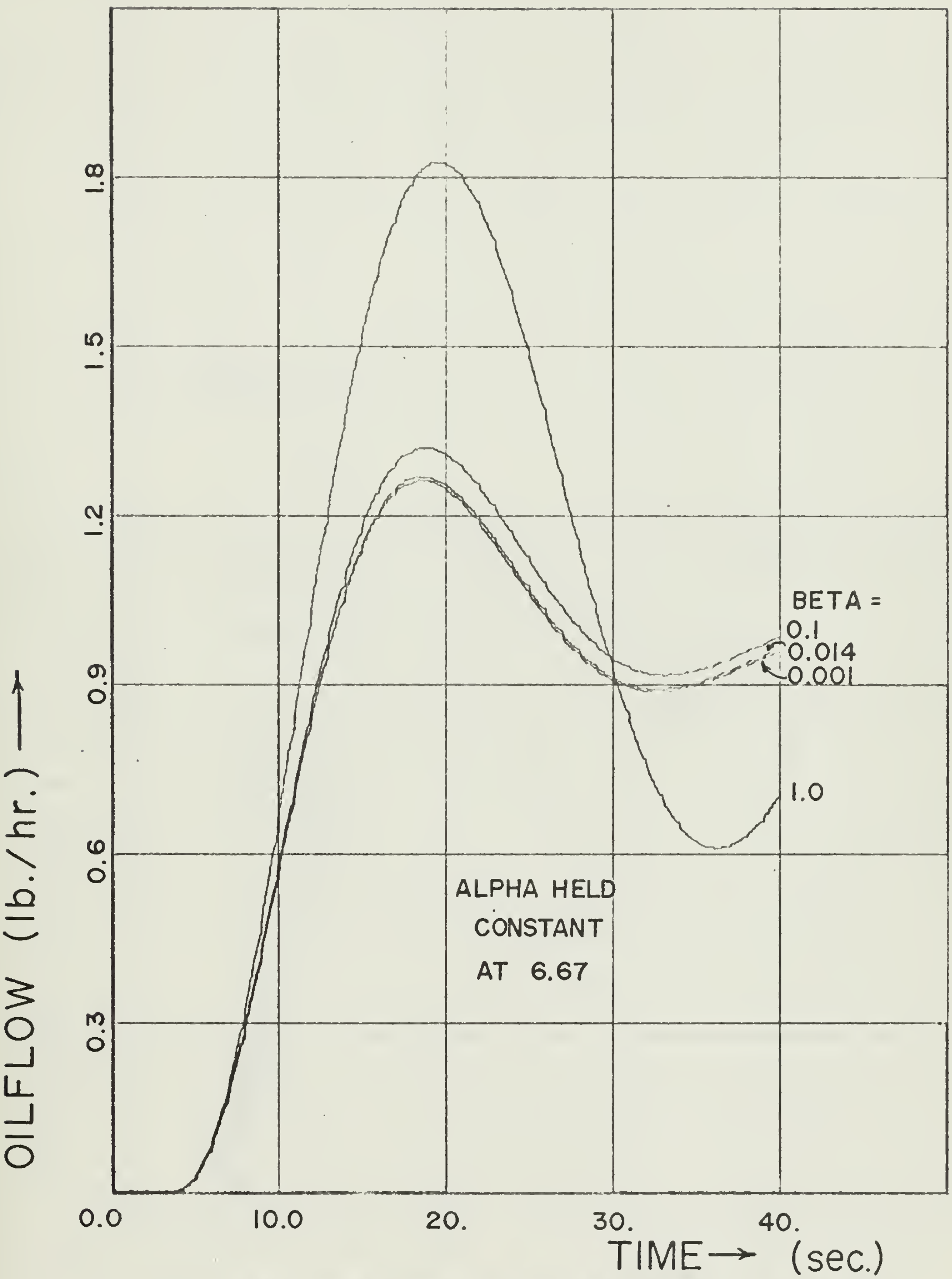

OILFLOW LOOP TRANSIENT
RESPONSE

FIGURE 17

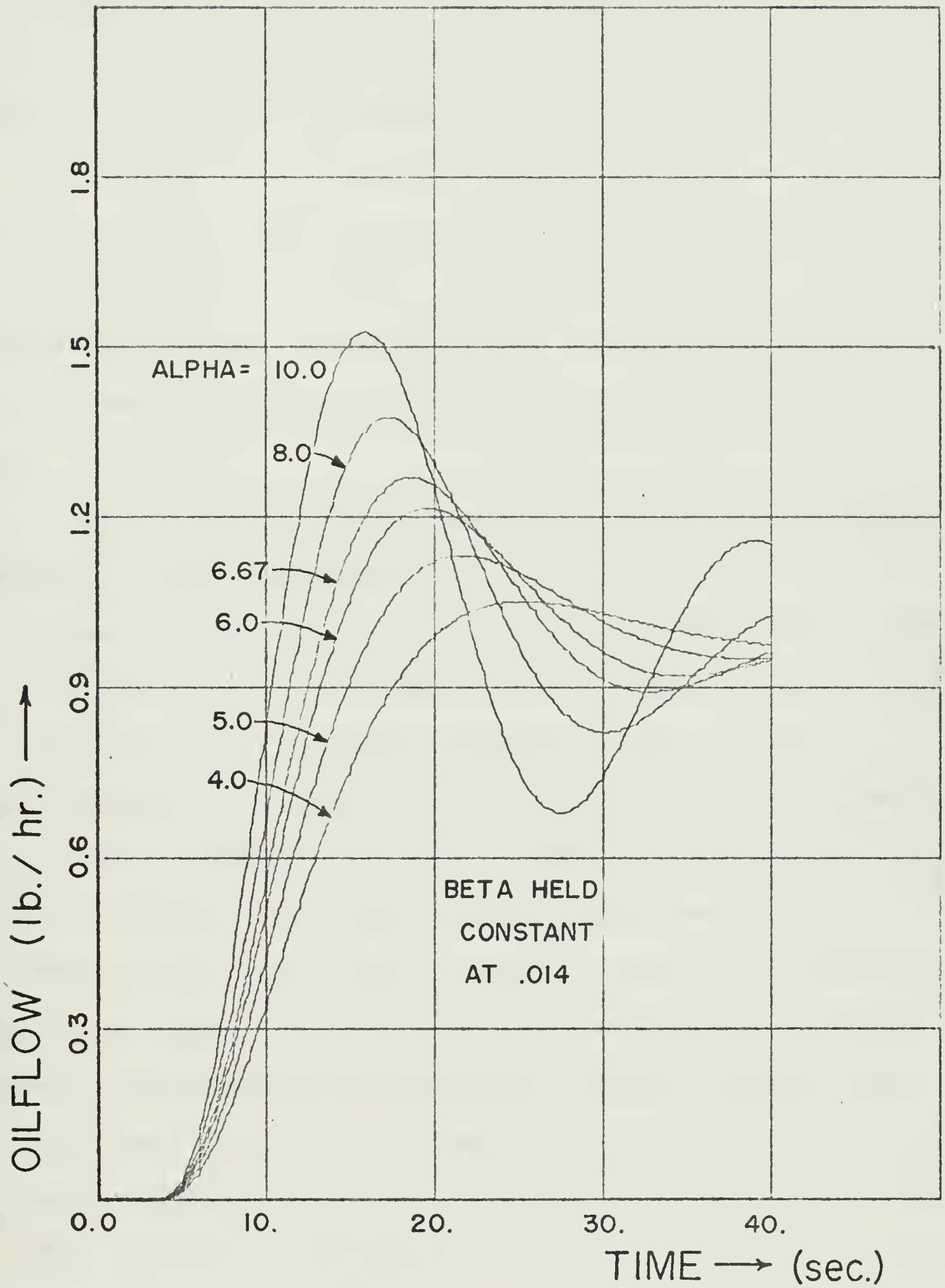

OILFLOW LOOP TRANSIENT RESPONSE

FIGURE 18

C. WATER FLOW LOOP ANALYSIS

The water flow control loop is shown in simplified form in Fig. 19. In order to maintain true closed-loop action for the resulting analysis, the loop had to be reduced as shown from the loop in Fig. 1(c).

The integration in the feedback circuit made the system characteristically type one. Hence, response to a step input contained no steady-state error, and for unity input, unity output was obtained. As was found in the original system response (see Fig. 6) the response of the water loop left something to be desired as far as oscillatory action was concerned.

The loop characteristic polynomial was determined using the FORMAC program and is given in Appendix C.

Choices for parameter plane variables were somewhat limited in this case. Since there was not a proportional plus integral controller present as in the oil and air loops, other variables had to be selected. A simple inspection of the loop of Fig. 19 revealed two likely parameters. The gain of the thermostat (2.37) was selected as alpha and the gain of one of the combining relay factors (0.014) was selected as beta.

Effects of the rather large (0.45 sec) time delay were questioned in Ref. 2, so several transient response runs were made of the entire system and results are shown and discussed in the next section, IV.D.

The parameter plane plot is shown in Fig. 20. Note that the operating point of the original system, $\alpha = 2.37$, $\beta = 0.147$, which is marked with an X, lies outside of the $\xi = 1.0$ curve. This indicated that the dominant roots were not complex, but real. A constant-sigma, or real root, line, $\sigma = 0.52$, passes through the operating point. This indicated that one

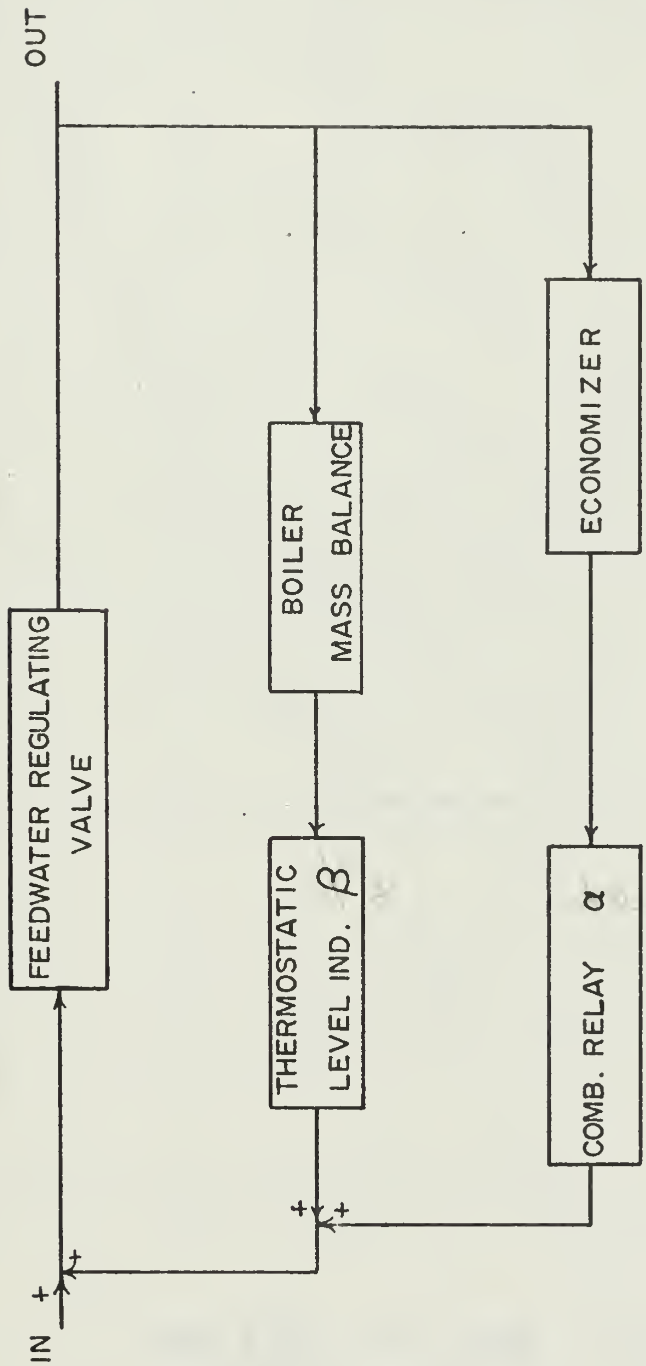

SIMPLIFIED WATER FLOW CONTROL LOOP

FIGURE 19

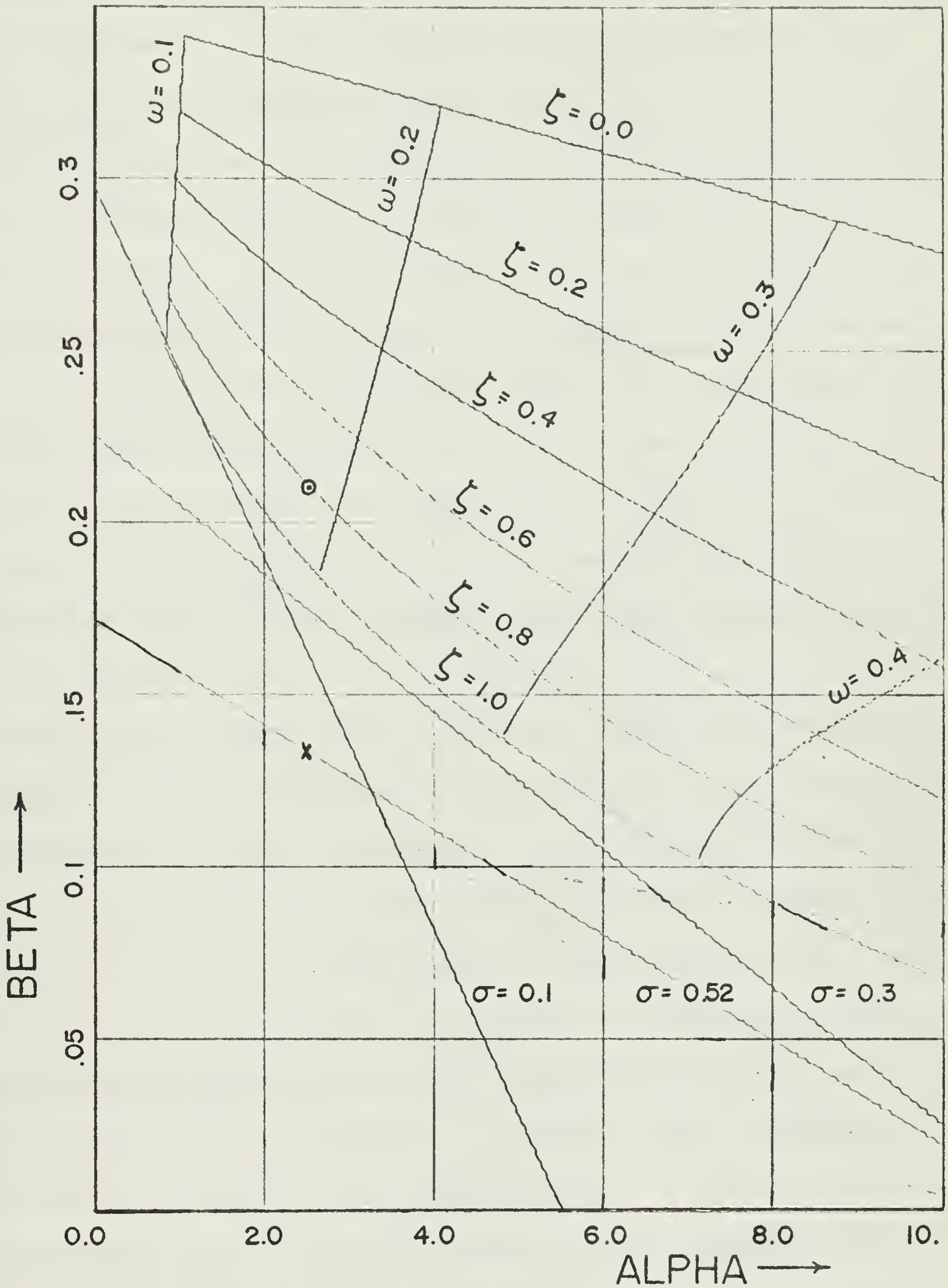

WATER FLOW LOOP
PARAMETER PLANE

FIGURE 20

of the dominant roots lies at $\sigma = -0.52$ on the root locus plot. In order to verify this result, a computerized root-locus plotting program, also developed at the Naval Postgraduate School, was used.

Since the root locus is a one-parameter method, it was decided to fix alpha (thermostat gain) at 2.37 and more vertically on the parameter plane along a straight line and vary beta from 0.1 to 1.0. Since $\beta = 1.0$ appears to be above the $\xi = 0.0$ curve on the parameter plane, it was expected that the roots would move into the right half of the s-plane on the root locus, indicating instability of the loop. It was further expected that when the constant-alpha line crossed the $\xi = 1.0$ line on the parameter plane, that the real roots on the root locus would come together on the real axis and reach their breakaway point. The resulting root-locus plot is shown in Fig. 21 and it was found to fully verify the results expected from parameter plane predictions. Additional roots which do not appear on this plot due to scale limitations were at $-12.873 \pm j3.8547$ and $-9.3502 \pm j11.811$. System zeros were at 0.0, $12.872 \pm j3.8544$ and $9.3502 \pm j11.811$. As expected, the real roots which appeared at -1.2176 and -0.039322 when beta had the value 0.1, moved together as beta increased. The left hand root was at -0.52 at $\beta = 0.147$ as predicted by the parameter plane and both real roots came together at $\beta = 0.192$ ($\xi = 1.0$). The roots then became complex and moved toward the right-half plane, crossing over at $\beta = 0.333$ as predicted by the parameter plane.

It was expected that closed-loop response could be improved by increasing beta, as predicted by the increase in damping ratio subsequently provided. The original system response to a step input is shown in Fig.22 with $\beta = 0.147$. Several other values of beta were tested and these results appear in Fig. 23. To verify both root-locus and parameter plane

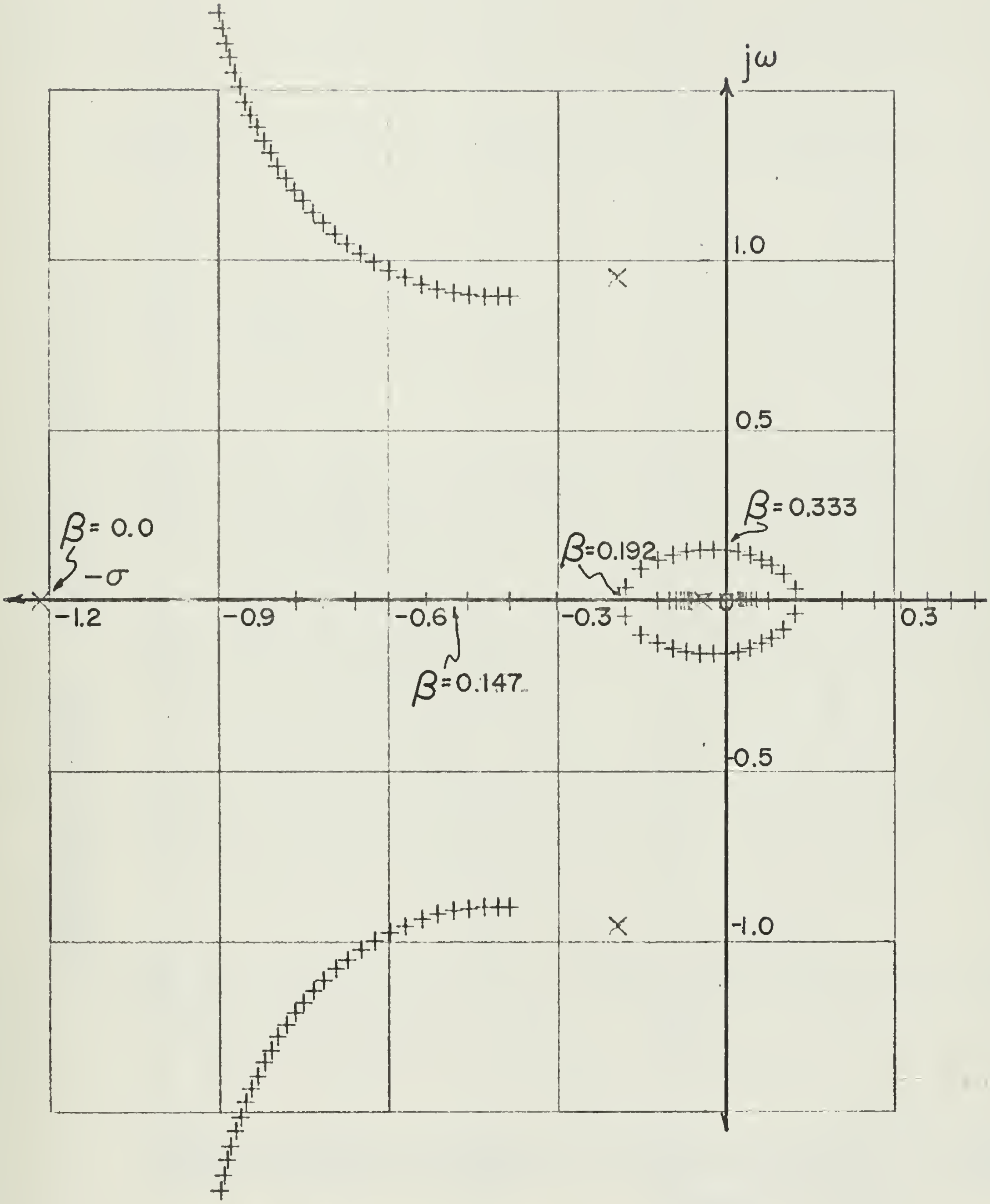

WATER FLOW LOOP
ROOT LOCUS

FIGURE 21

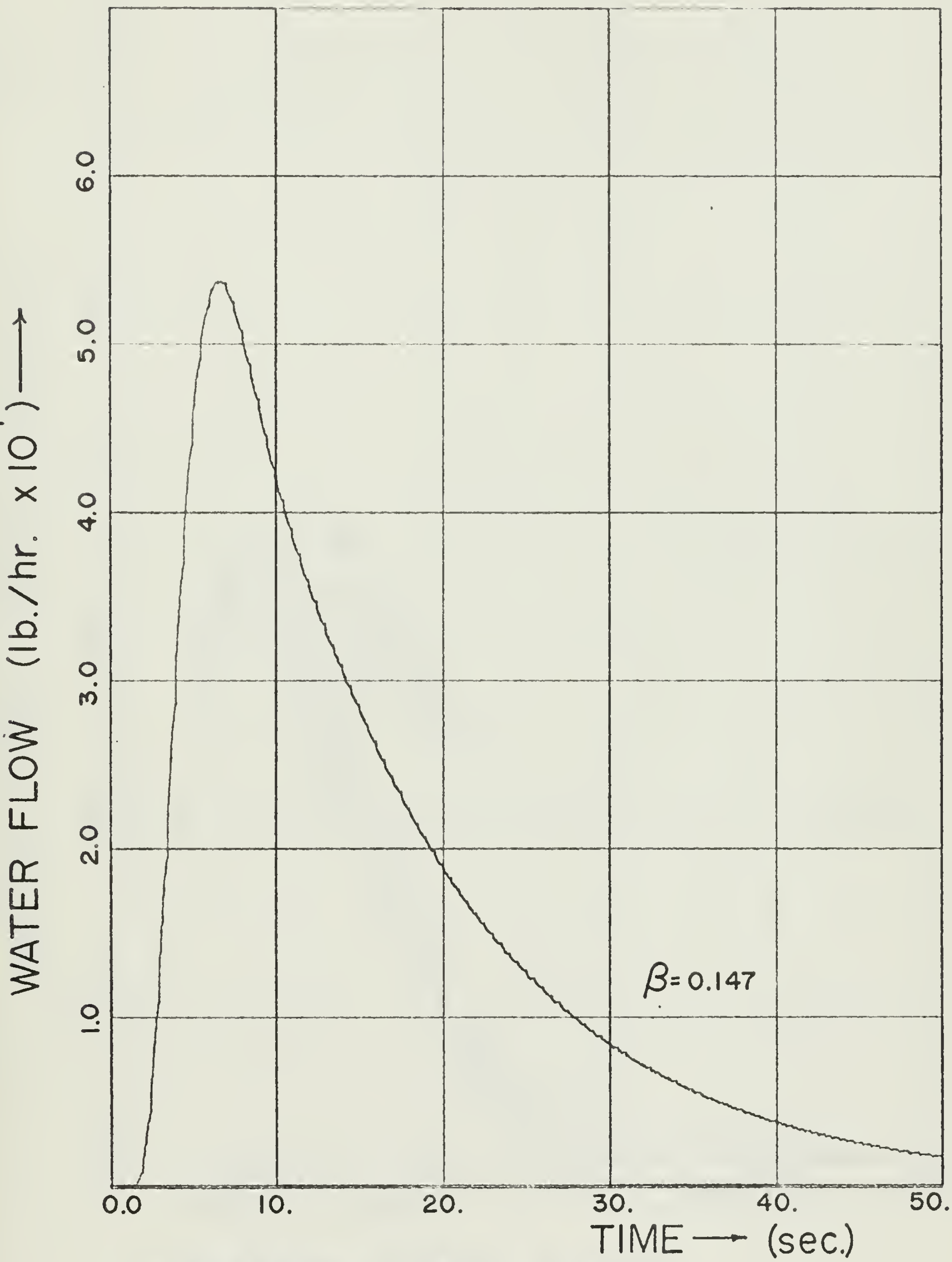

WATER FLOW LOOP
TRANSIENT RESPONSE

FIGURE 22

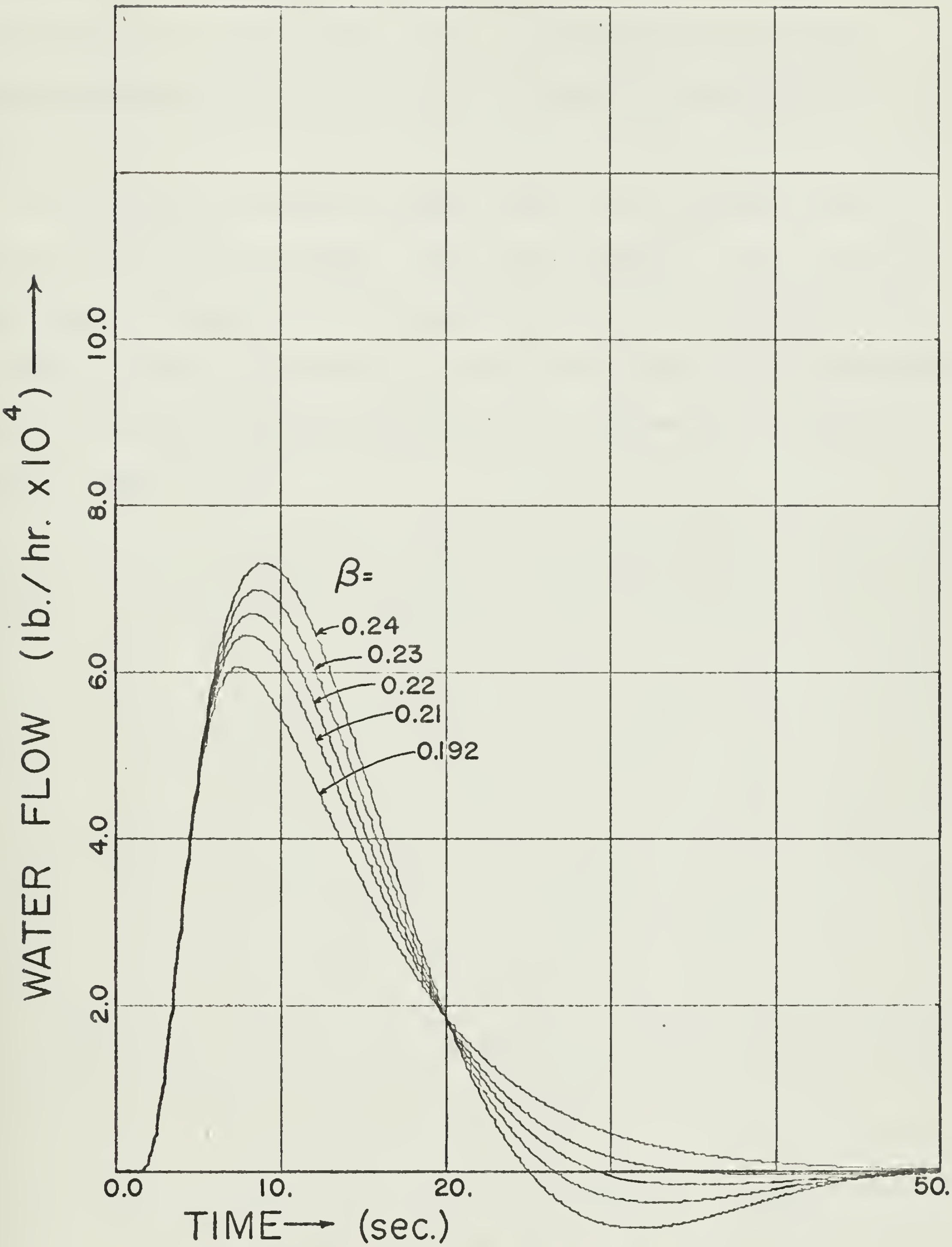

WATER FLOW LOOP
TRANSIENT RESPONSE

FIGURE 23

predictions of instability, a test with $\beta = 0.333$ was run and the resulting response is shown in Fig. 24. An almost undamped system was evident, characteristic of a system on the verge of instability with imaginary roots.

On the basis of transient response tests, a new operating point of $\alpha = 2.37$, $\beta = 0.21$ was chosen. Since the thermostatic level indicator transfer function information was somewhat doubtful as indicated in Ref. 2, it was felt that this parameter could not be varied with any meaningful results. The newly selected operating point is marked with a ⊙ on the parameter plane, Fig. 20.

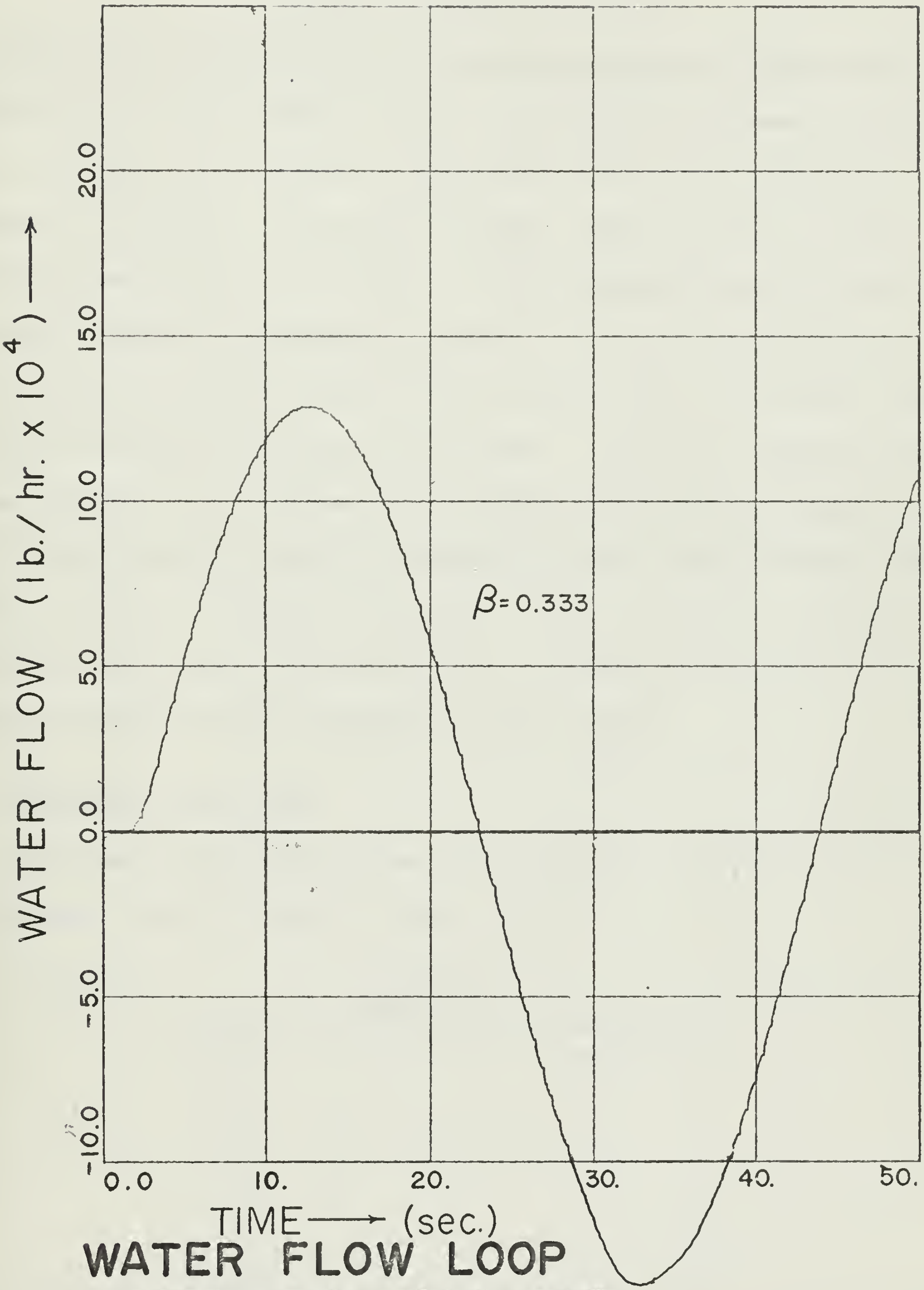

WATER FLOW LOOP
TRANSIENT RESPONSE

FIGURE 24

IV. SYSTEM RESPONSE TO VARIATIONS

Using the complete simulation program once again, the system was subjected to the input shown in Fig. 5. This time, the parameters used on the parameter plane graphs of the previous section were varied to observe their effects on the overall system. Note that while a total of six parameters were investigated, it was recommended that only three of them be changed for "optimum" response. In the air and oil loops, the proportional gain of a controller was varied while in the water loop, one of the combining relay gains was changed. For ease of identification, these variables were subsequently called AIR, OIL, and WAT, respectively.

It was decided to vary one parameter at a time first, to observe the effects, if any, of variable interaction. After this was accomplished, all three were changed in accordance with recommendations made in the previous section and the responses were again plotted.

A. VARIATIONS IN AIR LOOP

Table One indicates the values of the variable parameter AIR for the response curves of Figs. 25 through 29.

TABLE ONE

AIR	CURVE #
1.0	1
1.67	2*
2.0	3
2.5	4
3.0	5
3.5	6

*Original Operating Point

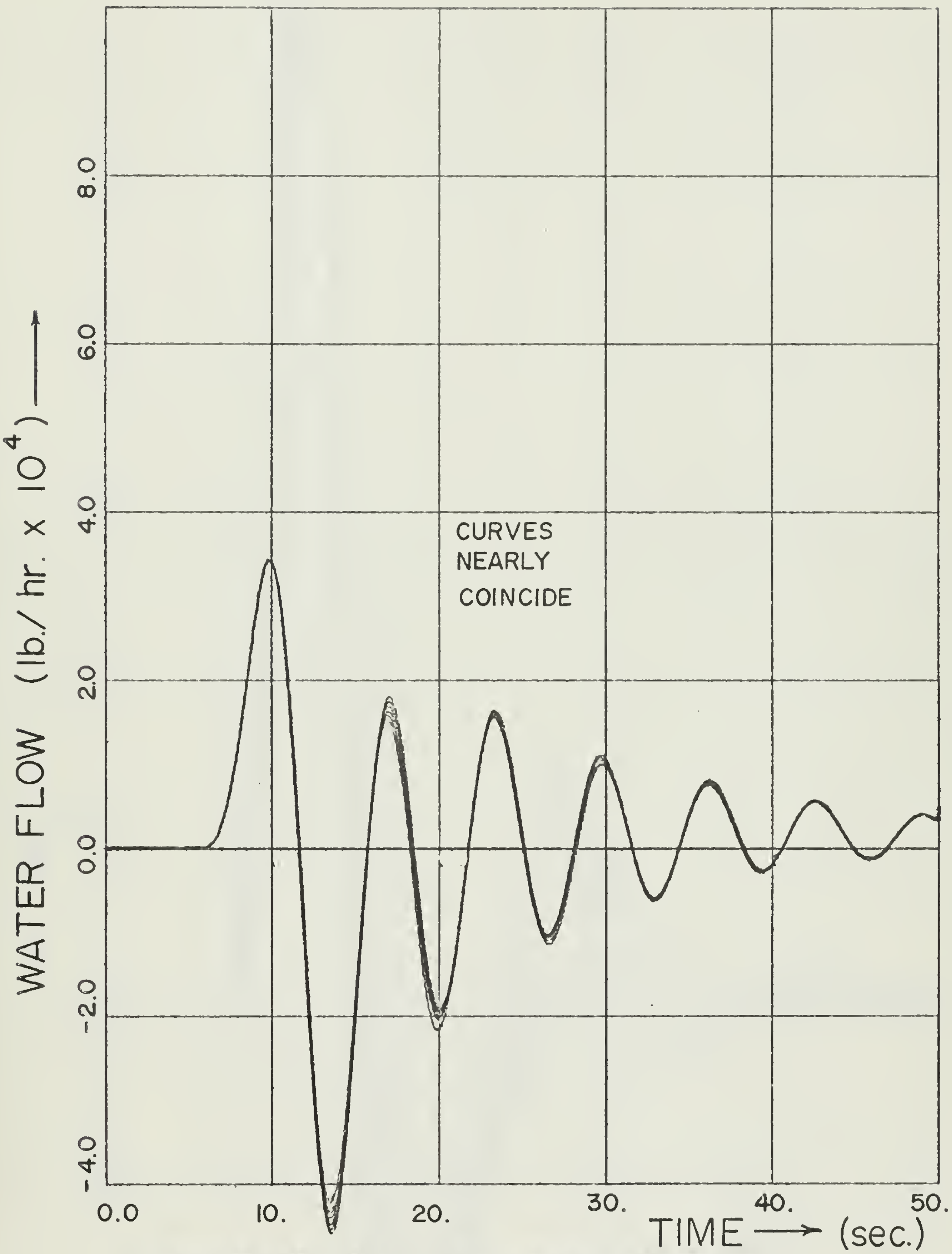

WATER FLOW RESPONSE TO AIR VARIATIONS

FIGURE 25

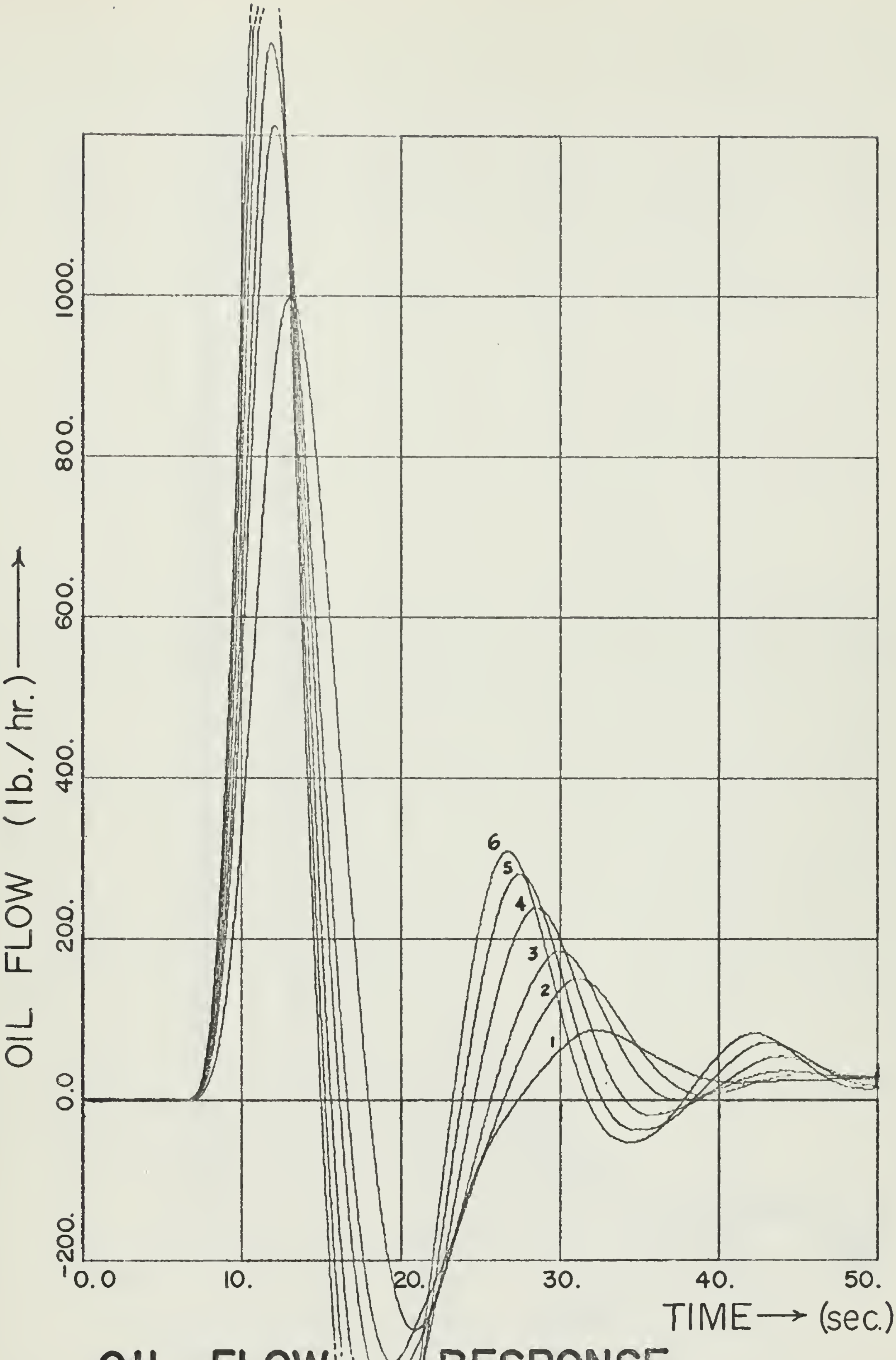

OIL FLOW RESPONSE TO AIR VARIATIONS

FIGURE 26

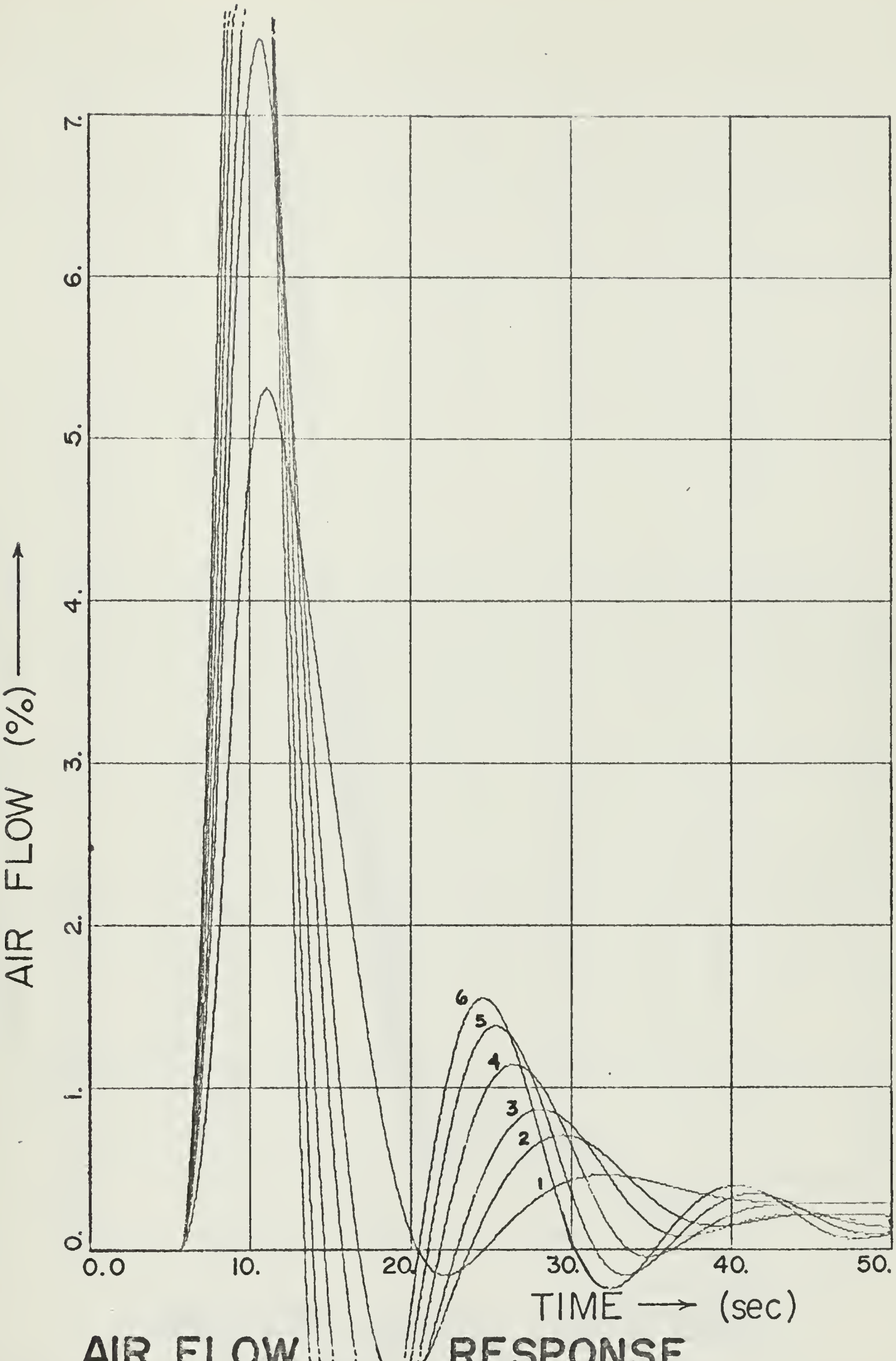

AIR FLOW RESPONSE
TO AIR VARIATIONS

FIGURE 27

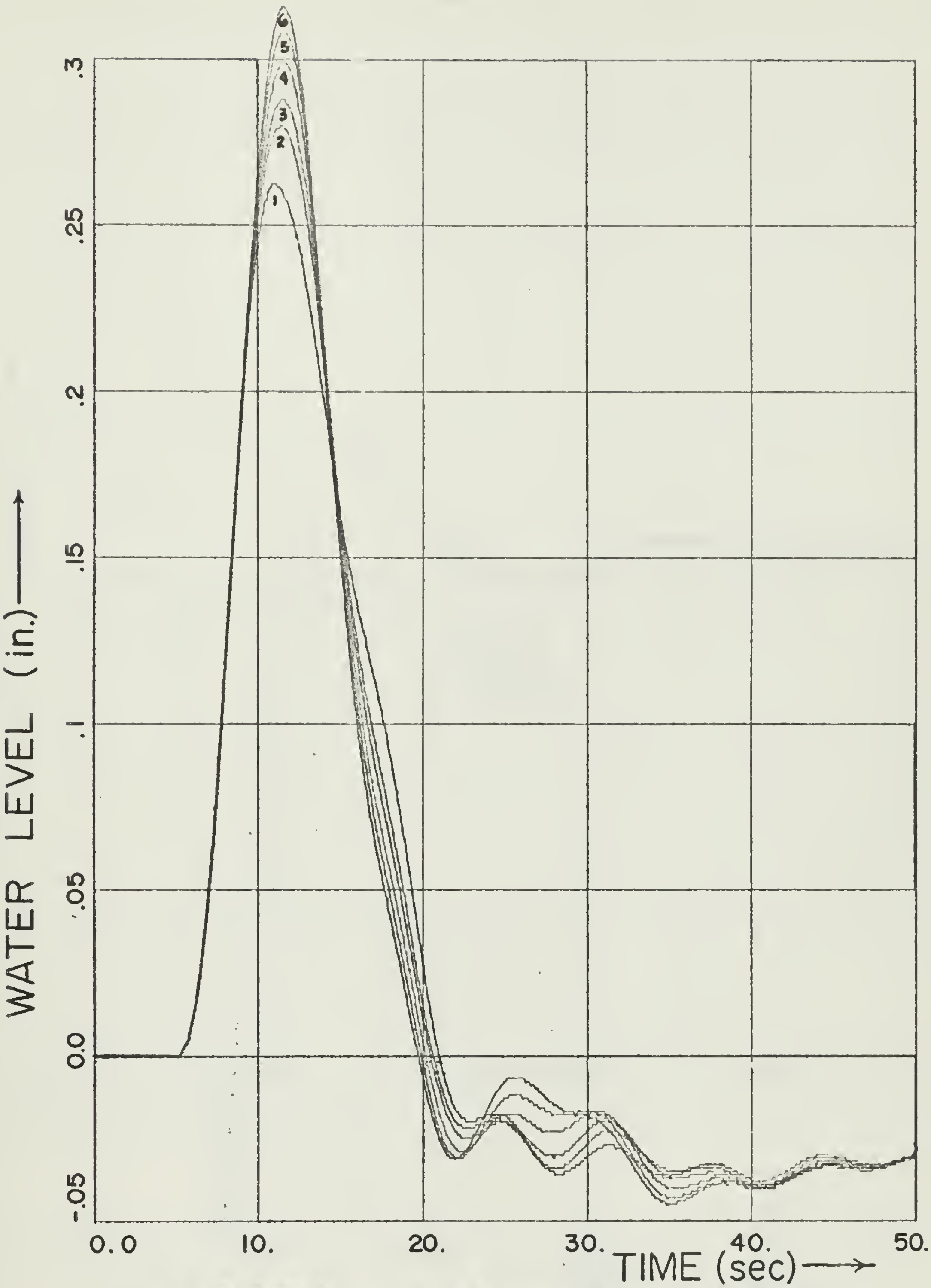

WATER LEVEL RESPONSE
TO AIR VARIATIONS

FIGURE 28

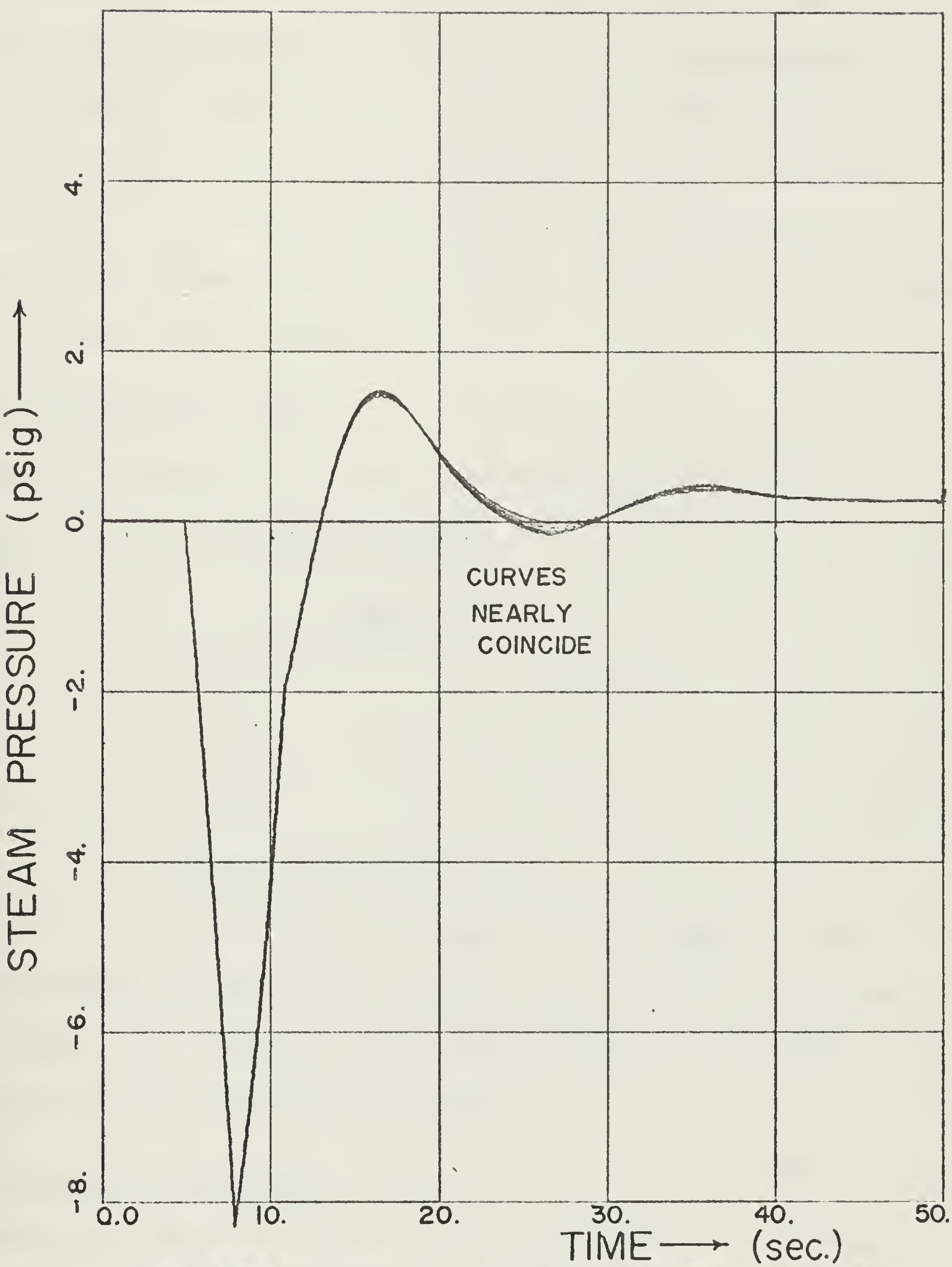

STEAM PRESSURE RESPONSE TO AIR VARIATIONS

FIGURE 29

Curve #4 was the result of using the operating point recommended from parameter plane predictions. It was a good deal faster than the original system as evidenced on the oil and air flow responses, Figs. 26 and 27. It made little difference in the two most important variables, steam pressure and water level, Figs. 28 and 29. Note the near absence of coupling of the variation of AIR to water flow as evidenced in Fig. 25, the water flow response. The curves nearly coincided and were indistinguishable as to which curve was which.

B. VARIATIONS IN OIL LOOP

Table Two indicates the value of the variable parameter OIL, for the response curves of Fig. 30 through 34.

TABLE TWO

OIL	CURVE #
4.0	1
5.0	2
6.67	3*

*Original Operating Point

As was evidenced from the five response curves, Figs. 30 through 34, any proportional gain (OIL) less than 6.67 slowed the system responses considerably. This indicated that an increased gain, as predicted by the parameter plane analysis, was in order.

C. VARIATIONS IN WATER LOOP

Table Three shows the values of the parameter WAT for the curves depicted in Figs. 35 through 39.

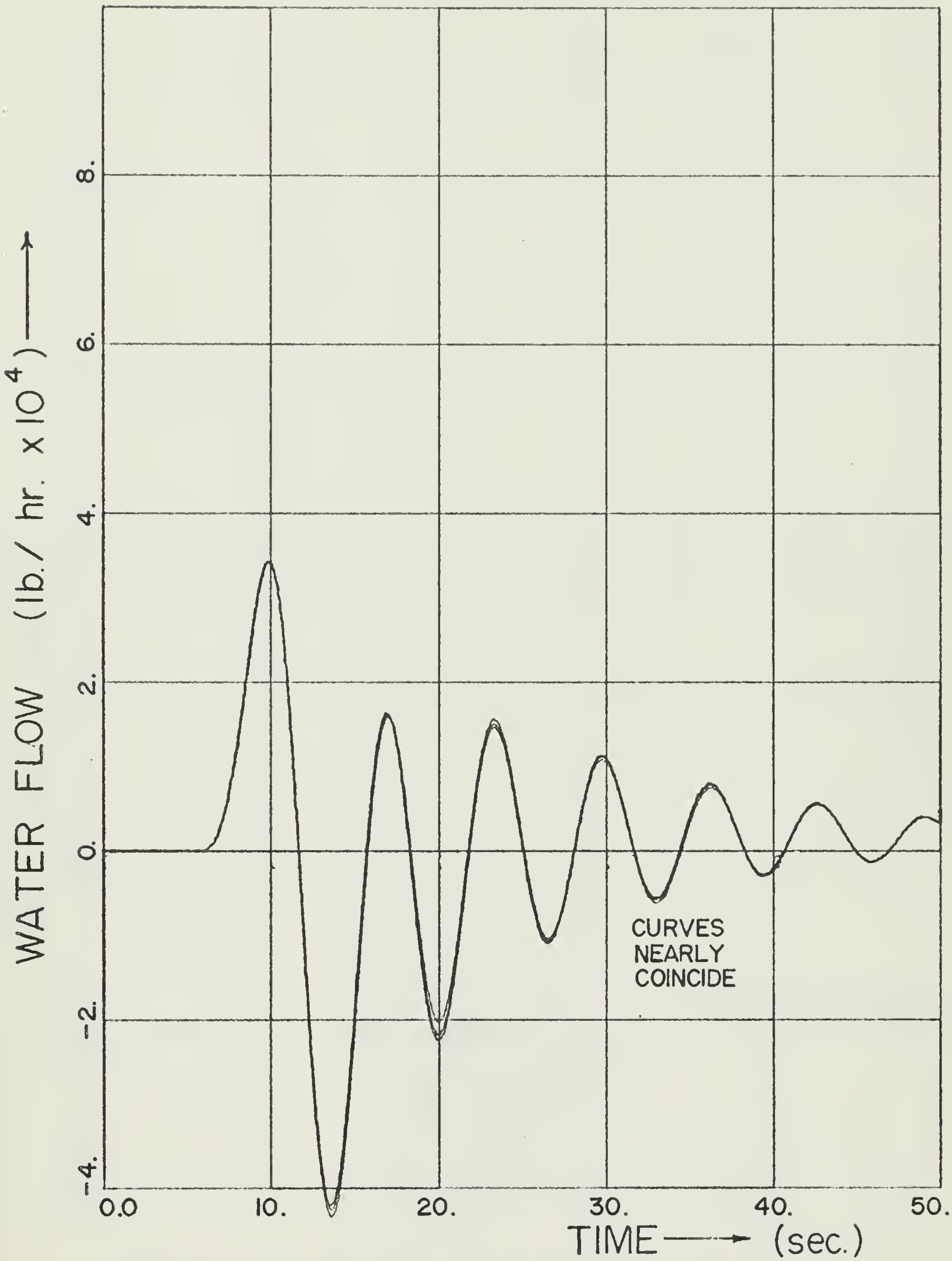

WATER FLOW RESPONSE
TO OIL VARIATIONS

FIGURE 30

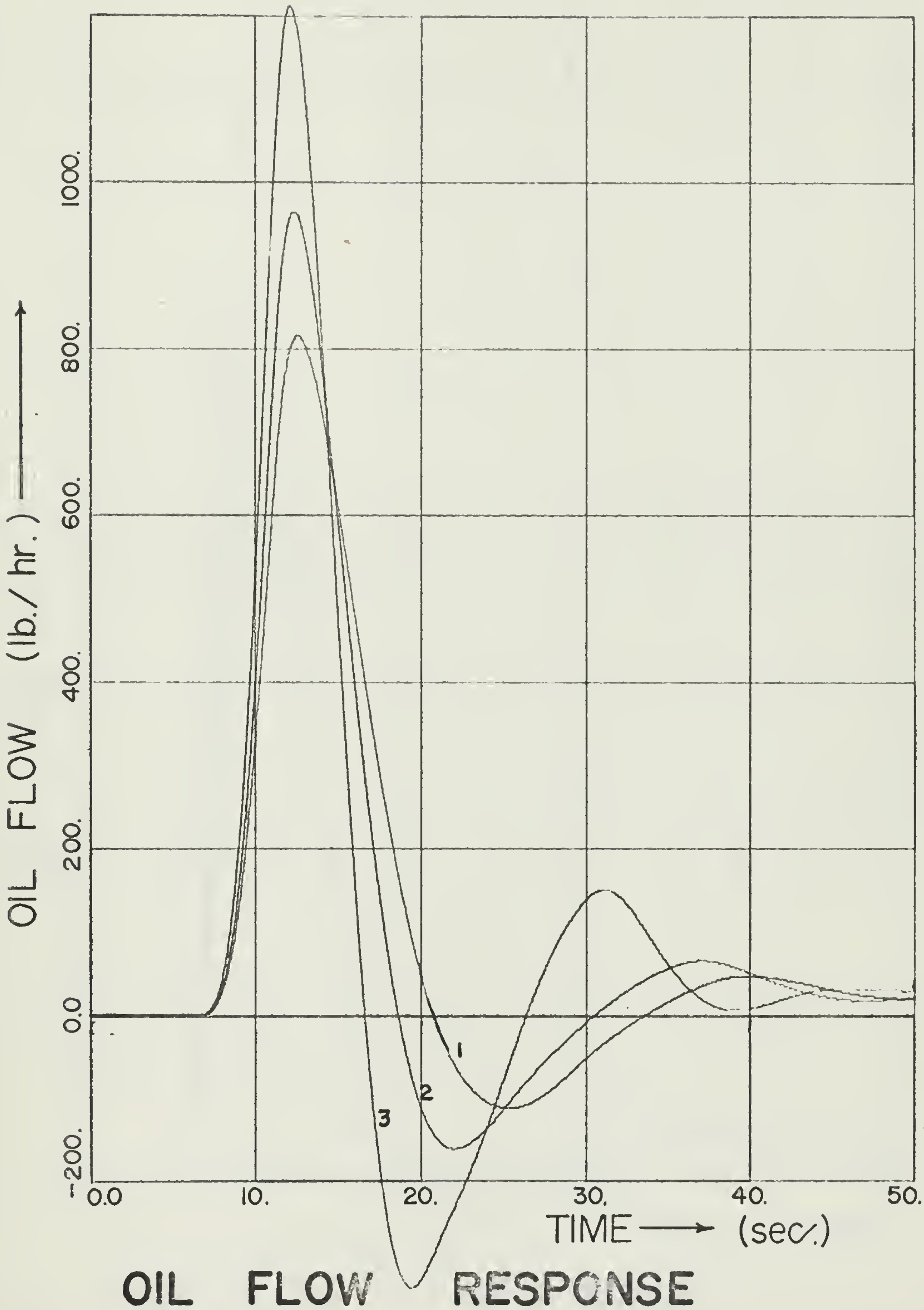

OIL FLOW RESPONSE TO OIL VARIATIONS

FIGURE 31

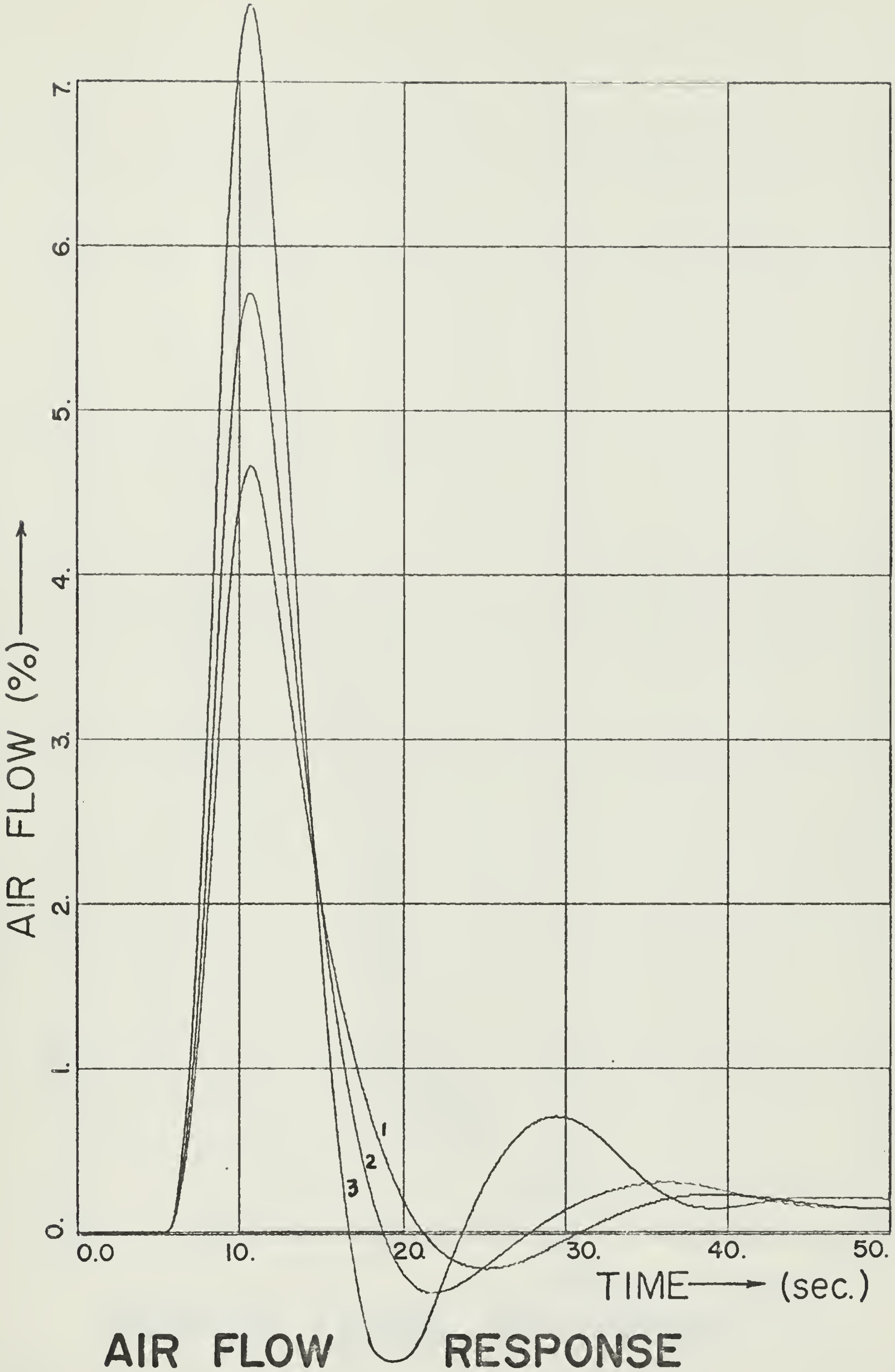

AIR FLOW RESPONSE
TO OIL VARIATIONS

FIGURE 32

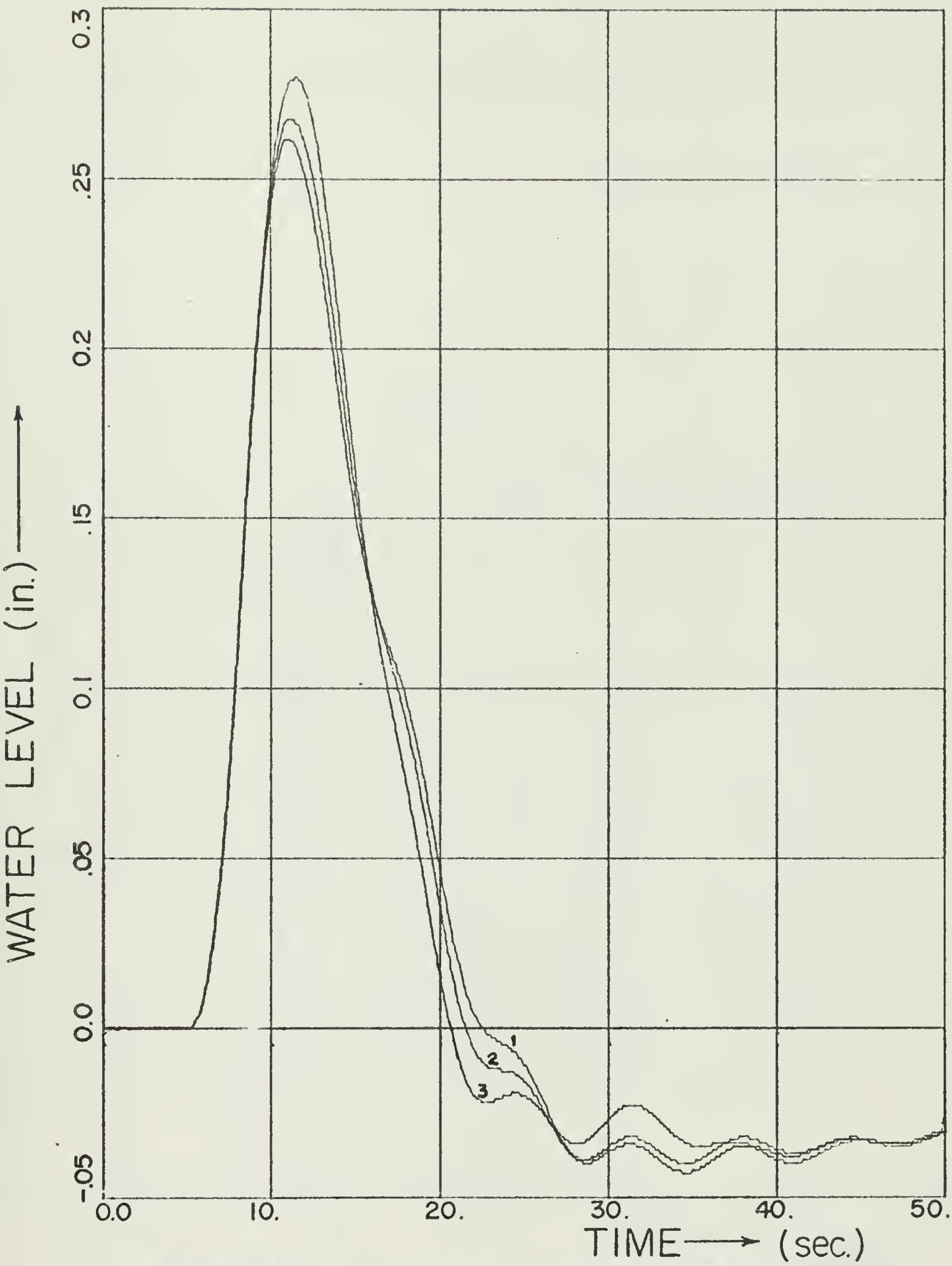

WATER LEVEL RESPONSE
TO OIL VARIATIONS

FIGURE 33

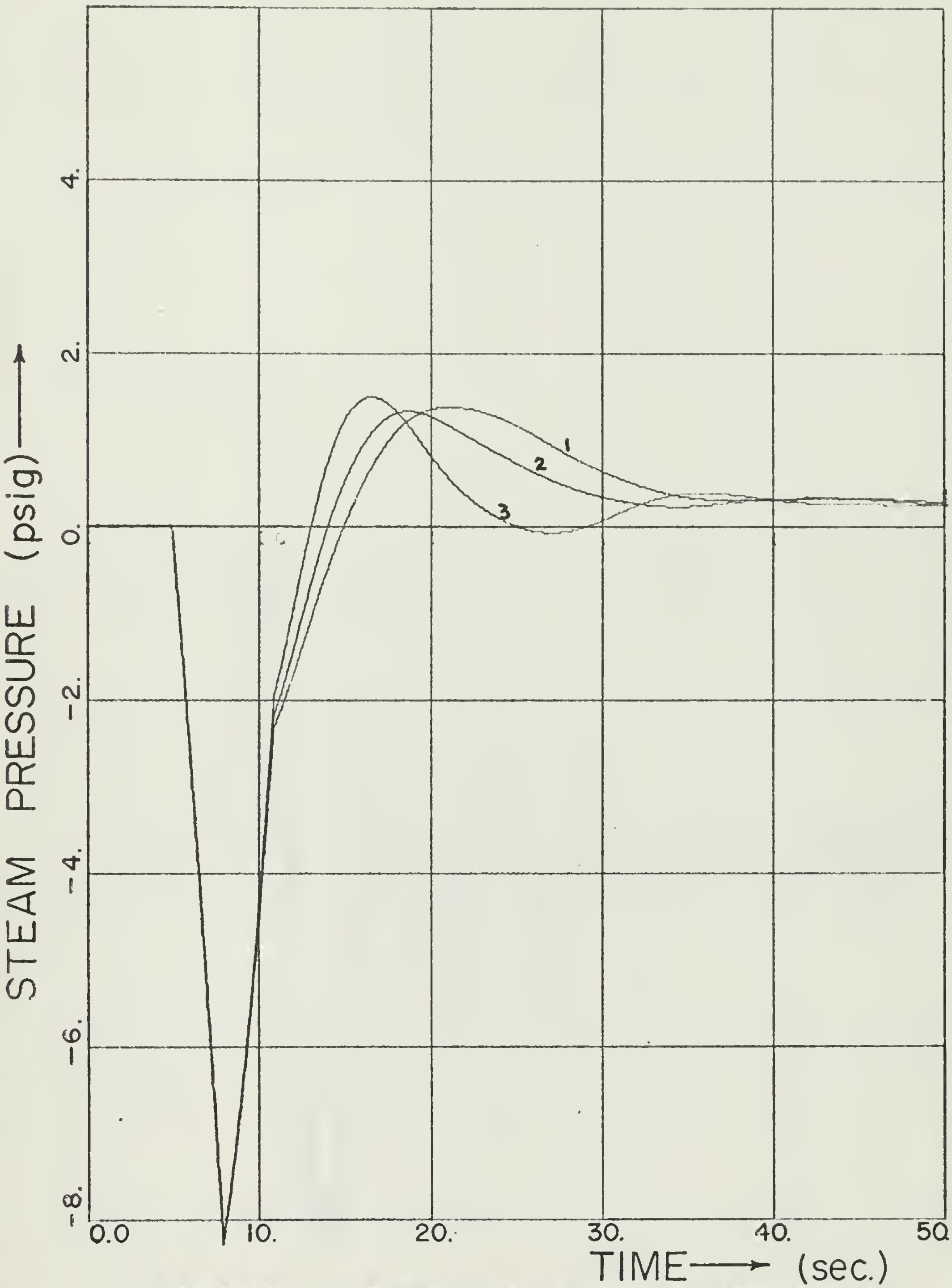

STEAM PRESSURE RESPONSE TO OIL VARIATIONS

FIGURE 34

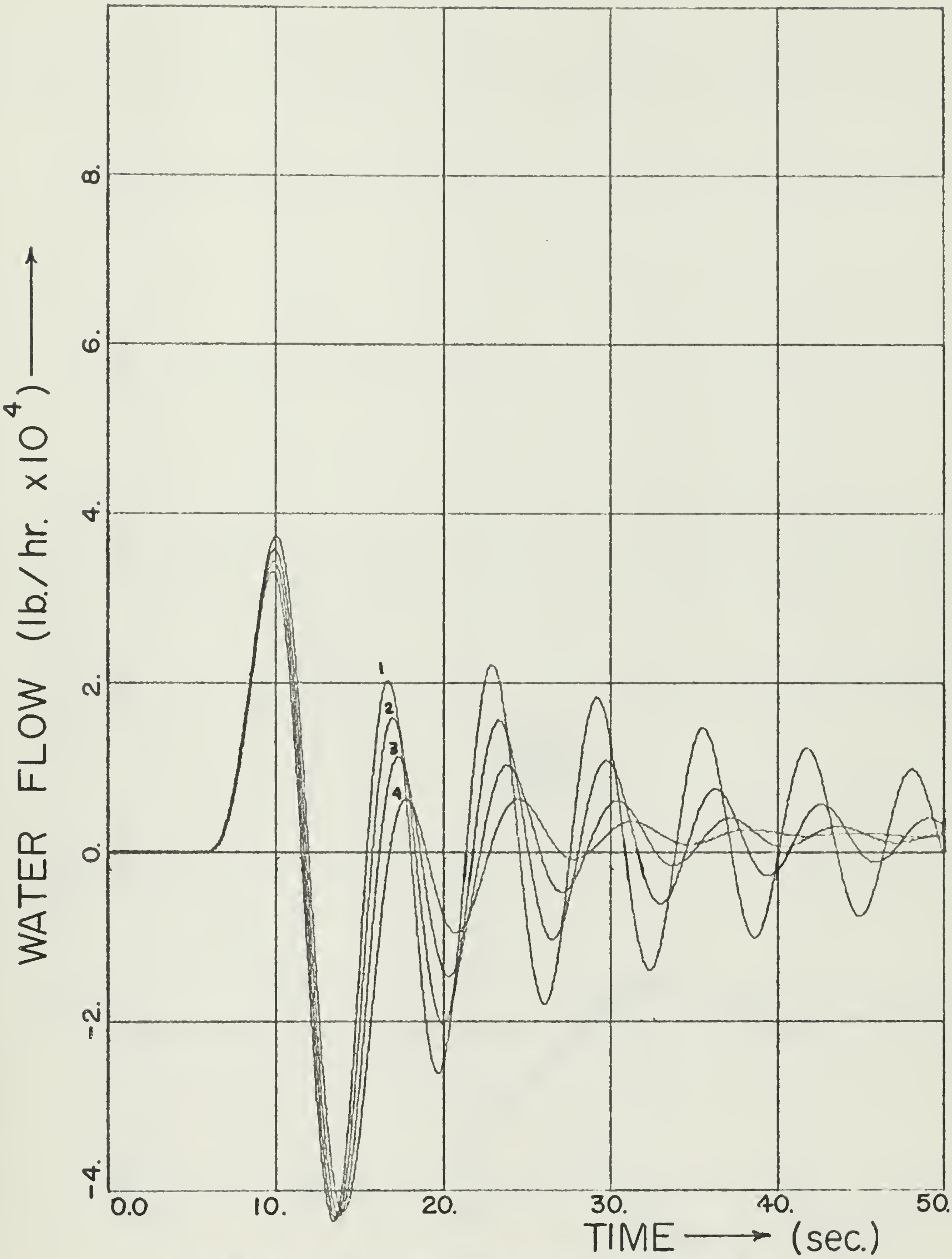

WATER ̇LOW RESPONSE TO WAT VARIATIONS

FIGURE 35

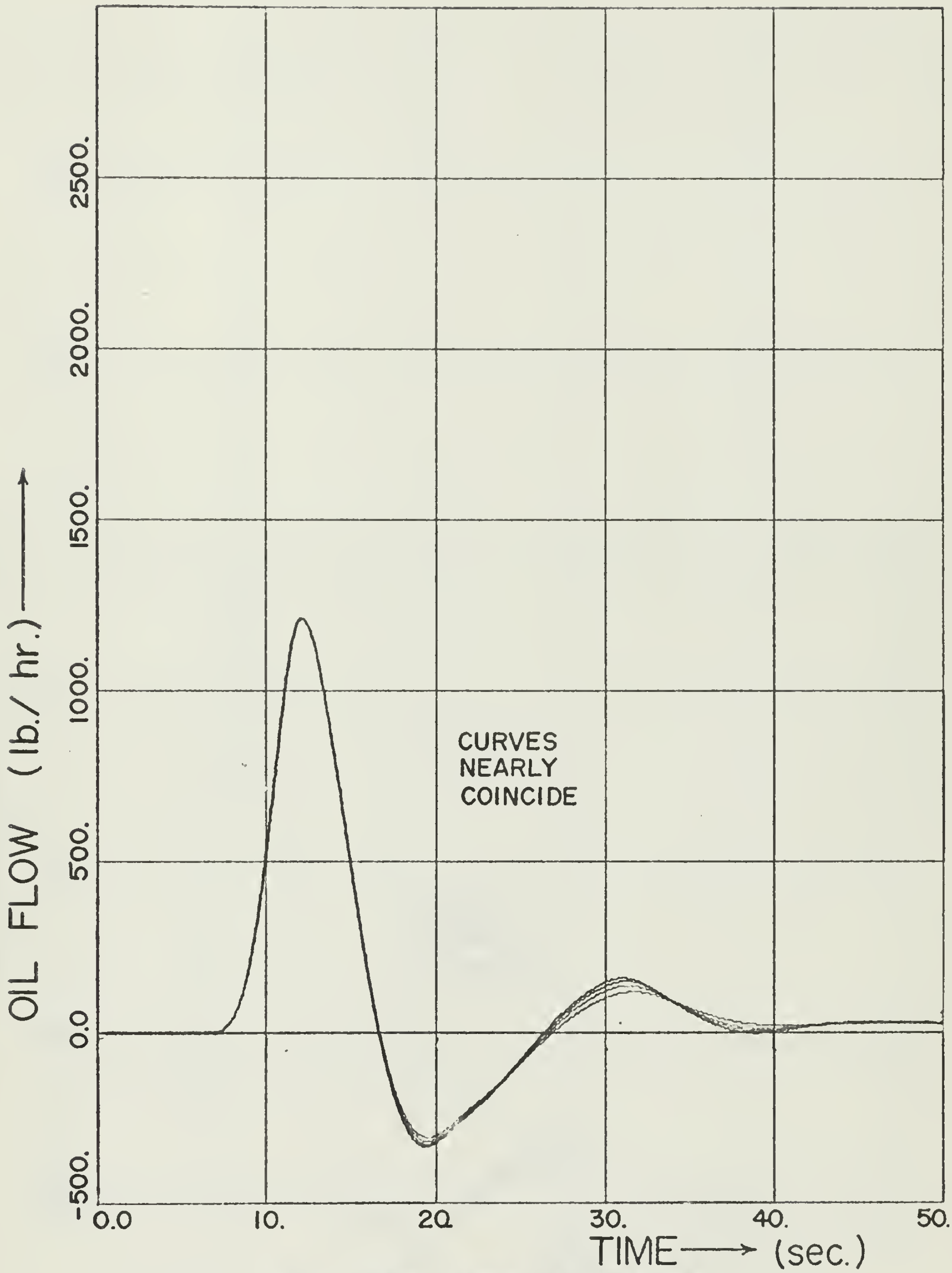

OIL FLOW RESPONSE
TO WAT VARIATIONS

FIGURE 36

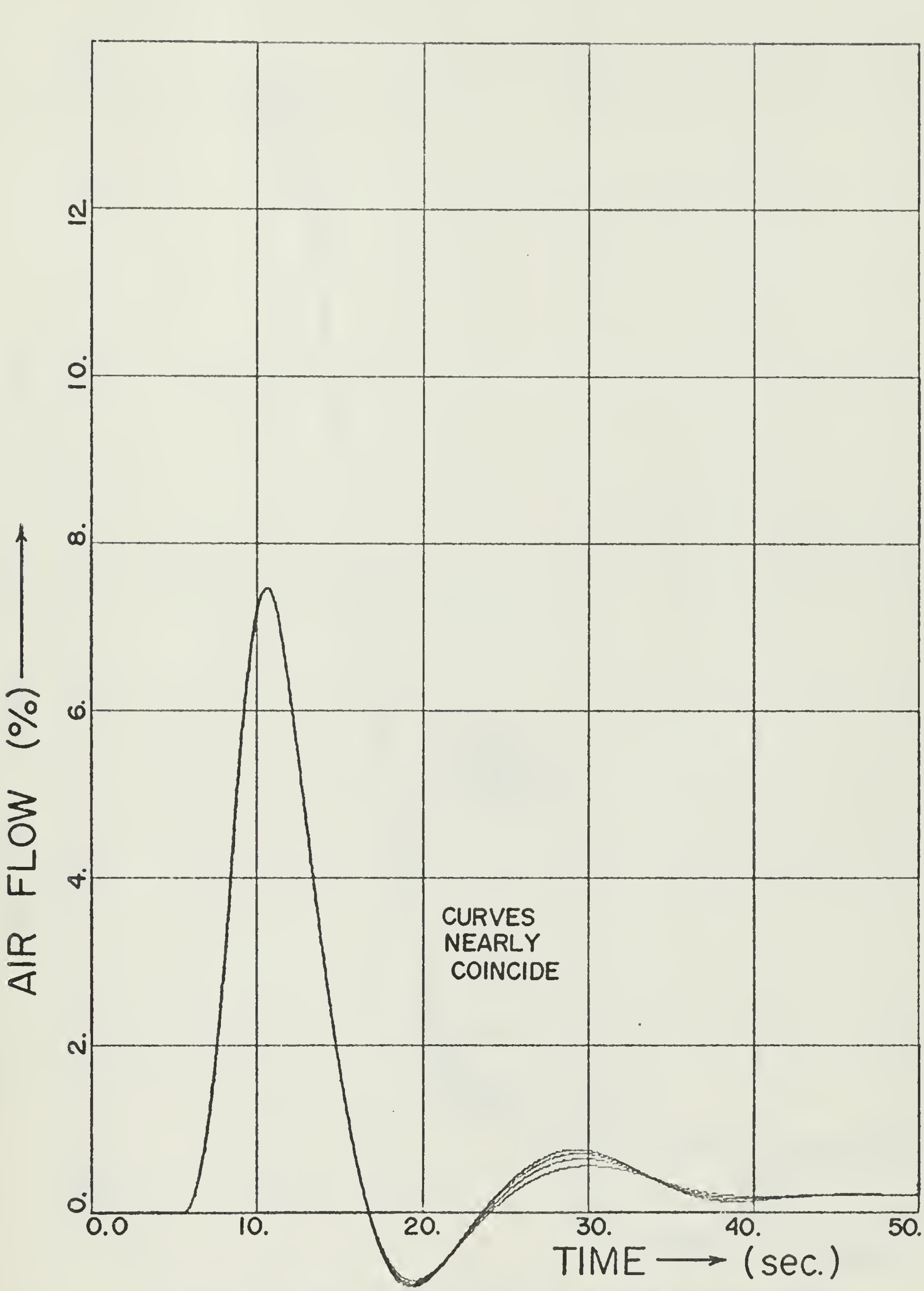

AIR FLOW RESPONSE
TO WAT VARIATIONS

FIGURE 37

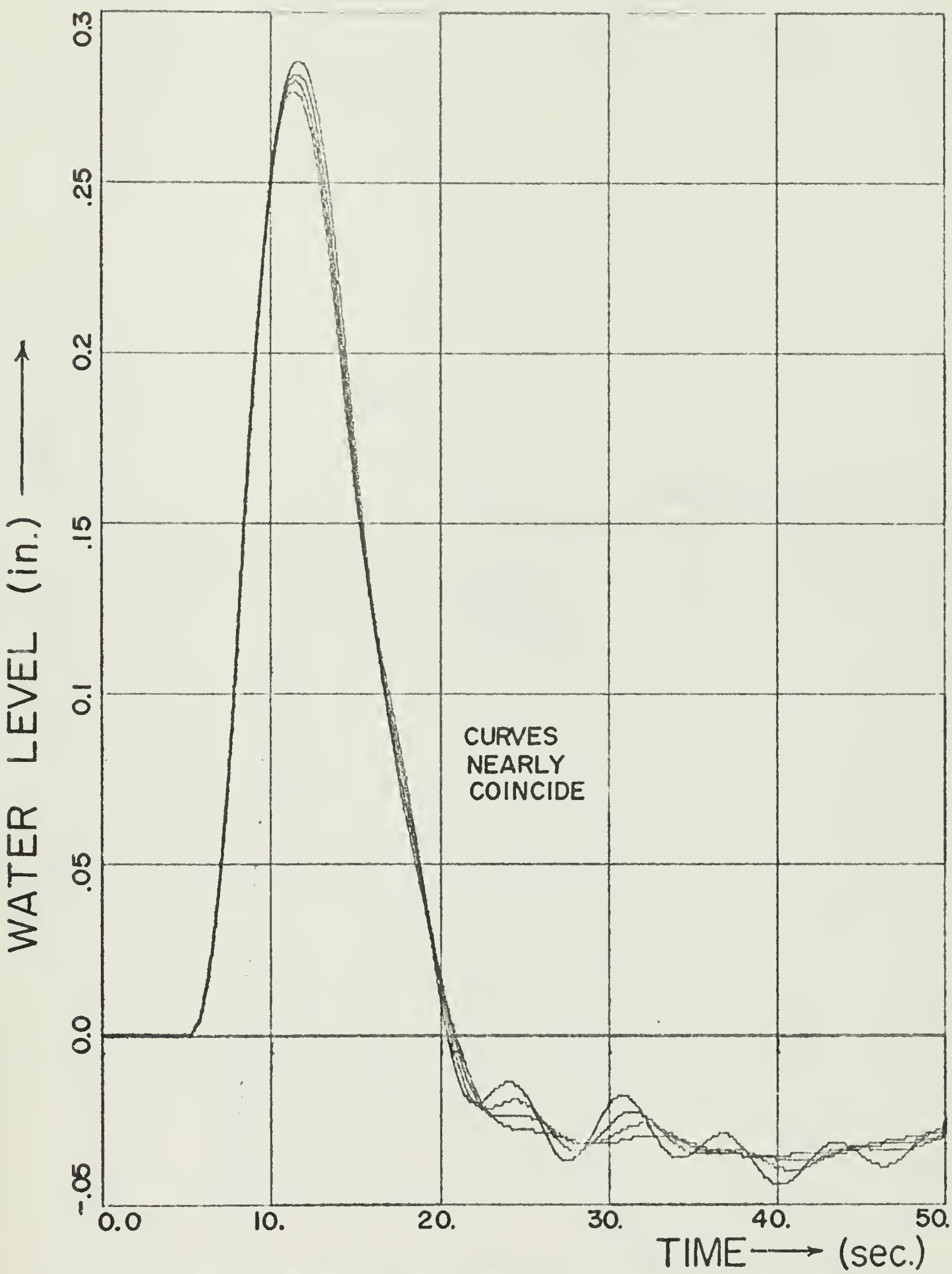

WATER LEVEL RESPONSE TO WAT VARIATIONS

FIGURE 38

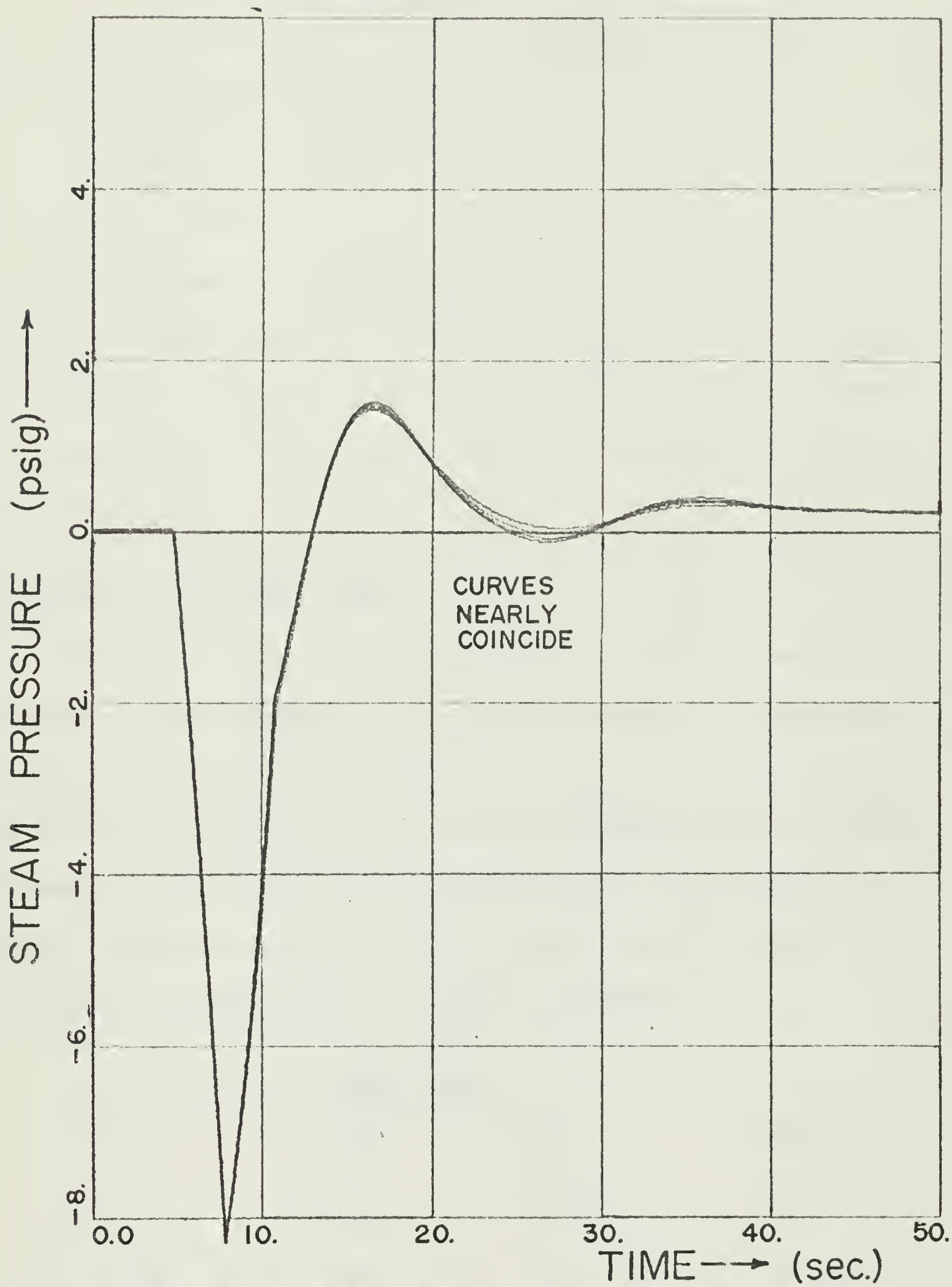

STEAM PRESSURE RESPONSE TO WAT VARIATIONS

FIGURE 39

TABLE THREE

WAT	CURVE #
0.21	1
0.147	2*
0.1	3
0.05	4

*Original Operating Point

All curves except those in Fig. 35 practically coincided with one another. Figure 35, the water flow rate response showed that the water responded faster with the new variable value (WAT = 0.21), as predicted on the parameter plane.

D. VARIATIONS IN ALL THREE LOOPS

As a final system test, all three parameters, AIR, OIL, and WAT were changed as was recommended in the previous section in accordance with parameter plane predictions. As a comparison, the old (original) response was plotted, along with a third curve representing the response if the parameters were moved in the opposite direction from that predicted by the parameter plane. Table Four gives parameter values along with corresponding curve numbers for Figs. 40 through 44.

TABLE FOUR

AIR	OIL	WAT	CURVE #
2.5	8.0	0.21	1
1.67	6.67	0.147	2*
1.0	4.0	0.1	3

*Original Operating Point

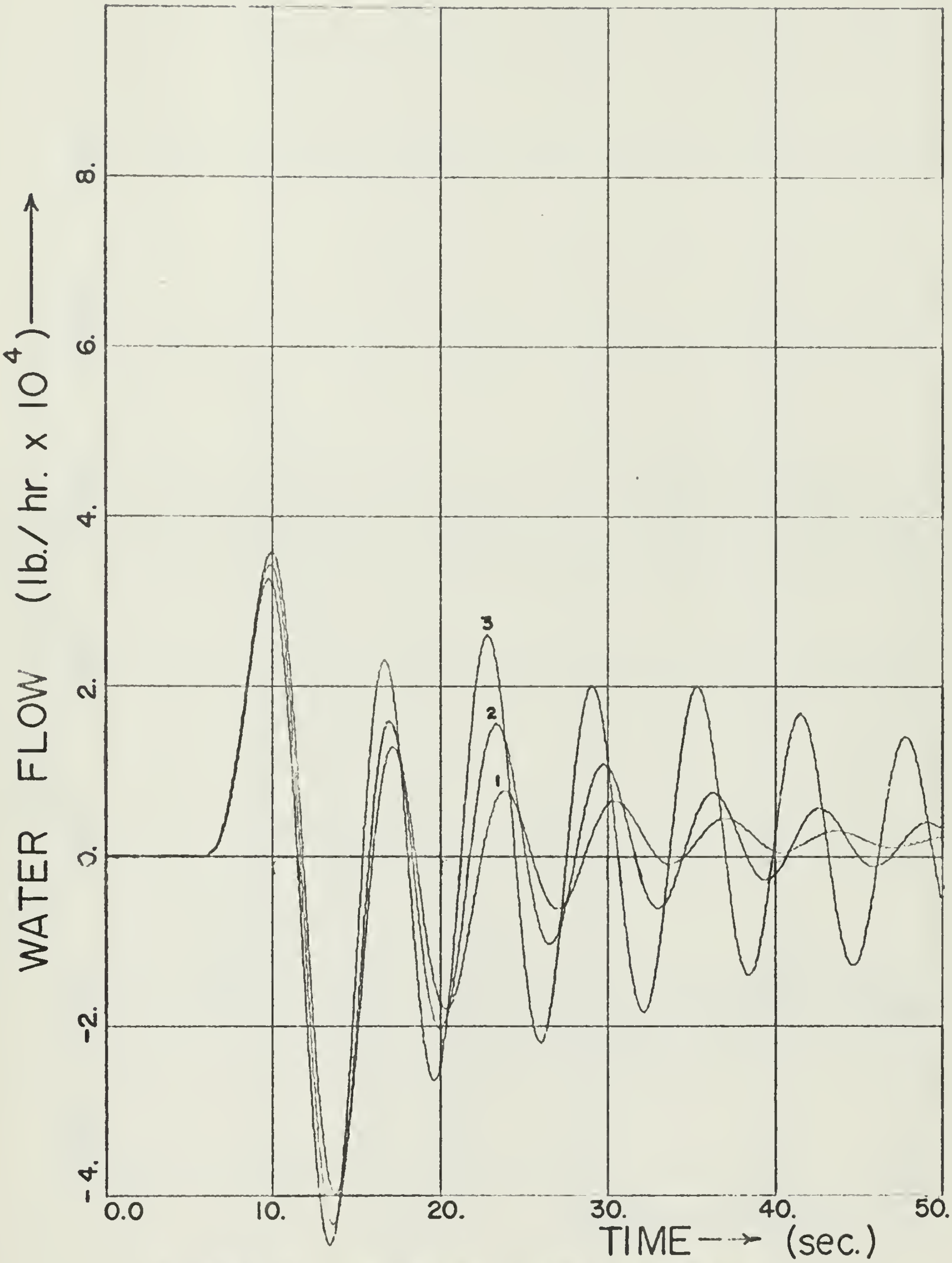

WATER FLOW RESPONSE
TO THREE VARIATIONS

FIGURE 40

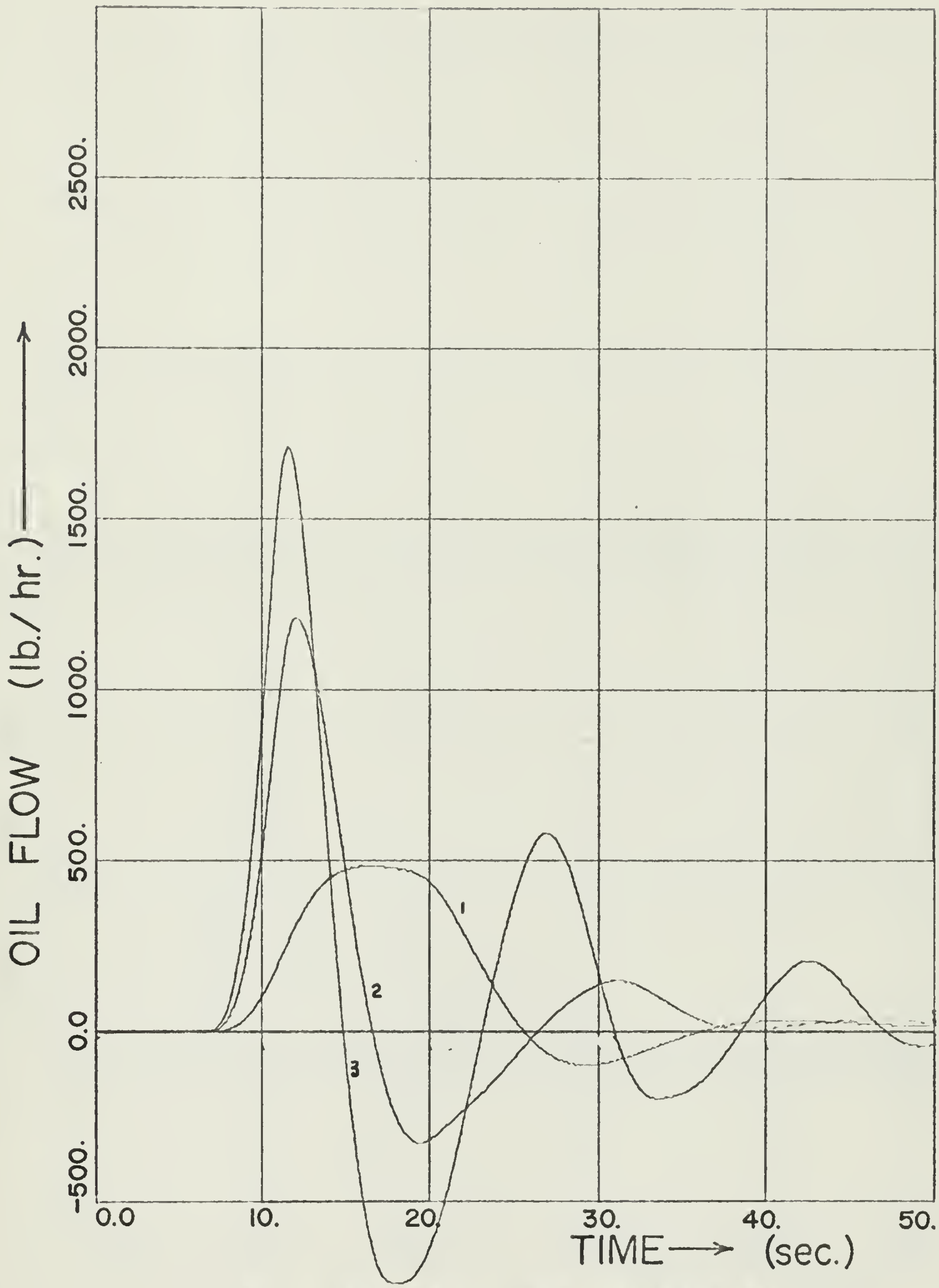

OIL FLOW RESPONSE
TO THREE VARIATIONS

FIGURE 41

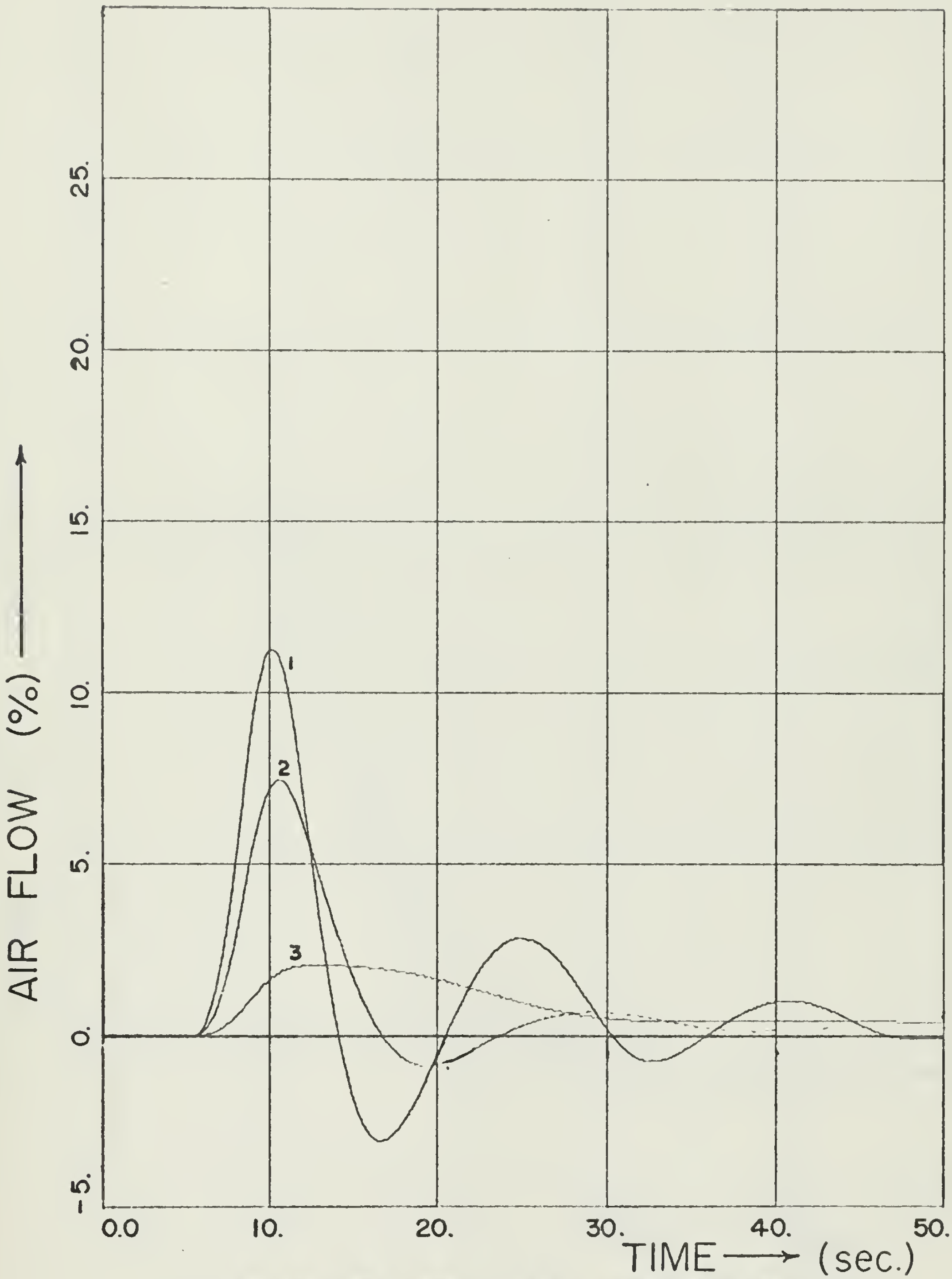

AIR FLOW RESPONSE
TO THREE VARIATIONS

FIGURE 42

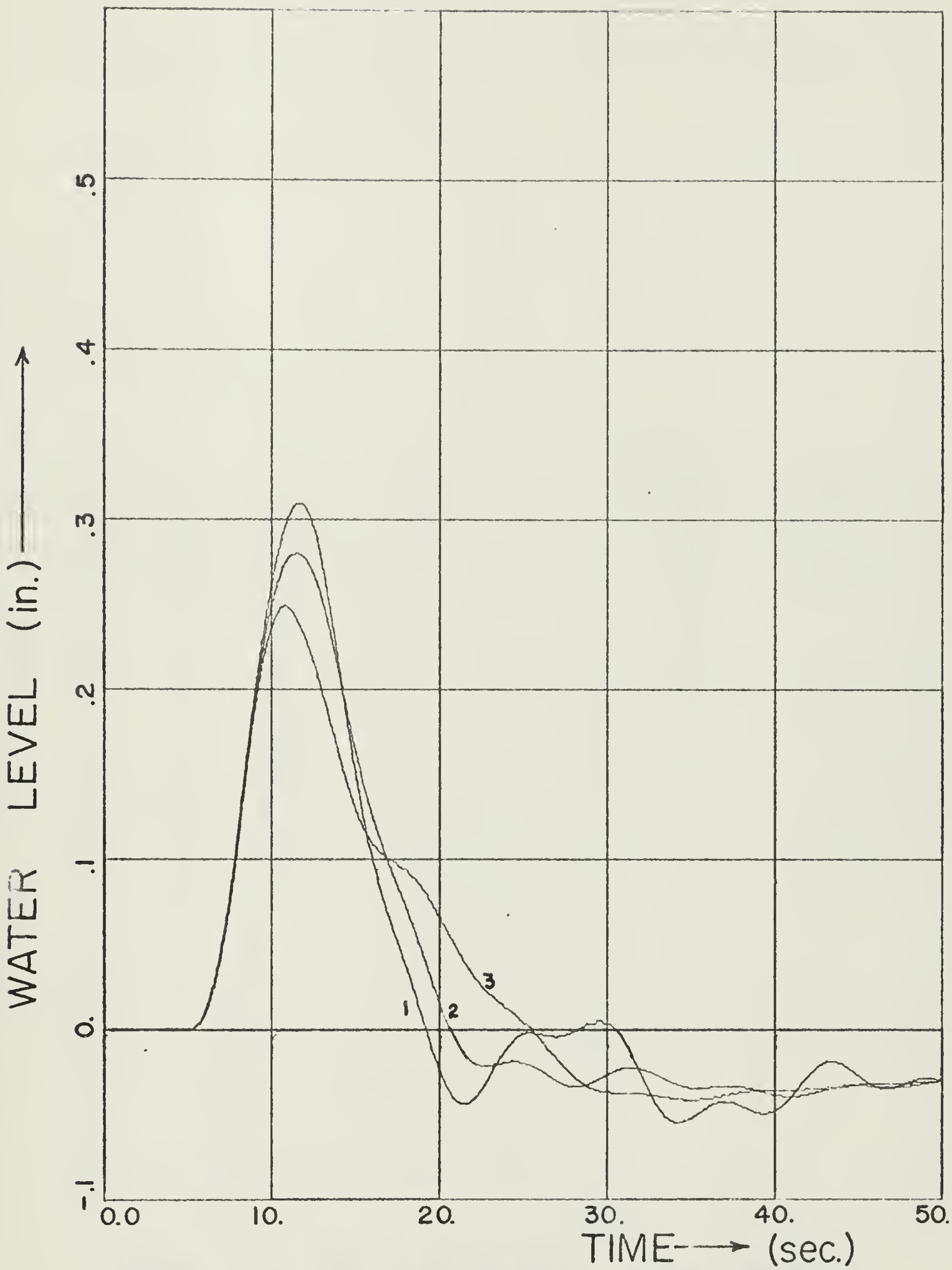

WATER LEVEL RESPONSE TO THREE VARIATIONS

FIGURE 43

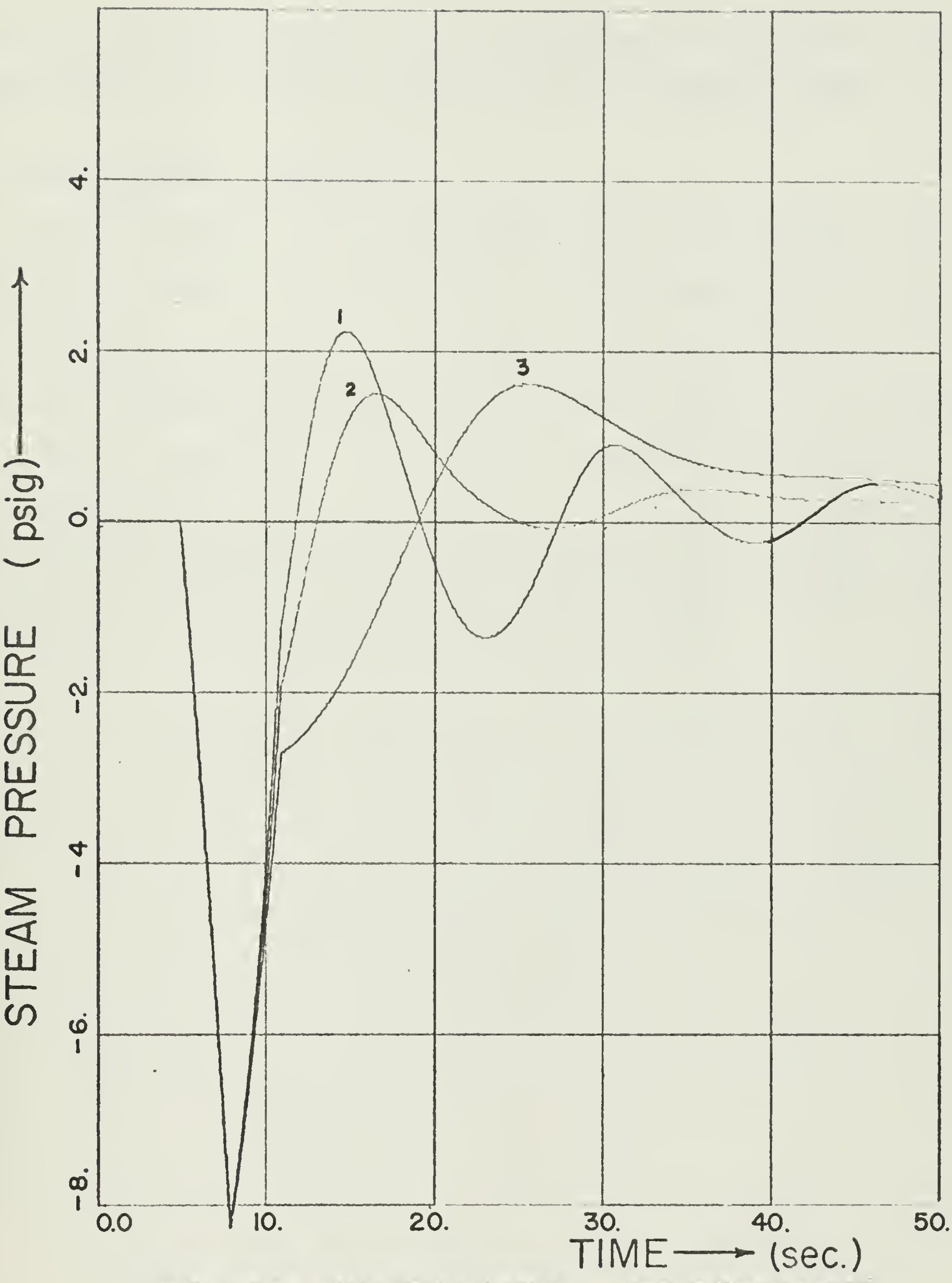

STEAM PRESSURE RESPONSE TO THREE VARIATIONS

FIGURE 44

In each case, it can be seen that the response is faster for curve #1 than for the original system. This proves the merits of design by the parameter plane. The curve #3 in each case was considerably slower.

E. ANOTHER PARAMETER VARIATION

It had been thought that the time delay (0.45 sec) in the feed water control valve contributed significantly to the oscillatory behavior of the water flow loop. The system was run using a variable time delay in the simulation to observe its effects. The time delays used were 0.45 (original) sec., 0.22 sec. (½), and 0.11 sec. (¼). The response of the water flow loop is shown in Fig. 45.

It can be seen that the variation in time delay did not affect the oscillations but did cause them to die out more quickly.

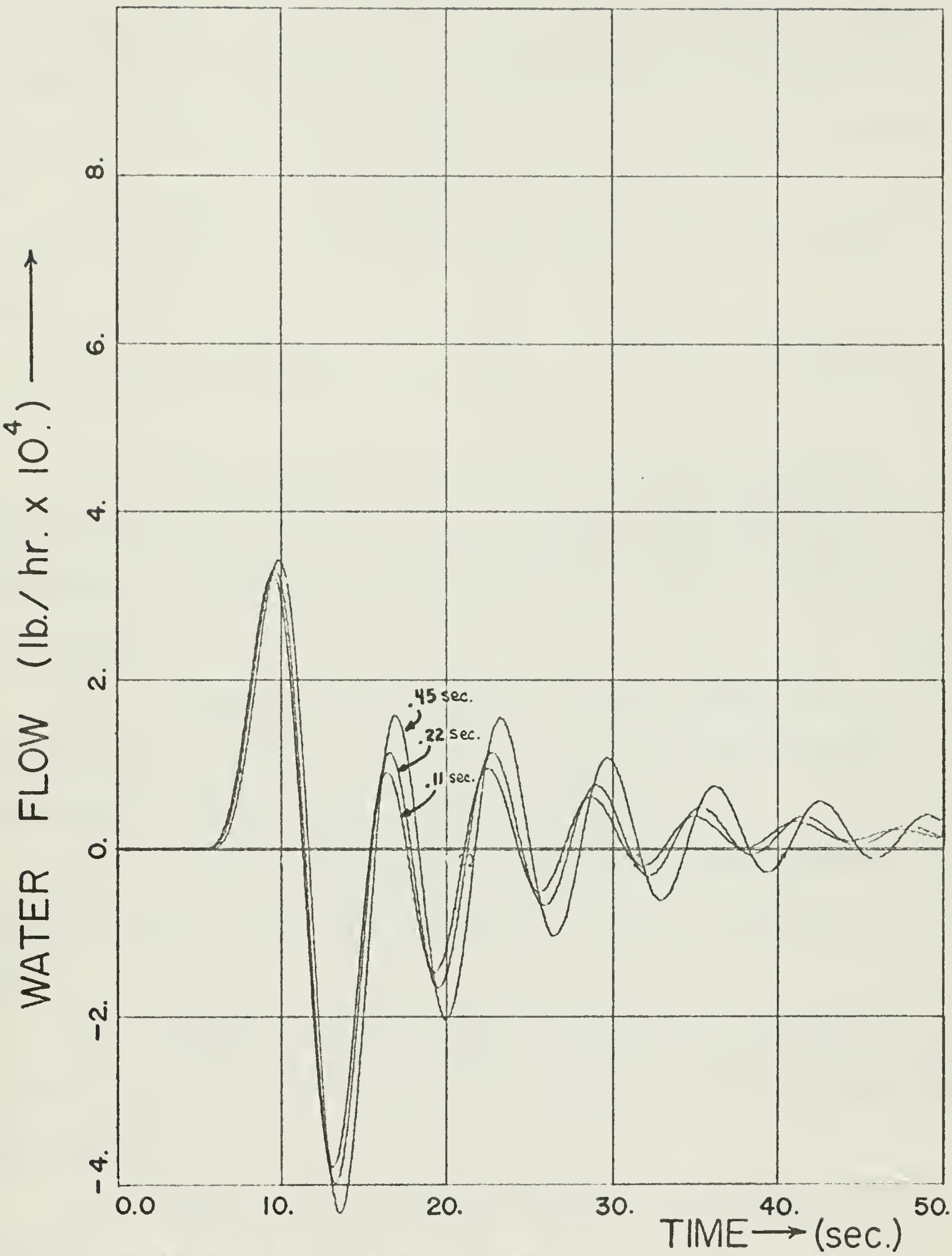

EFFECTS OF TIME DELAY ON WATER FLOW RESPONSE

FIGURE 45

V. CONCLUSIONS AND RECOMMENDATIONS

From this work, it can be seen that the use of a simulation program, particularly DSL, was valuable in the testing and analysis of a system of this type. The value of other computerized analysis tools was also demonstrated. The parameter plane proved to be most valuable and, even where interaction was ignored, proved useful in the design of boiler control systems.

The following recommendations are made as a result of this investigation:

1. Apply the simulation technique to other boiler control systems, on other ships which have the common pneumatic variety and on the newer ships to come which will have a state-of-the-art (probably fluidic) system.

2. Construct a three-dimensional parameter-space plot to depict the effects of varying the three parameters, OIL, AIR and WAT on the important variables, steam pressure and water level.

3. Investigate the effects of varying other system parameters or replacing certain system components, using the original simulation.

4. Extend the original system to be dynamically sound over the entire operating range of the boiler when other transient response data becomes available.

5. Continue work on the non-interacting controller shown in Appendix B.

It is not the belief of the author that the improvements were of

sufficient magnitude to recommend changes to the actual system. It is hoped, however, that the methods and techniques used in this thesis will be of sufficient value to aid in the further design and improvement of boiler automatic combustion control systems.

APPENDIX A

BOILER DESIGN AND PERFORMANCE DATA

DESIGN

Steam Generating Surface Area:		Sq. Ft.
Main tube bank	. . . .	4975
Screen tubes	. . . .	933
Front tubes	. . . .	40
Rear wall tubes	. . . .	158
Side and roof wall tubes	. . . .	274
Economizer	. . . .	7500
TOTAL WATER SURFACE		13880
Superheater	. . . .	2390
TOTAL SURFACE AREA		16720
Furance Volume:		1270 Cu. Ft.
Boiler Weight:		Lbs.
Dry	. . . .	230085
Water (Steaming Level)	. . . .	20080
TOTAL BOILER WEIGHT		250165

PERFORMANCE DATA

	CRUISING	FULL	OVERLOAD
Operating Rate, %	44.7	100	120
Total Steam Generated, lb/hr	117478	261450	313800
Drum Pressure, psig	1210	1245	1265
Superheater Outlet Pressure, psig	1200	1200	1200
Temperature, deg. F.	950	970	965
Air Flow, lb/hr	145000	321000	386000
Oil Flow, lb/hr	8645	20050	24100
Anticipated Efficiency, %	87.6	85.2	84.2
Number of Burners in Operation	4	6	6

APPENDIX B

A NON-INTERACTING BOILER CONTROLLER

The utility of a proportional plus reset type controller is limited in an environment which has many variables in which interaction is present. In the CVA-63 boiler control system, for example, a change in steam flow affects the drum water level as well as the pressure. When correction is applied to the water flow rate to bring the water level back to normal, the pressure is also affected which causes an adjustment to be made to the fuel flow rate.

It is desired to design a controller which will automatically limit the interaction between control system variables.

The major input variable to the boiler and control system is the steam flow rate.

$$\Delta P_d = K_{ps}\,\Delta W_s + K_{pf}\,\Delta W_f + K_{pi}\,\Delta W_i \tag{1a}$$

$$\Delta X = K_{xs}\,\Delta W_s + K_{xf}\,\Delta W_f + K_{xi}\,\Delta W_i \tag{1b}$$

These equations determine the change in drum pressure (ΔP_d) and water level (ΔX) in terms of steam flow rate change (ΔW_s), fuel flow rate change (ΔW_f), and feed water flow rate change (ΔW_i). The coefficients of Eqns. (1a) and (1b) are time dependent and are determined from boiler dynamic analysis.

The controller must adjust the fuel and water flow rates in a manner such that when the steam flow rate changes, neither the drum water level or the pressure is changed.

The controller will receive measurements of steam flow rate (W_s), drum pressure (P_d) and drum water level (X) from the boiler, compare the latter two with pre-determined set points, $\hat{P}_d$ and $\hat{X}$ and adjust flow of water and fuel accordingly. Refer to Fig. 46.

Hence, the controller equations may be written:

(2a) $$\Delta W_f = H_{fp}(e_p) + H_{fx}(e_x) + H_{fs}(\Delta W_s)$$

(2b) $$\Delta W_i = H_{ip}(e_p) + H_{ix}(e_x) + H_{is}(\Delta W_s)$$

where $e_p = \hat{P}_d - P_d$ and $e_x = \hat{X} - X$ are error signals. The time dependent coefficients K_{ij} are known (Fig. 46) as they represent boiler dynamic behavior. The H_{ij} coefficients are controller coefficients and are yet to be determined.

If the equations (2a) and (2b) are substituted into (1a) and (1b), the result is:

(3a) $$\Delta P_d = K_{ps}\Delta W_s + K_{pf}\left[H_{fp}(e_p) + H_{fx}(e_x) + H_{fs}\Delta W_s\right] + K_{pi}\left[H_{ip}(e_p) + H_{ix}(e_x) + H_{is}\Delta W_s\right]$$

(3b) $$\Delta X = K_{xs}\Delta W_s + K_{xf}\left[H_{fp}(e_p) + H_{fx}(e_x) + H_{fs}\Delta W_s\right] + K_{xi}\left[H_{ip}(e_p) + H_{ix}(e_x) + H_{is}\Delta W_s\right]$$

Rearranging the above equations and collecting terms, the above equations can be written:

(4a) $$\Delta P_d = (K_{ps} + K_{pf}H_{fs} + K_{pi}H_{is})\Delta W_s + (K_{pf}H_{fp} + K_{pi}H_{ip})e_p + (K_{pf}H_{fx} + K_{pi}H_{ix})e_x$$

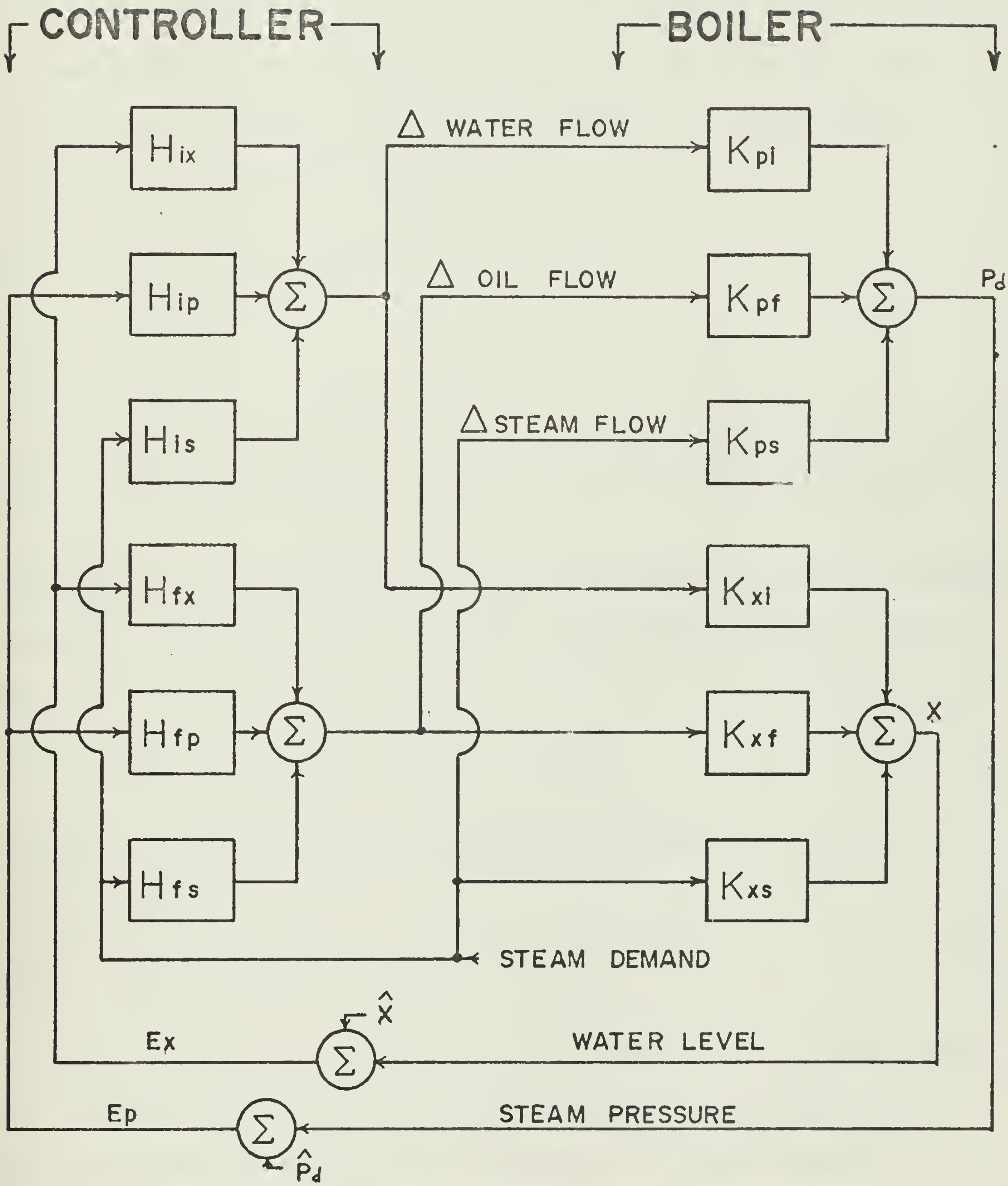

A NON-INTERACTING CONTROLLER

FIGURE 46

(4b) $\Delta X = (K_{xs} + K_{xf} H_{fs} + K_{xi} H_{is}) \Delta W_s + (K_{xf} H_{fp} + K_{xi} H_{ip}) e_p$

$$+ (K_{xf} H_{fx} + K_{xi} H_{ix}) e_x$$

Requirements for the non-interacting controller force ΔP_d and ΔX to be zero for any change in e_p or e_x . Therefore the coefficients of these terms must be zero identically.

(5a) $K_{pf} H_{fp} + K_{pi} H_{ip} \equiv 0$

(5b) $K_{pf} H_{fx} + K_{pi} H_{ix} \equiv 0$

(5c) $K_{xf} H_{fp} + K_{xi} H_{ip} \equiv 0$

(5d) $K_{xf} H_{fx} + K_{xi} H_{ix} \equiv 0$

Also present is the requirement t at when the pressure set point is changed, the pressure change must respond in some predetermined manner, say $G_p(s)$. Then

(5e) $K_{ps} + K_{pf} H_{fs} + K_{pi} H_{is} = G_p(s)$

Similarly, the water level must respond for a change in water level set point; therefore

(5f) $K_{xs} + K_{xf} H_{fs} + K_{xi} H_{is} = G_x(s)$

The six equations, (5a) through (5f), contain six controller transfer functions (H_{ij}) which are unknown, six boiler dynamic transfer functions which are known, and two "response to set point change" transfer functions which must be specified. Solving for the six unknowns yields

(6a) $$H_{fs} = (K_{xs} K_{pi} - K_{ps} K_{xi}) / C$$

(6b) $$H_{is} = (K_{xf} K_{ps} - K_{pf} K_{xs}) / C$$

(6c) $$H_{fx} = -(G_x K_{pi}) / C$$

where $$C = K_{pf} K_{xi} - K_{pi} K_{xf}$$

(6d) $$H_{ix} = (G_x K_{pf}) / C$$

(6e) $$H_{fp} = (G_p K_{xi}) / C$$

(6f) $$H_{ip} = -(G_p K_{xf}) / C$$

The simulation of this controller was attempted using DSL in the same fashion as the original control system. Several of the transfer functions contained more zeros than poles and the simulation failed.

Future work on this controller could involve the introduction of excess poles in the offending transfer functions which could be calculated to minimize any disturbing effects on the system.

APPENDIX C

I. PADE APPROXIMATIONS

The general form of the fourth-order Pade approximation used in the simulations was:

$$e^{-\tau s} \cong \frac{(\tau s)^4 - 20(\tau s)^3 + 180(\tau s)^2 - 840\,\tau s + 1680}{(\tau s)^4 + 20(\tau s)^3 + 180(\tau s)^2 + 840\,\tau s + 1680}$$

Specific approximations were as follows for the individual loops:

AIR:

$$e^{-.057s} \cong \frac{1.0551 \times 10^{-5}\, s^4 - .003703\, s^3 + .58482\, s^2 - 47.88\, s + 1680.}{1.0551 \times 10^{-5}\, s^4 + .003703\, s^3 + .58482\, s^2 + 47.88\, s + 1680.}$$

OIL:

$$e^{-.025s} \cong \frac{.39062 \times 10^{-6}\, s^4 - .3125 \times 10^{-3}\, s^3 + .1125\, s^2 - 21.\, s + 1680.}{.39062 \times 10^{-6}\, s^4 + .3125 \times 10^{-3}\, s^3 + .1125\, s^2 + 21.\, s + 1680.}$$

WATER:

$$e^{-.45s} \cong \frac{.04100625\, s^4 - 1.8225\, s^3 + 36.45\, s^2 - 378.\, s + 1680.}{.04100625\, s^4 + 1.8225\, s^3 + 36.45\, s^2 + 378.\, s + 1680.}$$

II. INDIVIDUAL LOOP CHARACTERISTIC POLYNOMIALS:

The following polynomials were calculated using the FORMAC computer program and were used in the parameter plane plotting routine:

AIR: $.1246 \times 10^{-11} S^{15} + .4831 \times 10^{-9} S^{14} + .8625 \times 10^{-7} S^{13} + .8598 \times 10^{-5} S^{12}$

$+ .4735 \times 10^{-3} S^{11} + .01329 S^{10} + .26135 S^{9} + 3.5134 S^{8} \ (35.736 +$

$.5289 \times 10^{-7} \alpha) S^{7} + (258.293 - .1691 \times 10^{-4} \alpha + .52897 \times 10^{-7} \beta) S^{6} +$

$(1433.6 + .002364 \alpha - .1691 \times 10^{-4} \beta) S^{5} + (5264.03 - .15295 \alpha + .002364 \beta) S^{4}$

$(14502.64 + 1.637 \alpha - .15295 \beta) S^{3} + (12894.84 + 204.603 \alpha + 1.637 \beta) S^{2}$

$(1680. + 2056.32 \alpha + 204.603 \beta) S + 2056.32 \beta$

OIL: $.2973 \times 10^{-7} S^{13} + .2611 \times 10^{-4} S^{12} + .0103 S^{11} + 2.144 S^{10}$

$+ 197.64 S^{9} + 1765.72 S^{8} + 15266.9 S^{7} + (85501.7 + .1104 \times 10^{-5} \alpha) S^{6}$

$+ (233383.7 - .96 \times 10^{-3} \alpha + .1104 \times 10^{-5} \beta) S^{5} + (286758.5 + .3756 \alpha - .96 \times 10^{-3} \beta) S^{4}$

$+ (123922. - 76.22 \alpha + .3756 \beta) S^{3} + (1680. + 6627.8 \alpha - 76.22 \beta) S^{2}$

$+ (29.856 \alpha + 6627.8 \beta) S + 29.856 \beta$

WATER: $.03346 S^{8} + 1.5422 S^{7} + 32.24 S^{6} + (359.64 + .127 \times 10^{-4} \beta) S^{5}$

$+ (1924.32 + .6381 \times 10^{-11} \alpha - .5469 \times 10^{-3} \beta) S^{4} + (2748. - .283 \times 10^{-9} \alpha +$

$.01129 \beta) S^{3} + (2400.72 + .5672 \times 10^{-8} \alpha + .11718 \beta) S^{2} + (1680. -$

$.58824 \times 10^{-7} \alpha + .5208 \beta) S + .2614 \times 10^{-6} \alpha$

```
TITLE  ***** CVA-63 BOILER AND ACC SYSTEM SIMULATION *******


*****  INPUT FORCING FUNCTION ********************************
AFGEN   STEAM=0.0,0.0,5.0,0.0,8.0,50000.,11.0,0.0,100.,0.0
        GS=AFGEN(STEAM,TIME)
*********************************************************************
*********************************************************************


*****  BOILER PORTION OF SIMULATION ***************************
        PDS=INTGRL(IC1,-19.E-06*GS)
        PDF=TRNFR(1,2,ICA,NUMA,DENA,GF)
        POW=TRNFR(0,3,ICB,NUMB,DENB,GW)
        PO=PDS+PDF+POW
        PSA=1.37E-04*GS
        POUT=PO-PSA
        LF=LEDLAG(IC2,14.2,1.42,5.11E-06*GF)
        LF1=INTGRL(IC1,LF)
        LW=INTGRL (IC3,5.02E-07*GW)
        LSA=CMPXPL(IC4,IC5,2.55,0.63,0.79E-05*GS)
        LSB=INTGRL(IC6,5.02E-07*GS)
        LST=LSA-LSB
        L=LF1+LW+LST
*********************************************************************
*********************************************************************


*****  OIL FLOW LOOP PORTION OF SIMULATION *****************
        PP=CMPXPL(IC7,IC8,.0422,7.09,POUT*1.25)
        PZP=PRP-PPL
        PMA=PZP*OIL
        PMB=INTGRL(IC9,0.14*PZP)
        PM=PMA+PMB
        SIGNAL=PQRL-PML
        PSF=FCNSW(SIGNAL,PQRL,PQRL,PML)
        PRF=CMPXPL(IC17,IC18,1.13,1.48,8.0*PSF)
        PFINT=CMPXPL(IC19,IC20,1.01,2.485,36.1*PRFL)
        PF=DELAY(10,0.23,PFINT)
        GF=117.*PF
*********************************************************************
*********************************************************************


*****  AIR FLOW LOOP PORTION OF SIMULATION *****************
        PEQ=PML-PQRL
        POAA=AIR*PEQ
        POAB=INTGRL(IC10,0.024*PEQ)
        POA=POAA+POAB
        PQA=CMPXPL(IC11,IC12,0.5,7.91,QA*6.)
        PQR=TRNFR(1,2,ICC,NUMC,DENC,POAL)
        PQ1=TRNFR(1,2,ICC,NUMC,DENC,POAL)
        GB1INT=CMPXPL(IC13,IC14,0.2237,5.59,PQ1*53000.)
        GB1=DELAY(10,0.05,GB1INT)
        QB1=CMPXPL(IC15,IC16,1.534,0.421,0.444E-03*GB1)
        QA=3.0*QB1
*********************************************************************
*********************************************************************


*****  WATER FLOW LOOP PORTION OF SIMULATION ***************
        PSW=.22*PSA-WAT*PWA
        PDW=PRL+PSL-PSW
        GWINT=TRNFR(0,3,ICD,NUMD,DEND,PDW)
        GW=DELAY(10,0.45,GWINT)
        PWA=0.925E-04*GW
        PL=2.37*L
        PSL=PS+PL
*********************************************************************
*********************************************************************
```

```
** LIMITING FOR CERTAIN PNEUMATIC SIGNALS **
      PPL=LIMIT(-20.,20.,PP)
      PML=LIMIT(-20.,20.,PM)
      PQRL=LIMIT(-20.,20.,PQR)
      PCAL=LIMIT(-20.C,20.,PQA)
      PRFL=LIMIT(-60.0,60.,PRF)
      PQAL=LIMIT(-20.,20.,PQA)
*****************************************************************
*****************************************************************


***** CONTROL PORTION OF SIMULATION *****************************
STORAG ICA(2),ICB(3),ICC(2),ICD(3),NUMA(2),DENA(3),NUMB(1),
      DENB(4),NUMC(2),DENC(3),NUMD(1),DEND(4)
TABLE ICA(1-2)=2*0.0,ICB(1-3)=3*0.0,ICC(1-2)=2*0.0,...
      ICD(1-3)=3*0.0,...
      NUMA(1-2)=.0628,3.18E-04,DENA(1-3)=71.4,1.0,0.0,...
      NUMB(1)=-4.42E-06,DENB(1-4)=10.1,2.54,1.0,0.0,...
      NUMC(1-2)=.064,1.0,DENC(1-3)=.0064,.08,1.0,...
      NUMD(1)=-3.1E04,DEND(1-4)=.816,1.5432,1.204,1.0

C        THESE PARAMETERS ARE FOR THE ORIGINAL SYSTEM
PARAM  OIL=6.67,AIR=1.67,WAT=.147
PARAM PRP=0.0,PRL=0.0,PS=0.0
CONTRL  FINTIM=50.,DELT=.05
INTEG RKSFX
END
STOP
```

REFERENCES

1. NavShips Technical Manual, Main Boilers, (CVA-63), 351-0652, June 1959.

2. Naval Boiler and Turbine Laboratory Technical Report of RDT&E Project B-502-II, SF013-06-06, Task 4182, Experimental Determination of Open-Loop Characteristics of CVA-63 Steam Generator System, by A. B. Macellaro, 30 November 1964.

3. Ulrich, J. L., Analysis of Boiler Dynamics for Single Furnace Natural Circulation Marine Steam Generator, N. E. and M. S. in N.A. and M. E. Thesis, MIT, 1964.

4. Naval Boiler and Turbine Laboratory Technical Report of RDT&E project B-452-I, SF013-06-06, Task 4200, Development of Simplified Combustion Controls for CVA-66, by J. W. Banham, Jr., 25 January 1962.

5. Beckman Instruments Technical Report, Navy Contract #Nobs-72280, Mathematical Analysis of Boiler Dynamics and a Non-Interacting Type Boiler Controller, by K. L. Chien, E. I. Ergin, C. Ling, 19 December 1957.

6. Naval Electronics Laboratory Center Technical Note TN-1444, Digital Control of Multivariable Systems, by D. G. Mudd, 4 November 1968.

7. Naval Electronics Laboratory Center Technical Report No. 1461, Digital Control of a Naval Steam Generating System, by T. Neff and D. G. Mudd, 23 May 1967.

8. Sowers, E. V., III and Banham, J. W., Jr., Development and Evaluation of a Steam Generator Fluidic Analog Control System, Instrumentation in the Chemical and Petroleum Industries, Vol., 4, Plenum Press, 1968.

9. Naval Boiler and Turbine Laboratory Technical Report of RTD&E Project B-452-I, SF013-06-06, Task 4200, Analysis of Automatic Control Systems Design for Main Propulsion Machinery, by J. W. Banham, Jr., 24 June 1964.

10. International Business Machines Company Technical Report, DSL-360 Digital Simulation Language Users Manual, by W. M. Syn, N. N. Turner, D. G. Wyman, November 1968.

11. Vinroot, C. A. and Thaler, G. J., An All Digital Simulation of the CVA-63 Boiler and Automatic Combustion Control System, paper published in the Proceedings of Second Ship Control Symposium, Annapolis, Md., 5 November 1969.

12. Naval Boiler and Turbine Laboratory Technical Report of RDT&E Project B-622, SR011-01-01, Task 0401, Development of Experimental Technique for Frequency Response Analysis by the Pulse Text Method, by J. W. Banham, Jr., 27 March 1964.

13. Creager, Fenick and O'Brien, Computer Investigation of a Destroyer Steam Generator, MSEE Thesis, NPGS, Monterey, California, June 1965.

14. Vinroot, C. A. and Thaler, G. J., Parameter Optimization in Boiler Control Loops, paper published in the Proceedings of Second Ship Control Symposium, Annapolis, Md., 5 November 1969.

15. Thaler, G. J., Algebraic Methods for Analysis and Design, paper presented at First Ship Control Symposium, Annapolis, Md., November 1966.

16. Holst, P. A., Pade Approximations and Analog Computer Simulation of Time Delays, Simulation, Vol. 12, Number 6, p. 277-290, June 1969.

17. Merzhauser, P. K., Symbolic Algebraic Manipulation by Digital Computer in Problems of Control Theory, MSEE Thesis, NPGS, Monterey, California, June 1970.

18. Sammet, J., Programming Languages, p. 474-491, Prentice-Hall, 1969.

INITIAL DISTRIBUTION LIST

		No. Copies
1.	Defense Documentation Center Cameron Station Alexandria, Virginia 22314	2
2.	Library, Code 0212 Naval Postgraduate School Monterey, California 93940	2
3.	Naval Ship Systems Command Department of the Navy Washington, D. C. 20360	1
4.	LT Charles A. Vinroot % Supervisor of Shipbuilding 97 East Howard Street Qunicy, Massachusetts 02169	1
5.	Professor M. L. Wilcox, Code 52Wx Department of Electrical Engineering Naval Postgraduate School Monterey, California 93940	1
6.	Dr. G. J. Thaler, Code 52Tr Naval Postgraduate School Monterey, California 93940	5
7.	Mr. J. W. Banham, Jr. Head, Machinery Automation Department Naval Ship Engineering Center Philadelphia, Pennsylvania 19112	1
8.	Mr. Ward Rosenberry Naval Ship Development Center Annapolis, Maryland 21402	1

Unclassified

Security Classification

DOCUMENT CONTROL DATA - R & D

(Security classification of title, body of abstract and indexing annotation must be entered when the overall report is classified)

1. ORIGINATING ACTIVITY (Corporate author) Naval Postgraduate School Monterey, California 93940	2a. REPORT SECURITY CLASSIFICATION Unclassified 2b. GROUP

3. REPORT TITLE

An All-Digital Simulation and Analysis of the CVA-63 Boiler and Automatic Combustion Control System

4. DESCRIPTIVE NOTES (Type of report and, inclusive dates)

Master's Thesis; June 1970

5. AUTHOR(S) (First name, middle initial, last name)

Charles Arthur Vinroot

6. REPORT DATE	7a. TOTAL NO. OF PAGES	7b. NO. OF REFS
June 1970	103	18

8a. CONTRACT OR GRANT NO.	9a. ORIGINATOR'S REPORT NUMBER(S)
b. PROJECT NO.	
c.	9b. OTHER REPORT NO(S) (Any other numbers that may be assigned this report)
d.	

10. DISTRIBUTION STATEMENT This document has been approved for public release and sale; its distribution is unlimited.

11. SUPPLEMENTARY NOTES	12. SPONSORING MILITARY ACTIVITY
	Naval Postgraduate School Monterey, California 93940

13. ABSTRACT

An all digital simulation of the existing boiler and control system of CVA-63 was carried out. A significant savings in computer time over previous simulations was realized.

The parameter-plane method was used to search for new operating points for each of the system minor control loops. Individual loop transient response was tested with a simulation program to demonstrate improved response with new operating points.

The entire system response was then investigated to demonstrate the overall effects. Recommendations were made for new controller settings along with component variations in order to improve over-all system response.

KEY WORDS	LINK A		LINK B		LINK C	
	ROLE	WT	ROLE	WT	ROLE	WT
oiler						
mulation						
mbustion Control						
rameter Plane						

Thesis 120073
V69 Vinroot
c.2 An all-digital simulation and analysis of the CVA-63 boiler and automatic combustion control system.